

# THE PROCEEDINGS OF THE PHYSICAL SOCIETY

## Section B

VOL. 63, PART 1

1 January 1950

No. 361 B

### CONTENTS

	PAGE
Editorial . . . . .	1
Mr. J. K. MACKENZIE. The Elastic Constants of a Solid containing Spherical Holes . . . . .	2
Prof. FRIEDRICH BLAHA. On Movements of Small Ferromagnetic Particles in Inhomogeneous Magnetic Fields . . . . .	12
Mr. B. COLLINGE. Dead Times of Self-Quenching Counters . . . . .	15
Mr. F. G. HEYMANN. Breakdown in Cold-Cathode Tubes at Low Pressure . . . . .	25
Mr. W. E. WILLSHAW and Mr. R. G. ROBERTSHAW. The Behaviour of Multiple Circuit Magnetrons in the Neighbourhood of the Critical Anode Voltage . . . . .	41
Mr. D. G. KIELY. Measurements of the Reflection Coefficient of Water at a Wavelength of 8.7 mm. . . . .	46
Mr. T. L. ECKERSLEY. Coupling of the Ordinary and Extraordinary Rays in the Ionosphere . . . . .	49
Letters to the Editor :	
Mr. A. N. HUNTER. The Debye Effect in Electrolytes . . . . .	58
Mr. C. E. CHALLICE. Electron Optics of the Three-Stage Electron Microscope . . . . .	59
Reviews of Books. . . . .	62
Contents for Section A . . . . .	63
Abstracts for Section A . . . . .	63

Price to non-members 10s. net, by post 6d. extra. Annual subscription: £5 5s.  
Composite subscription for both Sections A and B: £9 9s.

Published by  
THE PHYSICAL SOCIETY  
1 Lowther Gardens, Prince Consort Road, London S.W.7



THE PROCEEDINGS OF THE PHYSICAL SOCIETY  
**THE PHYSICAL SOCIETY**

Founded 1874.

Incorporated 1878.

**OFFICERS OF THE SOCIETY, 1949-50**

**President :** Professor S. CHAPMAN, M.A., D.Sc., F.R.S.

**Hon. Secretaries :** C. G. WYNNE, B.A. (*Business*). H. H. HOPKINS, Ph.D. (*Papers*).

**Hon. Foreign Secretary :** Professor E. N. da C. ANDRADE, Ph.D., D.Sc., F.R.S.

**Hon. Treasurer :** H. SHAW, D.Sc.

**Hon. Librarian :** R. W. B. PEARSE, D.Sc., Ph.D.

**SPECIALIST GROUPS**

**COLOUR GROUP**

**Chairman :** W. S. STILES, O.B.E., D.Sc., Ph.D.

**Hon. Secretary :** R. G. HORNER, B.A.

**OPTICAL GROUP**

**Chairman :** Professor L. C. MARTIN, D.Sc.

**Hon. Secretary :** G. S. SPEAK.

**LOW-TEMPERATURE GROUP**

**Chairman :** Professor F. E. SIMON, C.B.E., M.A.,  
D.Phil., F.R.S.

**Hon. Secretary :** G. G. HASELDEN, Ph.D.

**ACOUSTICS GROUP**

**Chairman :** H. L. KIRKE, C.B.E., M.I.E.E.

**Hon. Secretaries :** W. A. ALLEN, B.Arch.,  
A.R.I.B.A., and A. T. PICKLES, O.B.E., M.A.

*Secretary-Editor :* Miss A. C. STICKLAND, Ph.D.

*Offices and Library :* 1 Lowther Gardens, Prince Consort Road, London S.W. 7.

Telephone : KENsington 0048, 0049

**PROCEEDINGS OF THE PHYSICAL SOCIETY**

The *Proceedings* is now published monthly in two Sections.

**ADVISORY BOARD**

*Chairman :* The President of the Physical Society (S. CHAPMAN, M.A., D.Sc., F.R.S.).

E. N. da C. ANDRADE, Ph.D., D.Sc., F.R.S.  
Sir EDWARD APPLETON, G.B.E., K.C.B., D.Sc.,  
F.R.S.

L. F. BATES, Ph.D., D.Sc.

P. M. S. BLACKETT, M.A., F.R.S.

Sir LAWRENCE BRAGG, O.B.E., M.A., Sc.D.,  
D.Sc., F.R.S.

Sir JAMES CHADWICK, D.Sc., Ph.D., F.R.S.

Lord CHERWELL OF OXFORD, M.A., Ph.D.,  
F.R.S.

Sir JOHN COCKCROFT, C.B.E., M.A., Ph.D.,  
F.R.S.

Sir CHARLES DARWIN, K.B.E., M.C., M.A.,  
Sc.D., F.R.S.

N. FEATHER, Ph.D., F.R.S.

G. I. FINCH, M.B.E., D.Sc., F.R.S.

D. R. HARTREE, M.A., Ph.D., F.R.S.

N. F. MOTT, M.A., F.R.S.

M. L. OLIPHANT, Ph.D., D.Sc., F.R.S.

F. E. SIMON, C.B.E., M.A., D.Phil., F.R.S.

T. SMITH, M.A., F.R.S.

Sir GEORGE THOMSON, M.A., D.Sc., F.R.S.

Papers for publication in the *Proceedings* should be addressed to the Hon. Papers Secretary,  
Dr. H. H. HOPKINS, at the Office of the Physical Society, 1 Lowther Gardens, Prince  
Consort Road, London S.W.7. Telephone : KENsington 0048, 0049.

Detailed Instructions to Authors were included in the February 1948 issue of  
the *Proceedings* ; separate copies can be obtained from the Secretary-Editor.



## THE PHYSICAL SOCIETY

### MEMBERSHIP

Membership of the Society is open to all who are interested in Physics:

**FELLOWSHIP.** A candidate for election to Fellowship must as a rule be recommended by three Fellows, to two of whom he is known personally. Fellows may attend all meetings of the Society, are entitled to receive Publications 1 (either Section A or Section B), 4 and 5 below, and may obtain the other publications at much reduced rates.

**STUDENT MEMBERSHIP.** A candidate for election to Student Membership must be between 18 and 26 years of age and must be recommended from personal knowledge by a Fellow. Student Members may attend all meetings of the Society, are entitled to receive Publications 1 (either Section A or Section B) and 4, and may obtain the other publications at much reduced rates.

Books and periodicals may be read in the Society's Library, and a limited number of books may be borrowed by Fellows and Student Members on application to the Honorary Librarian.

Fellows and Student Members may become members of the *Colour Group*, the *Optical Group*, the *Low-Temperature Group* and the *Acoustics Group* (specialist Groups formed in the Society) without payment of additional annual subscription.

### PUBLICATIONS

1. *The Proceedings of the Physical Society*, published monthly in two Sections, contains original papers, lectures by specialists, reports of discussions and of demonstrations, and book reviews. Section A contains papers mainly on atomic and sub-atomic subjects; Section B contains papers on macroscopic physics.

2. *Reports on Progress in Physics*, published annually, is a comprehensive review by qualified physicists.

3. *The Handbook of the Physical Society's Annual Exhibition of Scientific Instruments and Apparatus*. This Exhibition is recognized as the most important function of its kind, and the Handbook is a valuable book of reference.

4. *The Bulletin*, issued at frequent intervals during the session, informs members of programmes of future meetings and of the business of the Society generally.

5. *Physics Abstracts (Science Abstracts A)*, published monthly in association with the Institution of Electrical Engineers, covers the whole field of contemporary physical research.

6. *Electrical Engineering Abstracts (Science Abstracts B)*, published monthly in association with the Institution of Electrical Engineers, covers the whole field of contemporary research in electrical engineering.

7. *Special Publications*, critical monographs and reports on special subjects prepared by experts or committees, are issued from time to time.

### MEETINGS

At approximately monthly intervals throughout each annual session, meetings are held for the reading and discussion of papers, for lectures, and for experimental demonstrations. Special lectures include: the *Guthrie Lecture*, in memory of the founder of the Society, given annually by a physicist of international reputation; the *Thomas Young Oration*, given biennially on an optical subject; the *Charles Chree Address*, given biennially on Geomagnetism, Atmospheric Electricity, or a cognate subject; and the biennial *Rutherford Memorial Lecture*. A Summer Meeting is generally held each year at a provincial centre, and from time to time meetings are arranged jointly with other Societies for the discussion of subjects of common interest.

Each of the four specialist Groups holds about five meetings in each session.

### SUBSCRIPTIONS

Fellows pay an Entrance Fee of £1 1s. and an Annual Subscription of £3 3s. Student Members pay only an Annual Subscription of 15s. Second Section of *Proceedings* 30s. No entrance fee is payable by a Student Member on transfer to Fellowship.

*Further information may be obtained from the Secretary-Editor  
at the Office of the Society:*

1 LOWTHER GARDENS, PRINCE CONSORT ROAD, LONDON S.W. 7  
Telephone: KENSington 0048, 0049



# THE OSRAM MINIATURES are becoming more popular every day . . .



## OSRAM BATTERY

### MINIATURES "17" RANGE

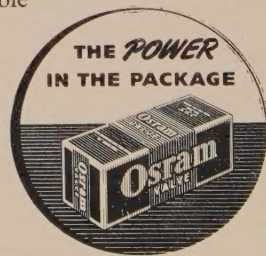
Left to Right: The X.17 Frequency Changer; W.17 Vari-Mu H. F. Pentode; ZD.17 Diode Pentode; N.17 Output Pentode

## and here's why

These valves, now extensively used by set manufacturers, have been specially designed with a view to H.T. current economy. The filaments, intended primarily to operate from a dry cell, maintain adequate emission during the whole useful life of the cell. Mounted on the popular B7G miniature base, they are compact and extremely robust. Ideal for battery operation in portable equipment such as personal receivers.

# Osram

V A L V E S

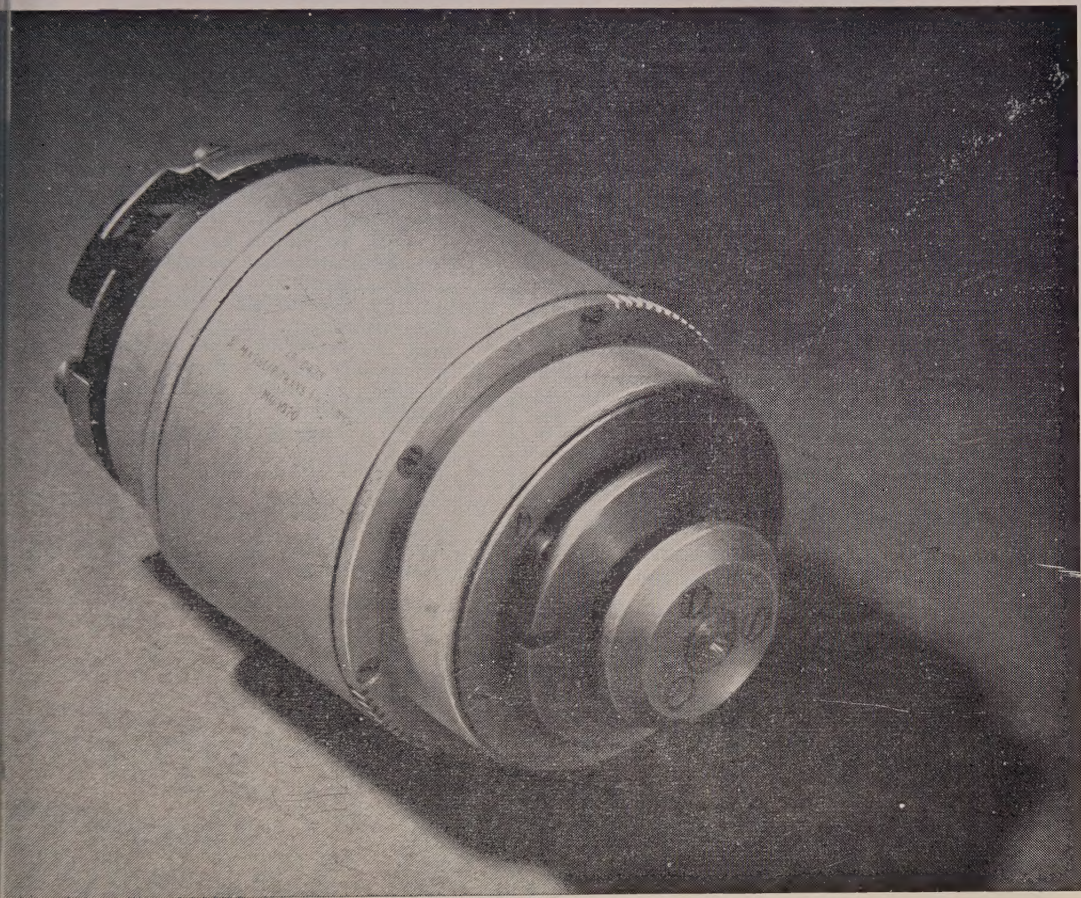


THE GENERAL ELECTRIC CO, LTD., MAGNET HOUSE, KINGSWAY, W.C.2



# Muirhead Magslips

*Measurements and Controls where you want them*



Designed by the Admiralty Research Laboratory and so widely used for war time service applications, these devices are now available for all.

Muirhead Magslips, which are backed by twelve years of manufacturing experience, may well solve many of your remote control and indication problems.

**DETAILS IN BULLETIN B-580, SENT ON REQUEST.**

---

**MUIRHEAD**

---

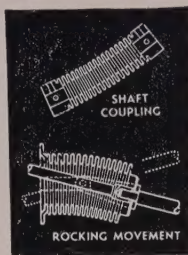
*Muirhead & Co., Ltd., Elmers End, Beckenham, Kent. Telephone: Beckenham 0041-2*

**OVER 60 YEARS DESIGNERS AND MAKERS OF PRECISION INSTRUMENTS**



# PLEASE tell us of OTHER applications

Drayton 'Hydroflex' Metal Bellows are an essential component part in Automatic coolant regulation . . . Movement for pressure change . . . Packless gland to seal spindle in high vacua . . . Reservoir to accept liquid expansion . . . Dashpot or delay device . . . Barometric measurement or control . . . Pressurised couplings where vibration or movement is present . . . Dust seal to prevent ingress of dirt . . . pressure reducing



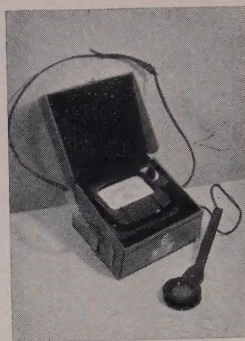
valves . . . Hydraulic transmission . . . Distance thermostatic control . . . Low torque flexible coupling . . . Pressure sealed rocking movement . . . Pressurised rotating shaft seals . . . Aircraft pressurised cabin control . . . Refrigeration expansion valves . . . Thermostatic Steam Traps . . . Pressure amplifiers . . . Differential pressure measurements . . . Thermostatic operation of louvre or damper.

## for HYDRAULICALLY FORMED

Seamless, one-piece, metal bellows combining the properties of a compression spring able to withstand repeated flexing, a packless gland and a container which can be hermetically sealed. Made by a process unique in this country, they are tough, resilient, with a uniformity of life, performance and reliability in operation unobtainable by any other method.

## Drayton METAL BELLOWS

Write for List No. V800-1 DRAYTON REGULATOR & INSTRUMENT CO. LTD.,  
WEST DRAYTON, MIDDLESEX. West Drayton 2611 B.8.



THE



PHOTOMETER

THE "EEL" PHOTOMETER measures, with an unusual degree of accuracy, light intensities not covered by the conventional exposure meter or light meter. Sturdily constructed in stout leather case, each instrument is especially assembled with a photocell and microammeter individually calibrated, the values being selected to cover customer's specific requirements.

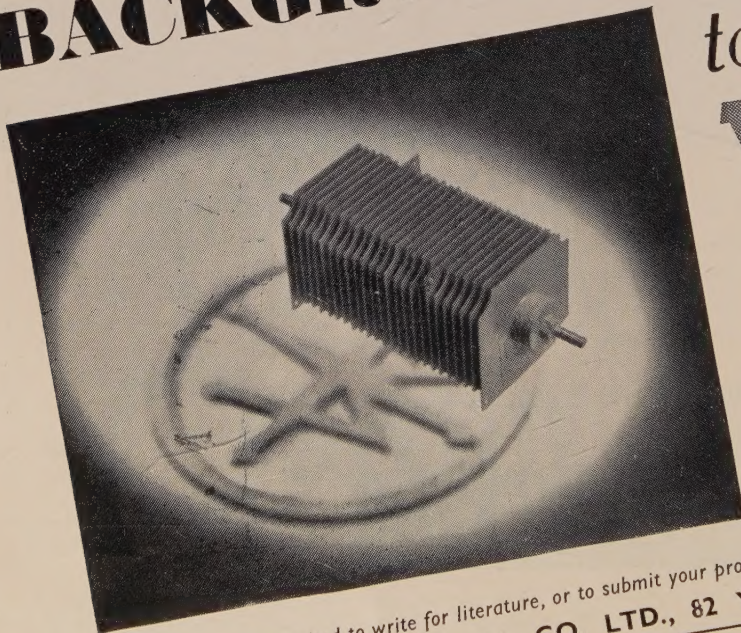
PRICE 20 Guineas

Complete in leather case with cell unit and handle on flexible lead.

Write for full particulars of this and other equipment incorporating the famous "EEL" selenium cell.

EVANS ELECTROSELENIUM LTD.  
SALES DIVISION 310 HARLOW ESSEX

# BACKGROUND



## to efficiency WESTINGHOUSE WESTALITE RECTIFIERS

have the very high efficiency of nearly 90% over a wide range of loading, and voltage regulation of about 5% with a current change from full load about 1/10th full load

You are invited to write for literature, or to submit your problems, to Dept. P.S.1

WESTINGHOUSE BRAKE & SIGNAL CO. LTD., 82 YORK WAY, LONDON,



# MICROID ADAPTABLE GALVANOMETERS

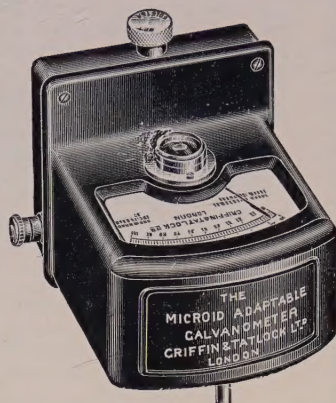
Microid Adaptable Galvanometers are inexpensive pointer-mirror instruments, available in two types:

- (a) UNIVERSAL MODEL with taut suspension which does not require levelling.
- (b) SENSITIVE MODEL with silver spiral current lead at bottom. This model requires levelling.

Each model is made in three resistances: 10, 50 or 375 ohms, either ballistic or dead-beat.

Full details on request.

The instrument is again in production. Delivery of 10 ohm ballistic Universal model from stock.



## GRIFFIN and TATLOCK Ltd

Established as Scientific Instrument Makers in 1826

**LONDON**  
Kemble St., W.C.2.

**MANCHESTER**  
19 Cheetham Hill Rd., 4.

**GLASGOW**  
45 Renfrew St., C.2.

**EDINBURGH**  
7 Teviot Place, 1.

**BIRMINGHAM** : STANDLEY BELCHER & MASON LTD., Church Street, 3.

### BINDING CASES for the PROCEEDINGS OF THE PHYSICAL SOCIETY

Binding cases for Sections A and B (separate) for Volume 62 (1949) may be obtained for 7s. each, post free, from the Offices of the Society.

The *Proceedings* may be bound in the Society's green cloth for 13s. 6d. each. Journals for binding should be sent direct to Messrs. Taylor and Francis, Ltd., Red Lion Court, Fleet Street, London E.C.4. Remittances should be sent to the Physical Society.

### THE HANDBOOK OF THE PHYSICAL SOCIETY'S 34th EXHIBITION OF SCIENTIFIC INSTRUMENTS AND APPARATUS, 1950

5s.; by post 6s.

To be published at the beginning of March

Copies of last year's Handbook are available, price 5s.

Orders, with remittances, should be sent to

THE PHYSICAL SOCIETY

1 Lowther Gardens, Prince Consort Rd., London, S.W.7

### SYMPOSIUM ON NOISE AND SOUND TRANSMISSION

*Report of the*  
1948 SUMMER SYMPOSIUM  
OF THE  
ACOUSTICS GROUP  
OF THE  
PHYSICAL SOCIETY

200 pages. 17s. 6d.; by post 18s.

(Price 10s. 6d., by post 11s., to Fellows of the Society and Members of the Acoustics Group)

Now ready

Orders, with remittances, to be sent to  
THE PHYSICAL SOCIETY  
1 Lowther Gardens, Prince Consort Road,  
London, S.W.7



## BULLETIN ANALYTIQUE

## Publication of the Centre National de la Recherche Scientifique, France

The *Bulletin Analytique* is an abstracting journal which appears monthly in two parts, Part I covering scientific and technical papers in the mathematical, chemical and physical sciences and their applications, Part II the biological sciences.

The *Bulletin*, which started on a modest scale in 1940 with an average of 10,000 abstracts per part, now averages 35 to 40,000 abstracts per part. The abstracts summarize briefly papers in scientific and technical periodicals received in Paris from all over the world and cover the majority of the more important journals in the world scientific press. The scope of the *Bulletin* is constantly being enlarged to include a wider selection of periodicals.

The *Bulletin* thus provides a valuable reference book both for the laboratory and for the individual research worker who wishes to keep in touch with advances in subjects bordering on his own.

A specially interesting feature of the *Bulletin* is the microfilm service. A microfilm is made of each article as it is abstracted and negative microfilm copies or prints from microfilm can be purchased from the editors.

The subscription rates for Great Britain are 4,000 frs. (£5) per annum for each part. Subscriptions can also be taken out to individual sections of the *Bulletin* as follows:

	frs.	
Pure and Applied Mathematics—Mathematics—Mechanics	550	14/6
Astronomy—Astrophysics—Geophysics .. .. .	700	18/-
General Physics—Thermodynamics—Heat—Optics—Elec- tricity and Magnetism .. .. .	900	22/6
Atomic Physics—Structure of Matter .. .. .	325	8/6
General Chemistry—Physical Chemistry .. .. .	325	8/6
Inorganic Chemistry—Organic Chemistry—Applied Chemistry—Metallurgy .. .. .	1,800	45/-
Engineering Sciences .. .. .	1,200	30/-
Mineralogy—Petrography—Geology—Paleontology ..	550	14/6
Biochemistry—Biophysics—Pharmacology .. .. .	900	22/6
Microbiology—Virus and Phages .. .. .	600	15/6
Animal Biology—Genetics—Plant Biology .. .. .	1,800	45/-
Agriculture—Nutrition and the Food Industries ..	550	14/6

Subscriptions can be paid directly to the editors: Centre National de la Recherche Scientifique, 18, rue Pierre-Curie, Paris 5ème. (Compte-chèque-postal 2,500-42, Paris), or through Messrs. H. K. Lewis & Co. Ltd., 136, Gower Street, London W.C. 1.

PROCEEDINGS OF THE  
PHYSICAL SOCIETY

## ADVERTISEMENT RATES

The *Proceedings* are divided into two parts, A and B. The charge for insertion is £18 for a full page in either Section A or Section B, £30 for a full page for insertion of the same advertisement in both Sections. The corresponding charges for part pages are:

$\frac{1}{2}$ page	£9 5 0	£15 10 0
$\frac{1}{4}$ page	£4 15 0	£8 0 0
$\frac{1}{8}$ page	£2 10 0	£4 5 0

Discount is 20% for a series of six similar insertions and 10% for a series of three.

The printed area of the page is  $8\frac{1}{2}'' \times 5\frac{1}{2}''$ , and the screen number is 120.

Copy should be received at the Offices of the Physical Society six weeks before the date of publication of the *Proceedings*.

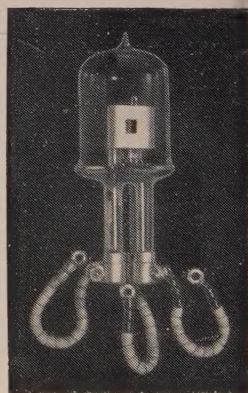
## VITREOSIL

(pure fused quartz)

## HYDROGEN

## DISCHARGE

## LAMPS



can be supplied with either circular hole source or slit source, as preferred, and the smaller size lamp can be inserted into Beckman Spectrophotometer housings without any extensions being necessary.

## Features:—

- Four patterns available.
- Provide a continuous spectrum from 3700 Å to 2100 Å.
- Have a useful operating life of about 500 hours.
- No water or other cooling arrangement necessary.
- Can be operated in any desired position.
- New filaments can be fitted and the quartz envelope can be repaired.

## THE THERMAL SYNDICATE LTD.

Head Office: Wallsend, Northumberland.

London Office: 12/14, Old Pye Street, Westminster, S.W.1.





## Infra - red Photo - conductive cells

### For Pyrometry, Spectroscopy, and the Detection of Radiant Heat

These lead sulphide cells are the fastest and most sensitive devices for the detection and measurement of infra-red radiation in the 1 to 3 micron wavelength

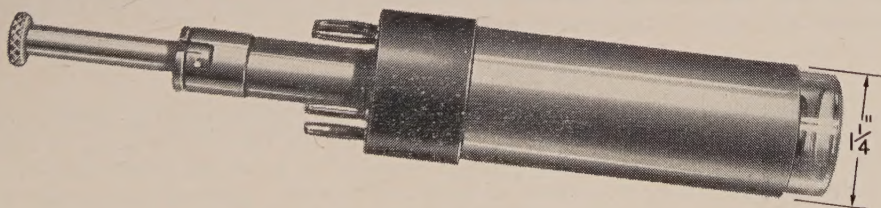
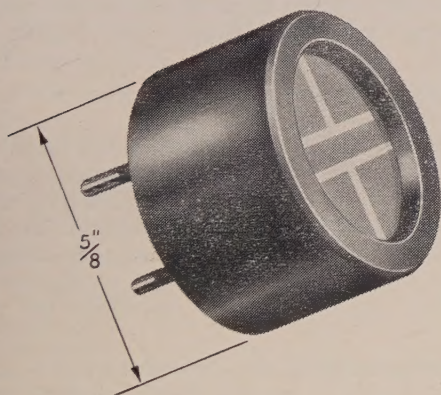
region of the spectrum. They are sensitive to source temperatures as low as 200°C, and they respond to temperature variations within 100 microseconds.

Left: Type "M", for detection and pyrometry, is of minimum dimensions and simple mechanical construction.

Below: Type "C.1", for detection and spectroscopy. This cell has provision for cooling by carbon dioxide, a feature which considerably increases its sensitivity.

Other BTH infra-red devices include: Nernst filaments (as infra-red sources), special infra-red transmitting glass, and semiconductor bolometers.

Full particulars on application.




---

**BRITISH THOMSON-HOUSTON**

THE BRITISH THOMSON-HOUSTON CO., LTD., RUGBY, ENGLAND

A 3984



# THE PHYSICAL SOCIETY

## NOTES ON THE PREPARATION OF PAPERS

The following instructions refer to the main points which have to be considered in the preparation of a paper for publication, and authors offering papers to the Physical Society for publication are asked to conform to these recommendations.

### MANUSCRIPTS

Manuscripts should be typed in *double* spacing on paper not wider than 8 in. and not longer than 13 in. Only one side of the paper should be used, and a margin of 1-1½ in. should be left. As alterations in the text cannot be allowed once the paper is set up in type, authors should aim at absolute clarity of meaning and of typing, and should check the typescript carefully before submission.

#### *Title and Sectional Headings.*

The title should be as concise as is compatible with lucidity. Papers are usually divided into sections beginning with §1. Introduction, and ending with § . Conclusion.

#### *Abstract.*

An abstract is printed at the beginning of the paper; it should state briefly the general aspects of the subject on which new information is presented and the main conclusions reached and final numerical results obtained. The abstract is placed immediately after the title, name(s) of author(s), and place of employment of author(s). The "title and abstract" page should be submitted in duplicate.

#### *Mathematics.*

It is not necessary to give detailed derivations of mathematical expressions and formulae in a published paper when the work is straightforward; it is quite sufficient to indicate the method of treatment and the final results. When interested readers are likely to find the argument difficult to follow, fuller treatment is called for. Extraordinary care should be taken with mathematical scripts, especially for expressions in the least complicated; legible long-hand is preferable to typing.

#### *References.*

In the text bibliographical references are made by giving the name of the author and the year of publication in brackets, e.g. (Jones 1942), and details are given in the last section, "References", where the references are arranged in alphabetical order of authors' names and in date order for each author.

### DRAWINGS

Drawings should be in Indian ink on tracing cloth, tracing paper or white card, with lettering in soft pencil. The drawings should in general be sufficiently large to allow of reduction in printing and the lines should therefore be bold; the frame lines of graphs should be slightly finer than those of the plotted curves. Essential photographs can be reproduced as plates, but they should be avoided when possible because of their expense. If authors are unable to submit drawings in the required form, arrangements can be made for these to be drawn and the cost price charged to the author. If the drawings are made on tracing cloth or paper, it is advisable to send a set of prints with the MS. so that the originals may not be handled unduly.

Full details are available in the Society's "Instructions to Authors", obtainable from the Secretary-Editor, The Physical Society, 1 Lowther Gardens, Prince Consort Road, London S.W. 7.



# THE PROCEEDINGS OF THE PHYSICAL SOCIETY

## Section B

VOL. 63, PART 1

1 January 1950

No. 361 B

## EDITORIAL

### PROCEEDINGS OF THE PHYSICAL SOCIETY SECTIONS A and B

In the light of experience gained over the course of the past year it is now possible to make a clearer statement of the basis on which division into the two Sections of the *Proceedings* is being made.

In general, it has been found that the division which best meets the needs of Fellows is one which brings papers on microphysics and the physics of elementary particles into the one Section, A, and papers on macroscopic physics into the other Section, B. While it is essential to maintain a certain amount of flexibility in the allocation of papers, a paper will, as far as possible, be put in the Section where the main interest lies, e.g. a paper on counter-technique would appear in B if the circuitry is the main interest, but would be in A if the applications to actual counting are of major importance.

A list indicating this subject division is given below.

A. C. STICKLAND,  
Secretary-Editor.

#### Section A

Thermodynamics  
Electrodynamics  
Statistical mechanics  
Quantum theory  
Nuclear physics  
Electron theory: metals, semiconductors, dielectrics  
Molecular and atomic structure  
Spectra of atoms and molecules over the whole frequency range

Physics of crystals (including luminescence as a means of investigating this)  
Photoconductivity  
Theory of solids, liquids and gases  
Magnetism (theoretical)  
Cosmic rays  
Low temperature physics  
Standards relevant to this Section

#### Section B

Thermal, magnetic, electrical, elastic, rheological and other mechanical properties of matter  
Hydrodynamics and aerodynamics  
Acoustics  
Metallography  
Geometrical optics, optical design and microscopy  
Interferometry, diffraction and classical physical optics generally  
Electric and electronic circuits  
Dielectrics and semiconductors: measurement and theory of measurement  
Electric discharges  
Electron optics  
Geophysics  
Radio  
Physics of the atmosphere and ionosphere  
Physics of the sensory processes

Colour physics  
Astrophysics and solar physics  
Applications of spectroscopy (e.g. chemical analysis, structure analysis)  
Analysis of crystal structure  
Radiography  
Luminescence  
Photoelectricity  
Thermoelectricity  
Piezoelectricity  
Photoconductivity  
Magnetic properties of materials (including methods of measurement)  
Production of low temperatures  
High pressure physics  
Vacuum physics  
Thermionic emission  
Standards relevant to this Section



# The Elastic Constants of a Solid containing Spherical Holes

By J. K. MACKENZIE \*

H. H. Wills Physical Laboratory, University of Bristol

*MS. received 4th August 1949*

**ABSTRACT.** The effective bulk and shear moduli are calculated by a self-consistent method due to Fröhlich and Sack. The bulk modulus  $k$  is determined by applying a hydrostatic pressure, and the shear modulus  $\mu$  by applying a simple homogeneous shear stress, to a large sphere. Each hole is surrounded by a spherical shell of real material, and the reaction of the rest of the material is estimated by replacing it by equivalent homogeneous material. For consistency, both the density and the displacement of the outer spherical boundary must be the same whether the hole and its surrounding shell are replaced by equivalent material or not. The effective elastic constants calculated from these conditions are

$$\begin{aligned} 1/k &= 1/k_0\rho + 3(1-\rho)/4\mu_0\rho + O[(1-\rho)^3], \\ (\mu_0 - \mu)/\mu_0 &= 5(1-\rho)(3k_0 + 4\mu_0)/(9k_0 + 8\mu_0) + O[(1-\rho)^2], \end{aligned}$$

where  $k_0$  and  $\mu_0$  refer to the real material and  $\rho$  is the density of the actual material relative to that of the real material; in the next approximation  $k$  depends on the standard deviation of the volumes of the holes.

The dilatation due to a distribution of pressures in the holes is  $\bar{p}(1/k - 1/k_0)$ , where  $\bar{p}$  is the mean obtained when the pressure in each hole has a weight proportional to the volume of the hole. By using the hydrodynamic analogue of the elastic problem, the theory is briefly applied to the theory of sintering, and used to discuss the effective viscosity of a liquid containing small air bubbles.

## §1. INTRODUCTION

WHILE developing a theory of sintering (Mackenzie and Shuttleworth 1949) it became necessary to calculate the compressibility of a solid containing spherical holes. In this paper all the holes were assumed to be of the same size and embedded in an incompressible medium. In this simple case it suffices to equate the stored elastic energy to the work done by the externally applied pressure in order to derive the effective compressibility. The original calculation, however, followed the lines of ordinary elasticity theory, and both the effective compressibility and the effective shear modulus were derived without assuming either holes of equal size or incompressibility of the real material. It is these calculations which are reported in the present paper. On the other hand, the present method can only be used when the relation between stress and strain is linear, while the energy method used in the paper on sintering is applicable when this relation is non-linear.

In §2 the problem is analysed in some detail and the self-consistent method of calculation is described. In §3 two problems are considered: (a) the calculation of the compressibility of a material full of small spherical holes of different sizes, and (b) the calculation of the dilatation due to different pressures acting in the holes; the shear modulus of a material full of small spherical holes is calculated in §4. Finally, in §5 the close similarity between the equations of hydrodynamics and elasticity is used to discuss briefly an application to the theory of sintering and to discuss the effective viscosity of a liquid containing small air bubbles.

The results of these calculations show that, to a good approximation, both the effective elastic moduli depend only on the relative density  $\rho$  and the elastic

\* Now at C.S.I.R.O., Division of Tribophysics, Melbourne, Australia.



constants of the real material; holes have a comparatively large effect on compressibility and only a small effect on the shear modulus. It may be conjectured that this is true in general no matter what the shape or size of the individual holes may be, provided of course that extremes are excluded. It is not clear how the numerical constants appearing in the results will depend on the particular shape of hole chosen for calculation, but it seems likely that the formulae obtained here will give the correct order of magnitude in most cases.

## § 2. THE METHOD OF CALCULATION

It will be assumed that the real material contains isolated spherical holes distributed at random throughout the volume of the material, and that the real material has homogeneous and isotropic elastic properties. It will also be assumed that the volume of all the holes is small compared with the total volume, and that the total volume contains a large number of holes. The calculation uses the notion of an equivalent homogeneous continuum introduced in the next paragraph.

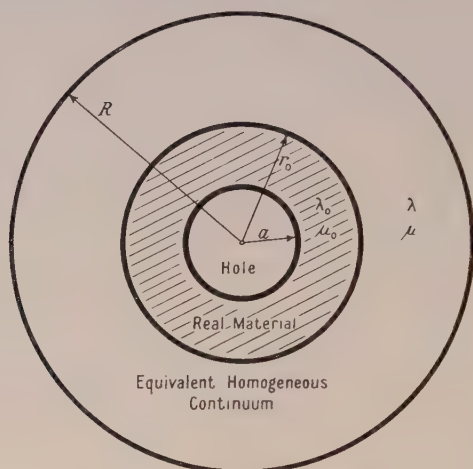
If attention is directed not to the detailed structure of the actual solid but to a volume element containing a large number of holes, then, because the distribution of the size of holes and of their position in space is statistically uniform, such a volume element can be regarded as forming part of a homogeneous isotropic continuum. The elastic constants of this equivalent homogeneous continuum will be calculated in terms of the elastic properties of the real material and the number and size distribution of the holes. When large volumes are concerned, the elastic properties of the actual solid will be independent of its external shape, and for simplicity it is convenient to choose this shape to be spherical. The effective elastic constants will be calculated by applying a stress to the outer spherical boundary and comparing the strains produced in the actual solid with the strains produced by the same stress in a homogeneous isotropic solid. A uniform hydrostatic pressure will be applied to determine the effective bulk modulus and a simple homogeneous shear stress (with no hydrostatic component) to calculate the effective shear modulus. The results obtained depend to some extent on the particular stress which is applied and, in general, the more complicated the stress the more the detailed structure of the actual solid will become apparent.

A convenient self-consistent method of calculation has been indicated by Fröhlich and Sack (1946). Their method is equivalent to a perturbation calculation, and is certainly valid when the volume of all the holes is sufficiently small compared with the total volume. The method depends on the fact that any macroscopic volume (i.e. one containing a large number of holes) can be replaced by equivalent homogeneous material without essentially changing the elastic behaviour of the solid. This is so because the mean stresses and displacements at the boundary of the volume are equal to those at the boundary of the same volume in the equivalent elastic continuum. The conditions for consistency, namely that the density and the displacement of the outer boundary shall be unchanged by such replacement, enable the effective elastic constants to be calculated. The particular method of calculation adopted is described in detail in the next paragraph.

Since the holes are isolated, every hole of radius  $a$  will be surrounded by a spherical shell of real material out to at least some radius  $r_0$  (see Figure), and this may be regarded as a typical volume element of the actual solid. The model used for the calculation of the effective elastic constants is then as follows. A hole of radius  $a$  is surrounded by a spherical shell of real material out to radius  $r_0$ , and this



in turn is surrounded by a spherical shell of equivalent homogeneous material (whose elastic constants are as yet unknown) out to some large radius  $R$ . A particular stress is applied to this outer spherical boundary and the displacements of the outer surface calculated; this displacement is then weighted according to the frequency of occurrence of holes of radius  $a$  and averaged over the size distribution of the holes. Finally, the resulting mean displacement is equated to the displacement which would have resulted had the sphere of radius  $R$  been completely filled with equivalent homogeneous material. Thus, one of the consistency conditions is satisfied and an equation for the effective elastic constants derived.



The model used for calculation.

The other condition determines  $r_0$ , since the density of a hole and its surrounding shell must be the same as that of the actual material. If  $f(a)da$  is the proportion of holes with radii lying in the range  $(a, a + da)$  then the volume of holes per unit volume of the real material is

$$\frac{1-\rho}{\rho} = \frac{4}{3}\pi n \int f(a)a^3 da = \frac{1}{\rho r_0^3} \int f(a)a^3 da, \quad \dots\dots(1)$$

where the integration is over the whole of the relevant range of  $a$ ,  $\rho$  is the relative density, and  $n$  is the number of holes per unit volume of the real material. Note that  $\int f(a) da = 1$ .

In general, when part of a solid is replaced by material of different elastic constants there is an additional term in the displacement of the outer boundary of the order of the ratio of the volume replaced to the total volume. If, however, the elastic constants of the new material are the same as the effective constants of the original material this term will disappear. In fact, the consistency condition will be expressed by equating this term of order  $r_0^3/R^3$  to zero. In addition, there will usually be terms of higher order which arise because the boundary conditions are never met exactly when part of the actual solid is replaced by equivalent continuum, but only on the average. These terms will be neglected.

In the following sections the method outlined above will be applied to the calculation of the bulk and shear moduli of a material containing small spherical holes.



## § 3. THE COMPRESSIBILITY

Two problems will be considered in this section: (a) the calculation of the compressibility of a material containing small spherical holes of different sizes, and (b) the calculation of the dilatation due to a distribution of pressures inside the holes; these pressures may be due to included gas or to surface tension in the boundary of the hole. The compressibility will be calculated by applying a hydrostatic pressure  $P$  to the outer spherical boundary and using the method described in the last section. The same model is also applicable when a pressure  $p$  is applied inside the central hole with zero pressure in all the other holes; in this case, the approximation consists in estimating the reaction of the part of the actual solid which lies outside a sphere of radius  $r_0$  by replacing it by equivalent homogeneous material. When there are pressures in all the holes the total displacement is found by adding the displacements due to each hole individually.

The detailed calculations fall naturally into three parts. In § 3 (i) the general equations for the elastic displacements will be written down, while in the two following sub-sections the effect of an externally and an internally applied pressure will be considered in turn. However, before proceeding it is convenient to show how the second problem may be reduced to the first.

Consider first the case where the pressure  $p$  is the same in every hole and there is no externally applied pressure. If an additional hydrostatic pressure  $-p$  is applied to the surfaces of all the holes and to the external surface, then the resultant pressure is zero in all the holes and  $-p$  on the external surface. Now when a hydrostatic pressure is applied to all the boundaries of a homogeneous elastic material the stress at all points inside the material is a hydrostatic pressure equal to that applied (Love 1944, p. 86). Hence, the displacements due to the extra hydrostatic pressure  $-p$  can readily be estimated by filling up all the holes with real material and applying the pressure  $-p$  to the outer boundary. (A comparison of the two situations shows that all the boundary conditions are met.) Thus the total dilatation is  $p(1/k - 1/k_0)$ , and the additional term is zero if the material is incompressible.

On the other hand, if the pressure is not the same in all the holes, then a fixed part of this pressure can be transferred to the outer boundary as explained in the last paragraph, and the effect of the pressures remaining in the holes estimated separately. If these remaining pressures produce no total dilatation they may be neglected. Now the displacement of the outer boundary when only one particular hole has a pressure in it is proportional to the pressure in the hole and to its volume. Therefore, if the pressure in each hole is given a weight proportional to the volume of the hole, then when the mean pressure so calculated is transferred to the outside the remaining distribution of pressures will produce no displacement of the external boundary. This statement will be verified in § 3 (iii).

(i) *General Elastic Equations*

First a word about notation. Symbols with subscript zero refer to the real material or to the intermediate boundary, while the same symbol without a subscript usually denotes the corresponding magnitude for the equivalent homogeneous continuum. Thus  $\lambda$  and  $\mu$  are the effective elastic constants which are to be calculated, while  $\lambda_0$  and  $\mu_0$  are the same constants for the real material; the constant  $\mu$  is the rigidity and the bulk modulus  $k = \lambda + \frac{2}{3}\mu$ .



It is required to find the displacements in the composite body illustrated in the Figure when hydrostatic pressures are applied to both boundaries. On account of the spherical symmetry, the displacements will be purely radial and given by (Love 1944, p. 142)

$$u = Ar + B/r^2,$$

while the normal pressure acting across the spherical boundary at the same radius is

$$(\lambda + 2\mu) \frac{\partial u}{\partial r} + 2\lambda \frac{u}{r}.$$

Then, using Love's results for a thick spherical shell, the radial displacement in the outer shell of equivalent homogeneous material is

$$u = \frac{r}{3k} \frac{p_0 r_0^3 - PR^3}{R^3 - r_0^3} + \frac{R^3 r_0^3}{4\mu r^2} \frac{p_0 - P}{R^3 - r_0^3},$$

and the radial displacement in the inner shell of real material is

$$u = \frac{r}{3k_0} \frac{pa^3 - p_0 r_0^3}{r_0^3 - a^3} + \frac{a^3 r_0^3}{4\mu_0 r^2} \frac{p - p_0}{r_0^3 - a^3},$$

where  $p$  is the pressure inside the hole (all other holes at zero pressure) and  $P$  is the externally applied pressure.

The pressure  $p_0$  at the intermediate boundary is determined by the boundary condition that requires the radial displacement to be continuous across this boundary. This condition gives, neglecting  $r_0^3/R^3$  and higher powers,

$$p_0 \left[ \frac{1}{4\mu} + \frac{1}{3k_0} \frac{r_0^3}{r_0^3 - a^3} + \frac{1}{4\mu_0} \frac{a^3}{r_0^3 - a^3} \right] = P \left[ \frac{1}{3k} + \frac{1}{4\mu} \right] + p \left[ \frac{1}{3k_0} + \frac{1}{4\mu_0} \right] \frac{a^3}{r_0^3 - a^3}. \quad \dots (2)$$

This equation for  $p_0$ , together with the expression for the displacement of the external boundary, namely

$$\frac{u}{R} = -\frac{P}{3k} + (p_0 - P) \left[ \frac{1}{3k} + \frac{1}{4\mu} \right] \frac{r_0^3}{R^3 - r_0^3}, \quad \dots (3)$$

completely determines the external change of volume. The detailed solution of the two problems can now be obtained quite simply.

### (ii) Pressure applied Externally

In this sub-section the effective compressibility  $k$  is determined when there are no pressures in the holes. When a pressure  $P$  is applied to the external surface, the resulting displacement of the external boundary due to holes of some particular radius  $a$  is given by equation (3). Averaging this displacement over the size distribution of the holes and equating the resulting mean displacement to the displacement of the external boundary when a pressure  $P$  is applied to a solid sphere of the equivalent homogeneous material, viz.  $-PR/3k$ , as required by the consistency condition, it follows that

$$P = \int p_0 f(a) da, \quad \dots (4)$$



where  $p_0$  is given by equation (2) and  $\int f(a) da = 1$ . If the holes are all the same size,  $p_0 = P$ , and (7) (with  $\sigma = 0$ ) follows from (2) immediately.

On putting  $p = 0$  into equation (2) and expanding in powers of  $a^3/r_0^3$ ,

$$\frac{p_0}{P} = \frac{1 + 4\mu}{1 + 4\mu/3k_0} \left[ 1 - \frac{a^3}{r_0^3} + \frac{(\mu_0 - \mu)/\mu_0}{1 + 4\mu/3k_0} \left\{ \frac{a^3}{r_0^3} - \frac{a^6}{r_0^6} \right\} + \dots \right].$$

Now it will be shown in § 4 that

$$(\mu_0 - \mu)/\mu_0 = \kappa(1 - \rho), \quad \dots\dots(5)$$

where  $\kappa$  depends only on  $k_0$  and  $\mu_0$  and is given by equation (20). Put

$$\int \frac{a^3}{r_0^3} f(a) da = 1 - \rho \quad \dots\dots(1)$$

and

$$\int \frac{a^6}{r_0^6} f(a) da = \sigma^2 + (1 - \rho)^2, \quad \dots\dots(6)$$

where  $4\pi\sigma r_0^3/3$  is the standard deviation of the volumes of the holes. Then it follows from (4), after some reduction, that

$$\frac{1}{k} = \frac{1}{k_0\rho} + \frac{3}{4\mu_0} \frac{1 - \rho}{\rho} (1 + \kappa\sigma^2). \quad \dots\dots(7)$$

This equation gives the effective compressibility up to and including terms of order  $(1 - \rho)^3$ . The value of  $\kappa$  is always about 2. It should be noted that a few holes in an otherwise incompressible medium can give rise to an appreciable finite compressibility.

It is not altogether certain that the model is adequate for the calculation of a third approximation to  $k$ . It is clear, however, that the effect of a distribution in the sizes of the holes is small, and that to a good approximation the effective compressibility depends only on  $\rho$  and the elastic constants of the real material. In fact, (7) gives the correct behaviour for the effective compressibility in the extreme cases as the density tends to unity or to zero. Thus it is plausible that this equation should be roughly correct for all relative densities.

### (iii) Pressure applied Internally

In this sub-section the effect of a distribution of pressures inside the holes is considered. If there are different pressures in holes of the same size it is clear that their effect is the same as the mean pressure  $\bar{p}$  acting in all of them. When a pressure  $p$  is applied in only one hole, equation (3), with  $P = 0$ , gives the resulting displacement of the external boundary. Then, on multiplying by the number of holes,  $R^3/r_0^3$ , and averaging over the size distribution, the mean displacement of the external surface is (neglecting  $r_0^3/R^3$  compared with unity)

$$u = R \left[ \frac{1}{3k} + \frac{1}{4\mu} \right] \int p_0 f(a) da = \bar{p} R \left[ \frac{1}{3k} - \frac{1}{3k_0} \right], \quad \dots\dots(8)$$

where  $\bar{p}$  is the mean pressure which is transferred to the external surface, and the last part of the equation follows from the discussion at the end of the introductory part of § 3. The last equation in (8) determines the mean effective pressure  $\bar{p}$ , which will now be calculated.



On putting  $P=0$  into equation (2), substituting the value of  $p_0$  into (8), and expanding in powers of  $a^3/r_0^3$ , it follows that

$$\bar{p} = \frac{1/3k_0 + 1/4\mu_0}{1/3k - 1/3k_0} \frac{1 + 4\mu/3k}{1 + 4\mu/3k_0} \int p \frac{a^3}{r_0^3} \left[ 1 + \frac{(\mu_0 - \mu)/\mu_0}{1 + 4\mu/3k_0} \frac{a^3}{r_0^3} \right] f(a) da.$$

Then, substituting for  $k$  from (7) and replacing  $p$  by  $\bar{p}$  when evaluating the correction term in the integral, it follows, after some reduction, that

$$\bar{p} = \frac{1}{a_0^3} \int p a^3 f(a) da, \quad \dots\dots(9)$$

where  $a_0^3 = (1 - \rho)r_0^3$ , or  $4\pi a_0^3/3$  is the mean volume of the holes. Although this expression is correct up to and including terms of order  $(1 - \rho)^3$ , it is not clear what error has been committed in replacing  $p$  by  $\bar{p}$  in the small correction term. Equation (9) justifies the statement made at the very end of the introductory part of §3.

Finally, returning to equation (8), it is clear that the dilatation caused by a distribution of pressures in the holes is  $\bar{p}/k'$ , where  $\bar{p}$  is given by (9) and

$$\frac{1}{k'} = \frac{1}{k} - \frac{1}{k_0} = \frac{1 - \rho}{\rho} \left[ \frac{1}{k_0} + \frac{3}{4\mu_0} (1 + \kappa\sigma^2) \right]. \quad \dots\dots(10)$$

#### §4. THE SHEAR MODULUS

The effective shear modulus will now be calculated by applying a simple type of homogeneous shear stress and calculating the resulting displacements of the external boundary both for the composite solid shown in the Figure and for a sphere of equivalent homogeneous material. As before, comparison of the two solutions gives an equation from which the effective shear modulus can be calculated.

Now the displacements which result from all the simple types of homogeneous shearing stress can be derived from solid spherical harmonics of degree two. Such a solid harmonic is of the form  $r^2 S_2$ , where  $S_2$  is a surface harmonic of degree two and determines the symmetry of the displacements; the solid harmonic  $r^{-3} S_2$  also has the same symmetry, and will therefore be expected to occur in the general solution.

The solution of the elastic equations, which is derived from the solid harmonic  $r^2 S_2$ , and for which the dilatation and the rotation are everywhere zero, is (Love 1944, p. 250)

$$\mathbf{u} = \text{grad}(r^2 S_2) = 2r S_2 \mathbf{r} + r S_2' \boldsymbol{\tau}, \quad \dots\dots(11)$$

and the corresponding stress across a spherical boundary at the same radius is

$$\mathbf{F} = 2\mu r^{-1} \text{grad}(r^2 S_2) = 4\mu S_2 \mathbf{r} + 2\mu S_2' \boldsymbol{\tau}, \quad \dots\dots(12)$$

where  $\mathbf{r}$  and  $\boldsymbol{\tau}$  are unit vectors normal and tangential to the spherical boundary and  $S_2'$  is independent of  $r$ . This solution gives the displacements when a shearing stress  $\mathbf{F}$ , which is the same at all points, is applied to a solid homogeneous sphere. This stress will now be applied to the composite solid and the resulting displacements calculated.

There are four independent solutions of the elastic equations which can be derived from solid harmonics with the same symmetry as  $S_2$ , and for which the rotation is everywhere zero. Writing

$$p S_2 \mathbf{r} + q S_2' \boldsymbol{\tau} = \{p, q\}, \quad \dots\dots(13)$$

these solutions are (Love 1944, p. 250):

$$\left. \begin{aligned} \mathbf{u}_1 &= \text{grad}(r^2 S_2) &= \{2, 1\}r, \\ \mathbf{u}_2 &= \text{grad}(r^{-3} S_2) &= \{-3, 1\}/r^4, \\ \mathbf{u}_3 &= r^2 \text{grad}(r^2 S_2) + \alpha_2 r^3 S_2 \mathbf{r} &= \left\{ \frac{6\lambda}{5\lambda + 7\mu}, 1 \right\} r^3, \\ \mathbf{u}_4 &= r^2 \text{grad}(r^{-3} S_2) + \alpha_{-3} r^{-2} S_2 \mathbf{r} &= \left\{ \frac{3\lambda + 5\mu}{\mu}, 1 \right\} / r^2; \end{aligned} \right\} \dots\dots (14)$$

the corresponding stresses acting across a spherical surface of radius  $r$  are, respectively,

$$\left. \begin{aligned} \mathbf{F}_1/\mu &= \{4, 2\}, \\ \mathbf{F}_2/\mu &= \{24, -8\}/r^5, \\ \mathbf{F}_3/\mu &= \left\{ \frac{-6\lambda}{5\lambda + 7\mu}, \frac{16\lambda + 14\mu}{5\lambda + 7\mu} \right\} r^2, \\ \mathbf{F}_4/\mu &= \left\{ -\frac{18\lambda + 20\mu}{\mu}, \frac{3\lambda + 2\mu}{\mu} \right\} / r^3. \end{aligned} \right\} \dots\dots (15)$$

Thus the general solution of the elastic equations in a thick spherical shell will be of the form

$$\mathbf{u} = A\mathbf{u}_1 + B\mathbf{u}_2 + C\mathbf{u}_3 + D\mathbf{u}_4. \quad \dots\dots (16)$$

This solution will apply as it stands in the outer shell containing equivalent homogeneous material; the corresponding solution for the inner shell containing the real material is derived simply by putting a subscript zero on all the constants. The whole solution then involves eight arbitrary constants which are determined by eight equations arising from the boundary conditions; two equations have to be satisfied for each of four boundary conditions.

The four boundary conditions are: (a) that the stress across the external boundary is  $\mu\{4, 2\}$ , (b) that the displacements are continuous across the intermediate boundary, (c) that the stress is continuous across the intermediate boundary, and (d) that the innermost boundary is stress-free. Using equations (14), (15) and (16), these boundary conditions lead to a set of equations whose formal solution can be written down immediately in a form involving eighth-order determinants. The solution can then be expanded quite simply in powers of  $r_0/R$ , and the result of doing this is

$$\left. \begin{aligned} A - 1 &= K_1 \frac{\Delta_2}{\Delta_1} \frac{r_0^3}{R^3}, & B/R^5 &= 0, \\ CR^2 &= K_2 \frac{\Delta_2}{\Delta_1} \frac{r_0^3}{R^3}, & D &= \frac{\Delta_2}{\Delta_1} \frac{r_0^3}{R^3}, \end{aligned} \right\} \dots\dots (17)$$

where powers of  $r_0/R$  higher than the third have been neglected,  $\Delta_1$  and  $\Delta_2$  are certain determinants of the sixth order, and  $K_1, K_2$  involve only  $\lambda$  and  $\mu$ . It is clear from this solution that the additional terms in the displacement due to the presence of the hole and its surrounding shell are of order  $r_0^3/R^3$ , as was stated at the end of § 2.



Substituting the values of the constants into (16), integrating over the size distribution, and comparing the results with the displacement given by equation (11), it follows that the condition for consistency is

$$\int_{\Delta_1}^{\Delta_2} f(a) da = 0. \quad \dots\dots(18)$$

Finally, expanding  $\Delta_1$  and  $\Delta_2$  in powers of  $a/r_0$ , and neglecting powers higher than the third in the quotient  $\Delta_2/\Delta_1$ , it follows that

$$\frac{\mu_0 - \mu}{\mu_0} = 5 \frac{3k_0 + 4\mu_0}{9k_0 + 8\mu_0} (1 - \rho). \quad \dots\dots(19)$$

This equation gives the fractional decrease in the modulus of rigidity due to the presence of the holes. The value of the constant  $\kappa$  introduced in equation (5) is

$$\kappa = 5 \frac{3k_0 + 4\mu_0}{9k_0 + 8\mu_0}. \quad \dots\dots(20)$$

### § 5. APPLICATIONS

The application of the results of the preceding calculations to determining the effective elastic constants of materials containing a large number of small holes is obvious and will not be discussed further. There is, however, a close similarity between the equations of elasticity and those of hydrodynamics (Goodier 1936), and it is the results which can be deduced from this similarity which will be briefly discussed in the following paragraphs.

If, in the hydrodynamic equations for slow steady motion (so that  $D_t Dt = 0$ ), the velocity  $\mathbf{v}$  is replaced by the displacement  $\mathbf{u}$ , the viscosity  $\eta$  by the rigidity  $\mu$ , and  $-p$  by  $k \operatorname{div} \mathbf{u}$ , then the equations of elasticity are obtained, and vice versa. Thus, by means of the above scheme of replacement, the velocities in a slow and steady viscous motion due to some system of stresses can be derived immediately from the elastic displacements resulting from the same stresses in the corresponding elastic problem. When making this transfer the bulk modulus will usually be taken as infinite because, although the shearing viscosity of a liquid is finite, the 'volume viscosity' (which is the analogue of  $k$ ) is usually considered to be infinite, i.e. there is no energy dissipated during a pure compression or expansion.

In the theory of sintering mentioned in the introduction, it was necessary to calculate the rate of increase of density of a compact consisting of spherical holes in an incompressible medium when a negative pressure  $-2\gamma/a$  due to surface tension acts in all the holes. In the case of glass the action of these pressures is resisted by viscous forces, and when this is so the resulting flow may be derived from the results of § 3 (iii) by means of the above substitution. Thus the rate of increase of density is

$$\frac{d\rho}{dt} = - \frac{\rho \bar{p}}{k'}, \quad \dots\dots(21)$$

where  $\bar{p}$  is given by equation (9) as

$$\left. \begin{aligned} \bar{p} &= - \frac{2\gamma}{a_0^3} \int a^2 f(a) da \\ &= - \frac{2}{3} \gamma \frac{\text{mean surface area of holes}}{\text{mean volume of holes}} \end{aligned} \right\} \quad \dots\dots(22)$$

If all the holes are of the same size, then using (10) with  $k_0 = \infty$  to determine  $k'$ ,

$$\frac{d\rho}{dt} = \frac{3}{2} \left( \frac{4\pi}{3} \right)^{\frac{1}{3}} \frac{\gamma n^{\frac{1}{3}}}{\eta} (1-\rho)^{\frac{2}{3}} \rho^{\frac{1}{3}}, \quad \dots\dots(23)$$

a formula previously derived in another way;  $n$  is the number of holes per unit volume of the real material.

Again, consider a liquid which contains a large number of small bubbles containing gas. These bubbles will be of such a size that the gas pressure is equal to the hydrostatic pressure in the liquid plus the pressure  $2\gamma/a$  due to surface tension. Now provided the liquid is sheared slowly and the bubbles retain approximately their spherical form, the analogue of equation (19) gives the fractional decrease in the viscosity due to the presence of the bubbles as

$$\frac{\eta_0 - \eta}{\eta_0} = \frac{5}{3} \alpha, \quad \dots\dots(24)$$

where  $\alpha$  is the fraction of the total volume which is occupied by the bubbles. This expression assumes that the bubbles deform freely during the motion so that, unless the motion is oscillatory, the bubbles will not remain spherical for long. In practice, both the gas pressure and the surface tension will tend to maintain the shape of the bubble approximately spherical and equation (24) will not apply. Taylor (1932) has shown that the presence of liquid spheres which remain spherical during the motion raises the effective viscosity rather than lowers it. If the viscosity of the liquid in the spheres is  $\eta'$ , Taylor shows that

$$-\frac{\eta_0 - \eta}{\eta_0} = \frac{5}{2} \frac{\eta' + 2\eta_0/5}{\eta' + \eta_0} \alpha. \quad \dots\dots(25)$$

When the spheres are rigid,  $\eta' = \infty$ , and this reduces to Einstein's result (1906, 1911), and when  $\eta' = 0$ ,

$$-\frac{\eta_0 - \eta}{\eta_0} = \alpha,$$

a result also obtained by Eizenschitz (1933) for the case where the liquid slips freely over the surface of a rigid sphere. It is clear therefore that boundary conditions assumed at the surface of the bubble play an important part in the results which are obtained.

#### ACKNOWLEDGMENT

The author wishes to thank Dr. R. Shuttleworth for a great deal of helpful discussion during the preparation of this paper.

#### REFERENCES

- EINSTEIN, A., 1906, *Ann. Phys., Lpz.*, **19**, 289 ; 1911, *Ibid.*, **34**, 591.  
 EISENSCHITZ, R., 1933, *Phys. Z.*, **34**, 411.  
 FRÖHLICH, H., and SACK, R., 1946, *Proc. Roy. Soc. A*, **185**, 415.  
 GOODIER, J. N., 1936, *Phil. Mag.*, **22**, 678.  
 LOVE, A. E. H., 1944, *Theory of Elasticity*, 4th edn. (New York : Dover).  
 MACKENZIE, J. K., and SHUTTLEWORTH, R., 1949, *Proc. Phys. Soc. B*, **62**, 833.  
 TAYLOR, G. I., 1932, *Proc. Roy. Soc. A*, **138**, 41.



# On Movements of Small Ferromagnetic Particles in Inhomogeneous Magnetic Fields

By FRIEDRICH BLAHA

Institute of Physics, University of Vienna

*Communicated by T. G. Hodgkinson ; MS. received 30th June 1949*

**ABSTRACT.** Ferromagnetic particles of diameter from  $10^{-3}$  to  $10^{-5}$  cm. when exposed to light move along the lines of force of an inhomogeneous magnetic field. It does not seem possible to explain the movement when only dipole properties of the particles are taken into account. Field strengths of  $10^{-2}$  gauss are sufficient to cause distinct movement. The motions resemble those of electrically charged particles in electric fields.

## § 1. INTRODUCTION

**S**MALL particles of iron powder show, when exposed to light in homogeneous magnetic fields, polar motions which are reversible with reversal of the field (magnetophotophoresis (Ehrenhaft 1930)). Since then many kinds of various substances have been found to show this behaviour. In continuation of researches on the phenomenon the following observations were carried out in simply formed, typical inhomogeneous fields. The method described for producing the particles is one of the most convenient and effective.

## § 2. EXPERIMENT

An electric arc between two iron electrodes in oxygen or air produces a sort of smoke consisting mainly of small particles of ferric oxide. Such particles of  $10^{-3}$  to  $10^{-5}$  cm. in diameter were collected in a small observation chamber which was surrounded by a small rectangular loop (3 mm.  $\times$  10 mm.) of thin copper wire (see Figure 1). The chamber was specially constructed to allow of illumination and observation near the wire. The particles were observed in a dark field by means of a microscope (magnification 30 to 100 times), the axis of which was parallel to the plane of the above-mentioned loop. The assembly consisting of chamber, microscope and surroundings was iron-free and the geomagnetic field was compensated over the region of observation.

## § 3. OBSERVATIONS

Under the conditions of the experiment most of the particles appear as diffraction discs, others have the form of short, often crooked, threads. They all fall uniformly in the resisting medium (air) with a Brownian movement superimposed. In very few cases is common photophoresis (positive or negative) visible.

As soon as a direct current flows through the wire of the loop (for instance 0.2 amp.), forming an inhomogeneous magnetic field in the cell, 10 to 20% of the particles visible as discs start moving along the magnetic lines of force, some in, some against, the direction of the magnetic field. They pass the plane of the loop unhindered. When the direction of the current is reversed, these particles instantaneously reverse their direction of motion. They stop immediately the current is cut off. The other particles, so far as they appear as discs, do not show any reaction to the weak magnetic field applied.

All the particles shaped like short threads behave like tiny compass needles: pointing in the direction of the acting magnetic field they turn through  $180^\circ$  when the field is reversed. Among these particles also, some show the above described phenomenon, that is to say they move along the magnetic lines of force



Figure 3. Time of exposure 10 sec.  
Magnification 40 times.



Figure 4. Time of exposure 2 sec.  
Total magnification 120 times.



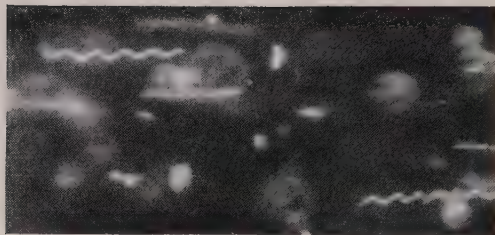


Figure 5. Time of exposure 0.4 sec.  
Magnification 80 times. Sunlight.

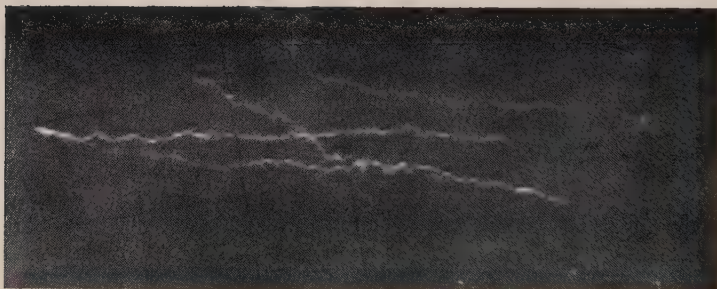


Figure 6. Time of exposure 13 sec.  
Magnification 80 times.

and pass the plane of the loop unhindered; reversal of the magnetic field causes a turn through  $180^\circ$  and reversal of the translatory movement.

Taking into account only dipole properties, from a theoretical point of view the particles should move from the right and the left towards the plane of the loop and the wire (provided that the gradient of the field is sufficient) without reversing their translatory movement.

The apparatus as above described did not permit the use of higher values of the inhomogeneous magnetic field. For this purpose the loop was replaced by a coil with iron core adjusted outside of the cell as shown in Figure 2. Small field strength (for example the remanent magnetism of the iron core) then caused movements analogous to those already described.

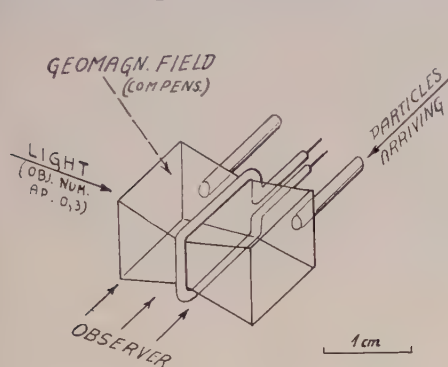


Figure 1.

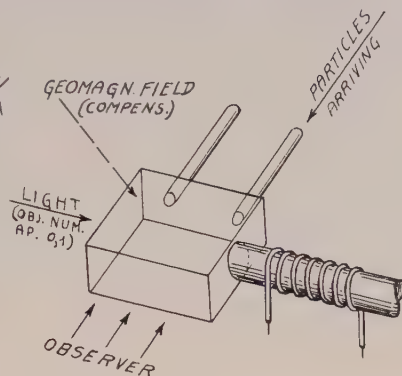


Figure 2.

When now the magnetic field strength was gradually increased, the different kinds of particles were affected in the following way:

(i) All particles which showed no translatory movement at first began gradually (from about 20 gauss/cm.) to move towards the denser lines of force (i.e. towards the magnet).

(ii) Those particles which were at first attracted by the magnet continued to move in this direction at an increasing velocity.

(iii) Those particles which were at first repelled by the magnet gradually decreased their velocity, came to a standstill, and finally also moved towards the magnet with gradually increasing velocity.

The same results can be achieved by steadily approaching a small permanent bar magnet to the cell instead of using a coil with iron core and increasing the current as described above.

#### § 4. TRACKS OF PARTICLES

Figure 3 is a general view showing tracks of some particles (the plane of the loop is vertical in the middle of the photograph). It is remarkable that the tracks often appear as dotted lines, which are in some cases enlarged to helix-like paths; this is illustrated by Figure 4, which shows the track of a single particle, and by Figure 5. Examination by means of a stereo-microscope proved these motions to be essentially rotatory, and not a sort of fluttering due to translatory motion.

Figure 6 shows for example the movements of a particle while the direction of the current in the loop was twice reversed. (Another particle showing only common photophoresis crossed the tracks of the first-mentioned particle.)



## § 5. FURTHER OBSERVATIONS

Ionization of the air in the cell by means of  $\gamma$ -rays did not influence the effect in any visible manner. Common radiometer forces play apparently only a small part in these movements, because the effect of common photophoresis was found to be only about 5 to 10% of the whole.

With care the same particle could be observed over a long period (half an hour and more), in course of which it did not lose the described property. Thus the explanation of the effect by assuming a jet-like emission of occluded gases caused by the impinging radiation, or as the result of a chemical action, cannot be accepted. Moreover, the velocity of the particles (in the direction of the magnetic field) is not constant, but increases with increase of field strength (up to about 120 gauss).

On an average the sensitivity of the particles in question is such that the method can be used for determining direction and intensity of weak magnetic fields (e.g. the geomagnetic one) when an accuracy of only  $\pm 0.03$  gauss is required.

## § 6. CONCLUSION

The described behaviour of the particles reminds one of equivalent experimental results, when electrically charged particles in inhomogeneous electric fields are observed, where the movements are described by the well-known equation

$$P = eE + f(\epsilon, K) \cdot \text{grad}(E^2), \quad \dots\dots(1)$$

in which  $P$  is the force acting on the particle,  $e$  the electric charge,  $E$  the electric field strength, and  $f$  a function of the dielectric constant  $\epsilon$  and the shape  $K$  of the particle. (Conductivity is neglected.)

Analogy suggests a trial of the equation

$$P = qH + f(\mu, K) \cdot \text{grad}(H^2), \quad \dots\dots(2)$$

where  $H$  is the magnetic field strength and  $\mu$  the magnetic permeability, but the coefficient of proportion  $q$  turns out to be a function of  $H$ , of intensity and composition of light. In addition to this a remanent dipole momentum has to be taken into account in (2), when ferromagnetic substances are used.

It is difficult to calculate values for  $q$ , because the shape of the particles (which can scarcely be assumed spherical as electron-optical photographs show) modifies Stokes' Law in a rather uncalculable manner. The values of  $q$  are approximately  $10^{-9}$  (c.g.s.) and smaller, under the above-described circumstances. The effect is not restricted to irregularly shaped particles; it was found to be of the same order of magnitude with iron powder (precipitated from carbonyl iron), the particles of which consist of spheres.

## ACKNOWLEDGMENT

I wish to thank Prof. Ehrenhaft for many discussions and stimulating suggestions. I am indebted to Mr. T. G. Hodgkinson for his advice and interest in this work.

## REFERENCES

- BEISCHER, F., 1939, *Z. Elektrochem.*, **45**, 310.  
 EHRENHAF, F., 1930, *C.R. Acad. Sci., Paris*, **190**, 263 ; 1942, *J. Franklin Inst.*, **233**, 235 ;  
 1947, *J. Phys. Radium*, **8**, 55 ; 1948, *C.R. Acad. Sci., Paris*, **225**, 926.  
 MAHL, H., 1940, *Z. techn. Phys.*, **21**, 17.  
 SCHEDLING, J. A., 1949, *Phys. Rev.*, **76**, 843.

# Dead Times of Self-Quenching Counters

By B. COLLINGE

George Holt Physics Laboratories, The University, Liverpool

*Communicated by J. Rotblat ; MS. received 30th May 1949*

**ABSTRACT.** Experiments on Geiger counters are described in which localization of the ion sheath was brought about by reducing the wire potential immediately after each count. The effect on the dead time is discussed. The dead time of a counter 30 cm. long was found to be 20  $\mu$ sec. and independent of the counting rate up to  $1.8 \times 10^6$  counts per minute. The reduction of the dead time of short counters was also investigated.

## § 1. INTRODUCTION

It is an inherent property of the Geiger counter that each discharge is followed by an insensitive period or 'dead time', which may be of several hundred microseconds duration. This has been defined as "the time interval, after recording a count, . . . (during which) the counter is completely insensitive and does not detect other ionizing events occurring inside it" (Korff 1946). Counts occurring during this period are missed and the registered counting rate must be corrected for their loss. The form of this correction is uncertain; Blackman and Michiels (1948) quote three different formulae for the correction factor and show theoretically that only one of them is valid under normal conditions. Further difficulties are introduced by the dependence of the dead time on the operating conditions, which may include the counting rate.

One way of evading these difficulties is to work with such low counting rates that uncertainties in the correction to be applied may be neglected. Hence for 10% losses the counting rate must be limited to  $10^4$  counts per minute, if the paralysis time of the recording equipment is 600  $\mu$ sec. At higher counting rates the difficulty of applying an accurate correction increases rapidly. An empirical method of obtaining the true counting rate, when the dead time varies with it, has been described by Kohman (1945). This method is, however, rather laborious.

Another expedient is the addition to the recording equipment of an electronically determined paralysis time, much longer than the dead time of the counter. The purpose of the paralysis time is to reduce spurious counts and eliminate variations in the counter dead time. However, this does not solve the problem because the effective dead time is still not constant. This is so because a subsequent discharge of the counter, during the paralysis time, may prolong it by as much as the dead time.

For many experiments the upper limit set to the counting rate by these considerations is too low. It would be desirable, therefore, to obtain an improvement, either by reducing the dead time, or by ensuring its constancy. Thus, reducing the dead time would allow higher counting rates to be used for a given percentage of losses, while with a constant dead time larger corrections for losses could be safely applied. It would, of course, be most desirable to improve both factors.

The dead time may be made constant by the use of a circuit which lowers the wire potential below the threshold of the Geiger region for a few hundred microseconds immediately after each count. The counter is then truly 'dead' during



this constant period. There are several advantages of such a method of operation and Putman (1948) has shown that self-quenching counters operated in this way show improved plateaux and become free from temperature drift.

A number of attempts have been made to obtain a reduction of the dead time. The discharge occurring in a counter operating in the Geiger region is stopped or quenched by positive ions produced during the discharge (Montgomery and Montgomery 1940). These ions form a sheath round the wire, reducing the field and preventing further multiple ionization. A second discharge is not possible until the sheath has moved to a critical distance from the wire, such that the field is sufficiently restored. The time required for this movement of the ions has been identified by Stever (1942) as the dead time.

Sherwin (see Smith 1948) has pointed out that, since the ion sheath is formed within a few tenths of a millimetre of the wire, it should be possible to collect these ions on the wire, immediately after a discharge, by reversing the applied field. Under these conditions, the times required for the positive ions to reach the wire would be relatively short and a considerable reduction in the dead time should be obtained. Following this suggestion Simpson (1944) and Hodson (1948) have used circuits which switched the wire potential a hundred or so volts negative with respect to the cylinder for a few microseconds after each count and then returned it to the working value. Both these workers used long counters up to 60 cm. Dead times of 20 to 30  $\mu\text{sec.}$  were obtained.

If the mechanism by which the ion sheath spreads along the counter wire is considered, then another explanation of the reduction in dead times obtained by Simpson and Hodson is possible. Complete spreading of the ion sheath along the full length of the wire is a characteristic of the discharge of a counter operating in the Geiger region. Stever (1942) has shown that the ion sheath rarely spreads past a bead mounted on the wire in self-quenching counters. In a similar way, reducing the wire potential below the threshold of the Geiger region during the spread of the discharge will cause localization of the ion sheath.

A consideration of the velocity of spread of the ion sheath (Wantuch 1947, Hill and Dunworth 1946) suggested that reversing circuits similar to those used by Simpson and Hodson, when used with long counters, should cause the wire potential to fall below the threshold of the Geiger region before the sheath has had time to travel far along the wire. The remainder of the counter would then be sensitive as soon as the wire potential is restored to its operating value. Thus the reduction of the dead time obtained with a switching circuit may be due to two causes: collection of positive ions or localization of the ion sheath. Some of the experiments described in § 3 of this paper show that localization of the ion sheath does occur in long counters and that the explanation given by Simpson (1944) and Hodson (1948) of the reduction of the dead time obtained by them in their experiments was not complete. This conclusion (Collinge 1948) is in agreement with the work of Smith (1948), Hodson (see Smith 1948) and Elliot (1949). In this paper further experiments are described in which was determined the effect on the dead time of momentarily changing the wire potential.

## § 2. THE CIRCUIT

The circuit which is shown in Figure 1 was intended for experimental purposes only. The cylinder of the counter is earthed and the wire is connected to the anode of the switching valve,  $V_{14}$ . The anode current of this valve is normally cut off by negative bias on the control grid. The cathode is returned to a preset

The valves  $V_2$  and  $V_4$  amplify the pulses from the counter and feed them to the flip-flop formed by valves  $V_6$  and  $V_9$ . The 'switching time' is determined by the grid resistance of  $V_9$  and may be varied from 1 to 10  $\mu$ sec.; its amplitude, and



The value of the switching voltage was measured by connecting the counter wire to the Y-plates of a cathode-ray oscillograph. The spot was normally biased off the screen by the high potential; each count caused it to be returned to the screen for the duration of the switching time and the switching voltage was read on a calibrated scale. This arrangement also enabled the drive to  $V_{14}$  to be adjusted so as to obtain square pulses.

### (i) Preliminary Work

PROC. PHYS. SOC. LXIII, I—B



time, the recovery time of the circuit and the time required for the wire potential to return to a point on the plateau where the counter pulses are large enough to operate the circuit.

To test this, several counters of lengths varying from 5 to 30 cm. and containing argon plus alcohol mixtures to a total pressure of about 11 cm. were used. Each counter was connected in turn to the circuit and the anode potential of  $V_{14}$  adjusted to the operating voltage for the counter. Pulses from the cathode of  $V_{12}$  were used to trigger an oscilloscope, whilst the pulses occurring at the control grid at  $V_6$  were fed to the Y-plates. A gamma ray source gave a convenient counting rate. The switching time was varied from 1 to 10  $\mu\text{sec.}$  and the switching voltage from plus to minus 500 volts.

Pulses were observed to occur on the cathode-ray oscillograph trace at all time intervals 2 or 3  $\mu\text{sec.}$  greater than the switching time. The recovery time of the circuit was about 3  $\mu\text{sec.}$ ; this includes the time required for the wire potential to be restored. This experiment seems to confirm therefore that localization of the sheath was taking place.

### (ii) Six-Cylinder Counter

Direct proof that localization of the ion sheath was occurring in these long counters was obtained using the six-cylinder counter shown in Figure 2. The cathode consists of six, separately insulated, identical cylinders, contained in a glass envelope. It was filled with 10 cm. of argon and 1 cm. of ethyl alcohol. The wire was connected to the anode of  $V_{14}$  and 1 M $\Omega$  resistances were connected

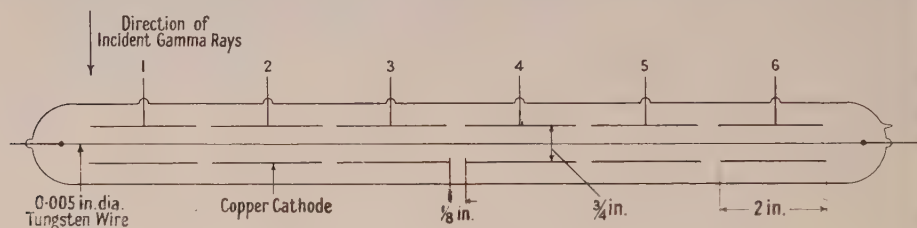


Figure 2. Six-cylinder counter.

Table 1

Counts per minute at cathode	No. 1	No. 2	No. 3
Circuit inoperative	1124	1150	1131
Circuit operative	918	97	43

between each of the cylinders and ground. A discharge, occurring in a particular cathode, caused a positive pulse to appear across the associated resistance. This counter was arranged so that a collimated beam of gamma rays was directed, at right angles to the wire, on to No. 1 cathode.

With a switching time of 1  $\mu\text{sec.}$  and zero switching voltage, the counting rates, at cathodes No. 1, 2 and 6, were determined by connecting an amplifier, discriminator and scale of 100 to each of the cathodes in turn. Readings were also obtained with the switching circuit made inoperative by disconnecting the condenser feeding the control grid of  $V_{14}$ . The results obtained are given in Table 1, which shows the average counting rate registered, at the three cathodes, after correcting for the background counting rate.

## (iii) Two-Window Counter

The counter shown in Figure 3 was used to obtain further confirmation in a similar way. It consists of a brass cathode with a mica window at each end, parallel to the wire. An RCA photo-multiplier tube was mounted opposite each window so that the light, produced during the discharge in that region of the counter, fell on the light sensitive surface. The voltage pulses, occurring at the collecting electrode, were recorded on a scaler via an amplifier and discriminator.

As before, the switching voltage was adjusted to zero and the switching time to 1  $\mu$ sec. Experiments were performed with either a collimated source of  $\gamma$ -rays

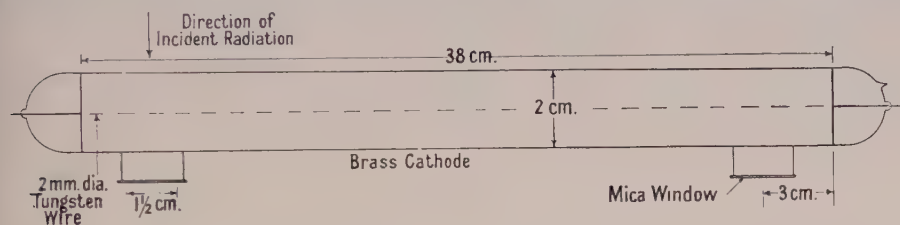


Figure 3. Two-window counter.

Table 2

Counts per minute	Window near source			Window remote from source		
	$\gamma$ -rays	$\beta$ -rays	$\beta$ -rays	$\gamma$ -rays	$\beta$ -rays	$\beta$ -rays
Circuit inoperative	2051	3614	1687	1693	3736	1674
Circuit operative	2087	3526	1568	220	42	16

Table 3

Counter	Six-cylinder		Two-window		
	$\gamma$	$\gamma$	$\gamma$	$\beta$	$\beta$
Distance between centres of detectors (cm.)	5	22.5	32	32	32
% of discharges remote from source	10.5	4.5	13.5	1	1

directed at one end of the cylinder or with a beam of  $\beta$ -rays from  $^{32}\text{P}$  passing into the counter at right angles to the wire, through an aluminium window. This window, not shown in Figure 3, was in the brass wall opposite one of the mica windows.

In Table 2 the number of counts per minute registered by the two photo-tubes are shown for both  $\beta$  and  $\gamma$ -rays. The figures are average values and have been corrected for the background.

## (iv) Discussion

The results of Tables 1 and 2 taken with the switching circuit operative are condensed in Table 3. The bottom line shows the percentage of discharges detected at various distances along the counters. These results show that localization of the ion sheath does occur.

A higher percentage of the discharges was localized when  $\beta$ -rays were used; this is explained by incomplete collimation and scattering of the  $\gamma$ -rays. Even so, the results for the six-cylinder counter show that about 90% of the discharges was confined to less than 5 cm. of the wire.



## § 4. DETERMINATION OF THE DEAD TIME OF A LONG COUNTER

(i) *The Paired Source Method*

It was stated in § 3 that the dead time of a long counter obtained from a triggered oscillograph was equal to the insensitive time of the switching circuit. The dead time determined by this method is independent of the length of the counter provided it is long enough for localization of the ion sheath to occur. Thus with a switching time of  $1 \mu\text{sec.}$ , dead times of 3 or 4  $\mu\text{sec.}$  were found for several counters of lengths greater than 5 cm. Although the result is consistent with Korff's definition of dead time, it is of no value for the correction of counting losses. This is because the whole of the counter is not sensitive to further counts immediately after the dead time. Regions of the counter where the ion sheath is localized remain insensitive for the normal dead time imposed by the ion sheath. The average losses depend on a number of factors which include the length of the counter. The true dead time must be obtained by a method giving the losses directly.

A convenient way of determining the true dead time involves the use of two sources. The average counting rate is noted when the sources are presented to the counter, separately and together.

If the registered counting rate is  $n_r$  then the true counting rate  $n_t$  is given by

$$\frac{n_r}{n_t} = \frac{1}{1 + n_t \tau}, \quad \dots\dots (1)$$

where  $\tau$  is the dead time.

From equation (1) Beers (1942) has derived a convenient formula for the dead time. Neglecting the background counting rate this may be written

$$\tau = \frac{\Delta}{2n_1 n_2} + \frac{n_{12} \Delta^2}{8n_1^2 n_2^2}, \quad \dots\dots (2)$$

where  $\Delta = n_1 + n_2 - n_{12}$  and the counting rates  $n_1$ ,  $n_2$  and  $n_{12}$  are derived from  $N_1$ ,  $N_2$  and  $N_{12}$  the total counts registered by the separate and combined sources during the intervals  $t_1$ ,  $t_2$  and  $t_{12}$  respectively.

The error in the dead time can be calculated approximately. Suppose that errors in time measurements are neglected and the errors in the total counts arranged to be of the same order by making  $N_1 \simeq N_2 \simeq N_{12} \simeq N$  say, then  $t_1 \simeq t_2 \simeq 2t_{12} \simeq t$  for roughly equal sources.

Then from equation (2) it can be shown that  $\delta\tau$ , the probable error in  $\tau$ , is given by equation (3) where  $\delta N$  is the probable error in  $N$ .

$$\delta\tau = \sqrt{\left(\frac{3}{2}\right) \frac{t \delta N}{N^2}}. \quad \dots\dots (3)$$

The probable error  $P_\tau$  due to statistical variations in the total number of counts is obtained by putting  $\delta N = \frac{2}{3} \sqrt{N}$

i.e.

$$P_\tau = \sqrt{\left(\frac{2}{3}\right) \frac{t}{N \sqrt{N}}},$$

from which it follows that

$$t = \frac{16}{3} \frac{(t_{12})^3}{(N_{12})^3} \frac{1}{P_\tau^2}. \quad \dots\dots (4)$$

Then for chosen values of  $P_\tau$  equation (4) gives the necessary counting period  $t$  for various values of  $t_{12}/N_{12}$ . Some values of  $t$  in minutes are given in Table 4, row 2, for  $P_\tau = 3\mu\text{sec}$ .

Table 4

Counting rate $n_{12}$ ( $\text{sec}^{-1}$ )	1,000	2,000	3,000	10,000	30,000
Minimum counting period $t$ necessary to ensure $P_\tau < 3\mu\text{sec}$ . (min.)	10	$<2$	$<2$	$\ll 2$	$\ll 2$
$P_\tau$ , the probable error in $\tau$ for $\alpha = \frac{1}{2}\%$ ( $\mu\text{sec}$ .)	12	6	5	1	0.3

Errors due to uncertainties in the wire potential may often be neglected when finding the dead time of a counter operated in the normal way. This is not true when a switching circuit is used which draws an average current which may be of the order of a milliampere, because of the difficulty of ensuring the same counter voltage at various counting rates.

If the probable error in  $N$ , due to setting the counter voltage supply is  $\delta N$ , then  $\delta N/N$  is the fractional error,  $\alpha$  say. Then from equation (3)

$$P_\tau = \sqrt{6\alpha t_{12}/N_{12}} \quad \dots\dots (5)$$

Row 3 of Table 4 shows the values of  $P_\tau$  for  $\alpha = \frac{1}{2}\%$  for various values of  $N_{12}/t_{12}$ .

### (ii) Experimental Details and Results

The counter used consisted of a brass cathode, 32 cm. long and 2 cm. inside diameter, with a 0.2 mm. tungsten wire, and filled with 10 cm. of argon and 1 cm. of ethyl alcohol. In order to minimize the effect of positive ion collection the switching voltage was set to zero and the switching time at  $1\mu\text{sec}$ . A scale of  $10^4$ , with a paralysis time of about  $5\mu\text{sec}$ . was used to record the counts. Two gamma-ray sources were used at a distance adjusted to give the desired counting rate. Readings were taken with the sources in several positions and the dead time determined as a function of the counting rate. A similar series of measurements was made with the circuit inoperative. The counting interval was always chosen from Table 4 so that the error due to statistical variation of the total counts could be neglected in comparison with  $\alpha$ .

The dead times obtained are shown in Figure 4 where they have been plotted against the counting rate. The values of the counting rate, obtained with the two sources together, have been plotted along the  $x$ -axis after correcting for losses. Curve (a) was taken with the circuit not working and (b) with it working.

### (iii) Discussion

As the experiment was arranged so that the statistical errors could be neglected we need only consider errors due to setting of the H.T. The experimental arrangement enabled its value to be determined to about 5 volts. The slope of the counter characteristic at the wire potential used was  $0.1\%$  per volt, determined under the conditions for the dead time measurements. Thus in this experiment  $\alpha = \frac{1}{2}\%$ . Hence the values of  $P_\tau$  applicable to the dead times obtained are not greater than those given in row 3 of Table 4. These errors apply to both graphs. The slope of  $0.1\%$  per volt is typical of the characteristic of a counter of this type, taken with a short paralysis time.



If the statistical dead time depends strongly on the counting rate, the value obtained from equation (2) loses its significance. Its meaning, in fact, is defined by this equation. This point has been discussed by Curran and Rae (1947). The values given in curve (a) Figure 4 are therefore somewhat artificial. The results show however the large changes which occur when the counting rate is high and emphasize the difficulties of correcting for large losses.

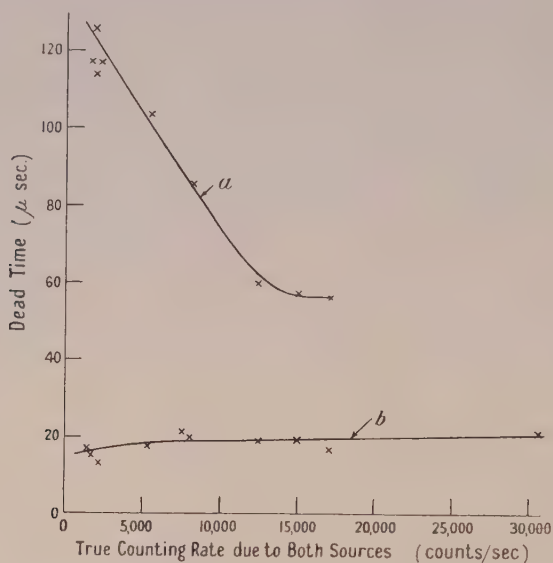


Figure 4. Dead time as a function of counting rate for a long counter.  
(a) Circuit inoperative; (b) Circuit operative.

The results shown in curve (b) obtained with the circuit operative show that not only is the dead time considerably reduced but its value is constant and independent of the counting rate within the experimental error. This is true up to counting rates of nearly  $2 \times 10^6$  counts per minute. It would be reasonable to correct for losses greater than 10% under these conditions. For a statistical dead time of 20 μsec. the losses would be 10% at a counting rate of  $3 \times 10^5$  counts per minute.

##### § 5. EXPERIMENTS WITH SHORT COUNTERS

In the experiment described in this section G.E.C. type G.M.2 counters were used; they are single ended argon-alcohol  $\beta$  counters. The tungsten wire is about 2 cm. long. Such a counter was connected to the circuit and a gamma-ray source used to provide a suitable counting rate.

The dead time of such a counter was observed on a triggered oscillograph in the manner previously described. Dead times considerably greater than the switching time and dependent on the circuit parameters were obtained, as would be expected if the wire is too short for localization of the ion sheath to occur. To show that localization was not occurring,  $V_5$  was used as a simple discriminator. The cathode was biased with a positive potential which was increased until triggering occurred only with pulses of maximum amplitude. This is a simple way of introducing a time delay to ensure that triggering occurs only when the ion sheath has had time to spread along the whole length of the wire. No change in the dead time was observed, showing that the ion sheath always spreads along the whole of the wire.

As complete spreading occurs in these counters it was considered reasonable to observe the dead time on a triggered oscillograph. The values obtained are of qualitative interest and are related to the values which would be obtained using the paired source method.

The dead times obtained for one of the counters which had a dead time of  $105 \mu\text{sec}$ . when the switching circuit was inoperative, have been plotted as a function of the switching time on Figure 5. Several curves are shown for various

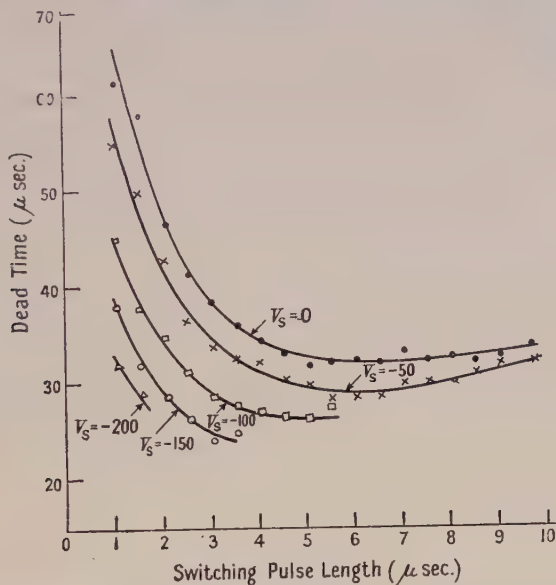


Figure 5. Variation of the dead time of a short counter with length of switching pulse.  $V_s$  is the switching potential.

values of the switching time. For these results the anode load of  $V_{14}$  was changed from  $10 \text{ k}\Omega$  to  $50 \text{ k}\Omega$ .

The curves show an expected initial decrease in dead time as the switching time increases. This is consistent with a progressive increase in the number of positive ions collected on the wire. As the minimum dead time is not the same for all the curves and is very much greater than the switching time, it is concluded that part only of the ion sheath is collected. This is in agreement with the observed distribution of pulse amplitudes which shows an increase in amplitude from zero at the dead time to a maximum value. It is presumed that the decreased dead time corresponds to the time taken for the reduced ion sheath to move to a critical distance from the wire at which Geiger avalanches can occur.

As the switching time is increased the rate of collection of positive ions decreases. This is because it is more difficult to collect ions remote from the wire away from the very high field region. The rate of collection decreases until the reduction in dead times obtained just equals the increase in the switching time. Thus the curves should have a minimum and a positive slope, approaching unity, for large values of the switching times. This conclusion is in agreement with the curves shown.

Some of the curves of Figure 5 do not include dead times for the full range of switching times. This is because for these conditions the cathode-ray oscillograph showed that very many spurious counts were occurring.



The reason why a reduction in dead times is obtained even when the switching voltage is negative has been discussed by Smith (1948). The charge induced by the sheath on the wire leads to large fields near the wire sufficient to cause collection of positive ions.

#### § 6. COUNTER CHARACTERISTICS

In general no significant changes in counter characteristics have been observed when using counters with the switching circuit. One counter had a somewhat longer plateau when the switching voltage was minus 150 volts. Three commercial gamma-counters had plateaux with slopes which became progressively worse as the switching voltage was made more negative. All the counters tested produced larger numbers of spurious counts when the switching voltage was very negative.

In order to reduce the chance of producing spurious counts, it is probably an advantage not to collect positive ions at the wire but to reduce the dead time of long counters by localizing the ion sheath. In this case a simpler circuit could be used to produce a very short negative pulse at the wire with an amplitude of 300 or 400 volts. It would be desirable that such a circuit should trigger on very small pulses in order to ensure that the time available for the ion sheath to spread is as small as possible. Not only is it desirable to limit the extent of the ion sheath, in order to obtain a short dead time, but also because the life of the counter is increased by reducing the number of positive ions involved in each discharge. Elliot (1949) describes some experiments in which the charge collected at the wire is shown to be reduced when a switching circuit is used and finds that under these conditions the life of the counter is prolonged.

#### ACKNOWLEDGMENTS

The author wishes to express his gratitude to the Department of Scientific and Industrial Research for the grant which made this work possible and to thank Sir James Chadwick for his interest and Dr. J. Rotblat and Dr. J. D. Craggs for many helpful discussions.

#### REFERENCES

- BEERS, Y., 1942, *Rev. Sci. Instrum.*, **13**, 72.  
 BLACKMAN, M., and MICHIELS, J. L., 1948, *Proc. Phys. Soc.*, **60**, 549.  
 COLLINGE, B., 1948, *Nature, Lond.*, **162**, 853.  
 CURRAN, S. C., and RAE, E. R., 1947, *Rev. Sci. Instrum.*, **8**, 871.  
 ELLIOT, H., 1949, *Proc. Phys. Soc. A*, **62**, 369.  
 HILL, J. M., and DUNWORTH, J. V., 1946, *Nature, Lond.*, **158**, 833.  
 HODSON, A. L., 1948, *J. Sci. Instrum.*, **25**, 11.  
 KOHMAN, T. P., 1945, *Atomic Energy Declassified Report*, MDDC. 905.  
 KORFF, S. A., 1946, *Electron and Nuclear Counters* (New York: Van Nostrand).  
 MONTGOMERY, C. G., and MONTGOMERY, D. D., 1940, *Phys. Rev.*, **57**, 1030.  
 PUTMAN, J. L., 1948, *Proc. Phys. Soc.*, **61**, 312.  
 SIMPSON, J. A., 1944, *Phys. Rev.*, **66**, 39.  
 SMITH, P. B., 1948, *Rev. Sci. Instrum.*, **19**, 453.  
 STEVER, H. G., 1942, *Phys. Rev.*, **61**, 38.  
 WANTUCH, E., 1947, *Phys. Rev.*, **71**, 464.

# Breakdown in Cold-Cathode Tubes at Low Pressure

By F. G. HEYMANN

University of the Witwatersrand, South Africa

*Communicated by G. I. Finch ; MS. received 17th May 1949*

**ABSTRACT.** When, in cold-cathode discharge tubes, electrode spacings and surface areas deviate from the ideal of infinite parallel planes, it is found that the breakdown voltage between electrodes increases. This is explained as a decrease in the effective  $\eta$  of the gas due to loss of electrons and positive ions by diffusion to the walls of the container. The loss factor per unit potential difference is shown theoretically to be inversely proportional to the field strength and tube radius, although this is not fully verified by experiment.

Paschen curves obtained experimentally for potassium and nickel cathodes in argon and in a neon-argon mixture at low pressures are shown and, from these, values of  $\gamma$  for the two cathode surfaces are obtained as a function of  $E/p_0$ . The apparatus used for measuring breakdown voltage is described.

Earlier theories of statistical and formative time delays are extended to cover the case of a rising overvoltage and also the case where the primary electrons appear in bursts as with ionization by  $\alpha$ -particles. The shape of the statistical distribution curve is an indication of whether the primary electrons have been produced singly or in bursts. The overvoltage  $\Delta V$  of breakdown due to formative lag and the rate of rise of the uniformly increasing applied voltage  $V$  are found to bear the relation  $\Delta V \propto \sqrt{(dV/dt)}$ . This has been experimentally verified.

## § 1. INTRODUCTION

THIS subject has been treated by quite a number of authors and experimental work has been carried out with various electrode materials and gases. The mechanism of breakdown is fairly well understood but the factor  $\gamma$  which represents the secondary mechanisms has not yet been fully explored because of the difficulty of direct determination. In the following pages some possibilities are set down in this connection.

When electrodes of finite dimensions are used in breakdown measurements, the special case of the similarity principle known as Paschen's law does not hold as will be shown later and an approximate theoretical approach will be attempted.

## § 2. INFINITE PARALLEL PLANE ELECTRODES

The simplest breakdown gap from a theoretical point of view is that between infinite parallel planes giving uniform field strength.

When all primary electrons are emitted from the cathode, the current density increases in the field direction according to the following relation (Penning and Druyvesteyn 1940, Rogowski 1940):

$$j_e = j_{ke} \exp \{ \eta (V - V_0) \}, \quad \dots\dots(1)$$

where  $V$  is the potential with respect to the cathode.

If all primary electrons are due to ionization in the gas by an external agent, the current relation is

$$j_e = j_s [\exp \{ \eta (V_a - V_0) \}] / \eta V. \quad \dots\dots(2)$$

In the steady state the positive ion current density at the cathode which corresponds to the electron current density of equation (1) is

$$j_{ki} = j_{ke} [\exp \{ \eta (V_a - V_0) \} - 1]. \quad \dots\dots(3)$$



The probability that a positive ion which reaches the cathode causes emission of an electron may be represented by  $\gamma_{ia}$  and the probability that the electron will not return to the cathode by diffusion by  $\gamma_{ib}$ . The probability that a positive ion will give rise to an active electron is thus:  $\gamma_i = \gamma_{ia}\gamma_{ib}$ .

Let there be  $\theta$  photons created in the gas for each ionization and let a fraction  $f_r$  fall on the cathode. The average probability that a photon will give rise to an active electron may be represented by  $\gamma_{ra}\gamma_{rb}$  in analogy to the case of positive ions. The secondary emission factor due to photons is then (Penning and Druyvesteyn 1940)

$$F_r\gamma_r = (\theta f_r)(\gamma_{ra}\gamma_{rb}).$$

The factor  $f_r$  depends on the geometry of the gap and on photon absorption in the gas. In the present case, if absorption is negligible,  $f_r = \frac{1}{2}$ .

$\theta$  is a function of the fundamental ratio  $E/p_0$  which is the main factor in discharge at low pressure (Penning and Druyvesteyn 1940, Penning 1933).

For metastable atoms an expression similar to that for photons will hold (Penning and Druyvesteyn 1940):  $F_m\gamma_m = (\psi f_m)(\gamma_{ma}\gamma_{mb})$ .  $\psi$  is analogous to  $\theta$ , both factors increasing with decreasing  $E/p_0$ .  $f_m$  depends on diffusion of the metastable atoms and is therefore related to the geometry of the gap, the pressure of the gas, and is also a function of time until the steady state is reached when metastable distribution between infinite parallel planes is (Rogowski 1940, Newton 1948)

$$m(x) = j_{ke} \frac{\psi}{\eta ED} [\{\exp\{\eta(V_a - V_0)\} - 1\} \frac{x}{d} - \{\exp\{\eta(V_x - V_0)\} - 1\}] \quad \dots\dots (4)$$

and

$$f_m = \frac{1}{\eta(V_a - V_0)} - \frac{1}{\exp\{\eta(V_a - V_0)\} - 1}. \quad \dots\dots (5)$$

The total secondary emission factor which relates the number of secondary electrons entering the discharge per second to the number of ionizations occurring in the gas per second is then (Penning and Druyvesteyn 1940)

$$\gamma = \gamma_i + F_r\gamma_r + F_m\gamma_m. \quad \dots\dots (6)$$

The factors  $\gamma_{ia}$ ,  $\gamma_{ra}$  and  $\gamma_{ma}$  are similar since they represent the efficiency of secondary emission. It has been shown by Penning (1930) and Oliphant (1929, 1930) that the kinetic energies of ions and metastable atoms have little effect on these factors when the energies are low and of the order encountered in low pressure discharge. The excitation energies are therefore responsible for secondary emission (Meili 1945) which means that the  $\gamma_a$  factors should be substantially constant over a large range of field strength and pressure.

The factors  $\gamma_{ib}$ ,  $\gamma_{rb}$  and  $\gamma_{mb}$  represent the effect of back-diffusion which has been treated by several writers (Hertz 1927, Pose 1928-9, Thomson 1928, Loeb 1939, Meili 1945).

The general expression derived is (Pose 1928-9)

$$\gamma_b = \left\{ 1 + \frac{3\bar{V}}{4\lambda_0 E/p_0} \log \left( \frac{V_0}{\bar{V}} + 1 \right) \right\}^{-1}. \quad \dots\dots (7)$$

(This holds on the assumption that only elastic collisions occur in the distance  $V_0/E$  from the cathode, which is approximately true.) It is evident from the expression that  $\gamma_b$  is a function of  $E/p_0$ .

It has thus been indicated that all the factors in equation (6) depend directly on  $E/p_0$  or are constants, except  $f_m$ , in the case of infinite parallel planes. If the contribution of the metastable atoms or the variation in  $f_m$  is not large,  $\gamma$  will approximately be a function of  $E/p_0$  alone.

In the steady state  $f_m$  is a constant and if this state is approximately reached before final breakdown takes place  $\gamma$  will be a function of  $E/p_0$ .

The breakdown relation may be written in the form (Penning and Druyvesteyn 1940)

$$V_B = V_0 + \frac{1}{\eta} \log \left( 1 + \frac{1}{\gamma} \right). \quad \dots\dots (8)$$

The factors  $V_0$  and  $\eta$  have been determined experimentally (Penning and Druyvesteyn 1940, Kruithof 1940) and are functions of  $E/p_0$  for pure gases.

Thus the breakdown voltage  $V_B$  will be a function of  $E/p_0$  in the case of infinite parallel plane electrodes.

Since the field is uniform

$$p_0 d = \frac{V_B}{E/p_0}, \quad \dots\dots (9)$$

so that  $V_B$  will be a function of  $p_0 d$  alone, which is a statement of Paschen's law.

The minimum breakdown voltage corresponds roughly with the maximum value of  $\eta$  (Penning and Druyvesteyn 1940) which for the rare gases is approximately  $1/3 V_i$ .

The factor  $\gamma$  varies enormously amongst various metals, being the greatest for the alkali metals and smallest for iron according to measurements made up to the present in the rare gases.

### § 3. FINITE PLANE ELECTRODES

When plane electrodes are used in measurements they have to be very large compared with their distance of separation to approximate to infinite planes. Loss of ionization products occur at the boundaries of the gap due to diffusion and the main cause of increase of breakdown voltage is the decrease in the effective  $\eta$  as a result of the loss of electrons and ions. The change in  $\gamma$  will not be very great since only the factors  $F_r$  and  $F_m$  are reduced. When these factors become important at low values of  $E/p_0$  this may not be true but changes in  $\gamma$  do not affect the breakdown voltage so much, since it occurs in a logarithmic function.

The greater part of the decrease in  $\eta$  is due to electron loss because of the large mean energy and consequent high rate of diffusion.

In the breakdown or Townsend region at low pressure, space charge is unimportant (Penning and Druyvesteyn 1940) and it may be assumed that the diffusion of electrons and ions depends on their respective concentrations.

At a distance  $x$  from the cathode the potential in a uniform field is  $V_x = Ex$  and the potential difference over a distance  $dx$  is  $dV = E dx$ .

The increment of electron current density due to ionization by collision is  $\eta j_e dV$  whilst the loss by diffusion may be represented by  $\sigma_e j_e dV$ .

Thus:

$$dj_e = (\eta - \sigma_e) j_e dV, \\ j_e = j_{ke} \exp \{ (\eta - \sigma_e)(V_x - V_0) \}. \quad \dots\dots (10)$$

The increment of ions is  $\eta j_e dV$  and the loss  $\sigma_i j_i dV$ . Therefore

$$dj_i = -\eta j_e dV + \sigma_i j_i dV.$$



Substituting for  $j_e$  and solving

$$j_i = A \exp \{ \sigma_i (V_x - V_0) \} - \frac{\eta j_{ke}}{\eta - \sigma_e - \sigma_i} \exp \{ (\eta - \sigma_e) (V_x - V_0) \}.$$

Setting  $\sigma = \sigma_e + \sigma_i$  and at the anode  $V_x = V_a$ ,  $j_i = 0$ ,

$$j_i = j_{ke} \frac{\eta \exp \{ \sigma_i (V_x - V_0) \}}{\eta - \sigma} [\exp \{ (\eta - \sigma) (V_a - V_0) \} - \exp \{ (\eta - \sigma) (V_x - V_0) \}]. \quad \dots\dots (11)$$

The positive ion current at the cathode is the same as at  $V_x = V_0$ ,

$$j_{ki} = j_{ke} \frac{\eta}{\eta - \sigma} [\exp \{ (\eta - \sigma) (V_a - V_0) \} - 1]. \quad \dots\dots (12)$$

Breakdown will occur when  $j_{ki} = j_{ke}$ ,

$$\begin{aligned} \frac{\gamma \eta}{\eta - \sigma} [\exp \{ (\eta - \sigma) (V_B - V_0) \} - 1] &= 1, \\ (\eta - \sigma) (V_B - V_0) &= \log \left( 1 + \frac{\eta - \sigma}{\gamma \eta} \right) \simeq \log \left( 1 + \frac{1}{\gamma} \right) - \frac{\sigma}{\eta(1 + \gamma)}, \\ &\simeq \eta (V_{B0} - V_0) - \frac{\sigma}{\eta(1 + \gamma)}, \\ V_B - V_{B0} &= \Delta V; \quad V_{B0} - V_0 - \frac{1}{\eta(1 + \gamma)} = V_R, \\ \Delta V &= \frac{\sigma}{\eta - \sigma} V_R; \quad \frac{\sigma}{\eta} = \frac{\Delta V}{\Delta V + V_R}. \quad \dots\dots (13) \end{aligned}$$

These are approximate expressions linking up the increase in breakdown voltage with the loss of electrons and ions due to diffusion.

The factor  $\sigma_e$  is difficult to determine theoretically and the following derivation gives mainly a qualitative result:

If the discharge is confined to the diameter of the electrodes of radius  $R$  by a glass envelope of slightly larger diameter and the electron concentration near the glass wall is  $n_w$ , then the number striking unit area on the glass wall per second is  $q_w = n_w \bar{c}_e / 4$ . The average electron concentration in the tube is  $j_e / eu_e$  ( $j_e$  is average current density).

Let  $n_w$  be related to this density by a factor  $a$  such that  $n_w = aj_e / eu_e$ . The loss per elemental distance  $dx$  is then

$$2\pi R q_w dx = 2\pi R \frac{aj_e \bar{c}_e}{4eu_e} dx,$$

now

$$u_e = K_e \frac{E}{p_0} = \text{const.} \times \frac{\lambda p_0}{\sqrt{\bar{V}_e}} \frac{E}{p_0}$$

and

$$\bar{c}_e \propto \sqrt{\bar{V}_e}.$$

Therefore the loss factor per unit potential difference is

$$\sigma_e = \text{const.} \times \frac{a \bar{V}_e p_0}{\lambda p_0} \frac{I_e}{E ER}. \quad \dots\dots (14)$$

This is probably the main part of  $\sigma$  and if  $\sigma_i$  is assumed to lead to a similar relation, the factor  $\sigma/\eta$  is approximately given by

$$\frac{\sigma}{\eta} = \text{const.} \times \frac{\bar{V}_c}{\lambda p_0} \frac{a p_0}{\eta E} \frac{I}{ER}. \quad \dots\dots(15)$$

At constant  $E p_0$  the only variables are  $E$  and  $R$  and with constant  $R$ ,  $\sigma/\eta$  should be inversely proportional to  $E$  if the factor  $a$  does not vary.

Mierdel and Steenbeck (1937) approach the problem differently by assuming the average life of an electron or ion to be  $T = R^2/(2.4)^2 D$ . On this assumption  $\sigma/\eta$  becomes inversely proportional to  $E^2 R^2$ .

In the experimental section the relative merits of the two derivations will be discussed with reference to the actual results.

#### § 4. MEASUREMENT OF BREAKDOWN VOLTAGE

A diagram of the apparatus together with a sketch of the type of experimental tube used are shown in Figure 1. In measuring breakdown voltage, a steady

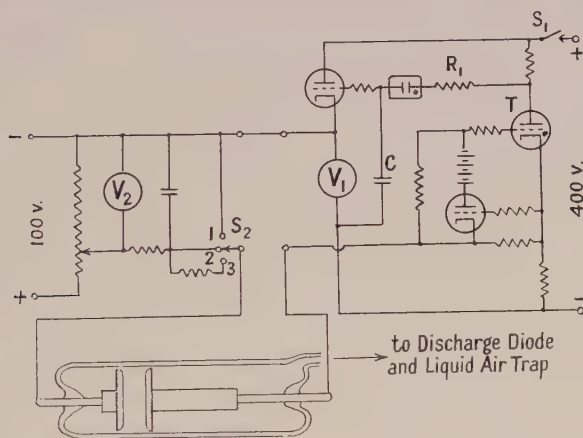


Figure 1. Apparatus for measuring breakdown potential and a typical experimental tube.

potential about 100 to 200 volts less than the expected breakdown voltage was applied through the potentiometer shown and the magnitude was indicated on voltmeter  $V_2$ . On closing switch  $S_1$ , the capacitance  $C$  charged through resistor  $R_1$  and the potential across  $V_1$  rose at the same rate, thus adding a further potential across the tube. When breakdown occurred, thyatron  $T$  fired, thus stopping the charging of  $C$  and applying an inverse voltage in series with  $V_1$  and  $V_2$  to reduce or extinguish the current through the tube, depending on the voltage.  $V_1$  could read up to 240 volts and the inverse voltage was about 170 volts.

The final value attained by  $V_1$  together with  $V_2$  is the maximum voltage across the tube just before a discharge passes. We may thus define breakdown potential as measured by this equipment as the maximum voltage between the electrodes prior to the negative slope transition region.

The cathodes of the experimental diodes were illuminated sufficiently in order to reduce statistical spread and as will be seen later (Figure 8), the overvoltage at the rate of rise of  $V_1$  of 40 volts per second is negligible.

The experimental tube consisted of two mild steel electrodes enclosed by a close-fitting hard glass tube. One of the electrodes was made to slide on a  $\frac{1}{8}$  in.

diameter tungsten rod and could be moved by using an external magnet. The tube was evacuated and baked at  $400^{\circ}\text{C}$ . for some time and the electrodes were brought to a dull red heat by eddy current heating. In almost all the cases potassium-activation was used and a good, reproducible potassium layer could be deposited on the electrodes by vacuum distillation.

Rare gases were used in the spectrally pure state and further purified by keeping in a vessel in which a continuous discharge was maintained between potassium-activated electrodes. Condensable vapours were removed in a double liquid-oxygen trap and as a last safeguard a potassium-activated diode passing a continuous discharge was permanently connected in the inlet to the main tube.

Three sizes of tube (dimensions in centimetres) were used:

Tube	Electrode diameter	Tube diameter	Maximum electrode separation
1	1.5	1.6	2.5
2	2.8	3.0	2.6
3	6.0	6.5	3.75

Breakdown voltage was measured as a function of electrode separation at various pressures in argon and in a mixture of neon and argon which contained 6.6% argon (potassium-activated cathode).

Some representative curves for tube 2 are shown in Figure 2. Breakdown voltages are plotted as functions of  $p_0d$  and it is evident that the curves at the lower pressures do not follow Paschen's law.

In Figure 3 the curves of breakdown voltage in argon are plotted for all three tubes as functions of  $E/p_0$ , assuming uniform field distribution. As was to be expected, the differences between curves are greatest for the smallest tube and least for the largest, for the same differences in pressure. At higher pressures the curves tend to merge in all cases and the curves for the various tubes show good correspondence at the pressures at which the losses by diffusion become small.

In order to determine the effect of the nearness of the glass wall to the edges of the electrodes, a tube with 1.5 cm. diameter electrodes and a 3 cm. diameter glass envelope was constructed. The values of breakdown voltage were not greatly different from those in tube 1 at the lower pressures, and it was therefore decided that the glass wall had only a small effect.

In order to check the validity of the theoretical expression for  $\sigma/\eta$  given in equation (15), the curves in Figure 4(a) were drawn, using equation (13) to determine  $\sigma/\eta$ . The theory predicts that  $\sigma/\eta$  should be inversely proportional to  $E$  at constant  $E/p_0$  and it has been found that there is reasonable correspondence as shown by the experimental points in Figure 4(a).

These points were calculated at various values of  $E/p_0$  (from 50 to 200 volt/cm.mm.), and it seems that for each tube a single factor of proportionality will represent all the points satisfactorily. The correspondence is not exact and partly due to experimental and graphical errors. Furthermore the theory is only approximate.

The correspondence amongst the three tubes is not so good, the theory predicting that the slopes of the lines in Figure 4(a) should be inversely proportional to the electrode diameters, which is not the case. It is probable that there is a further factor which has been overlooked in the theoretical derivation or it may be that the factor  $a$  in equation (15) is a function of  $R$ .



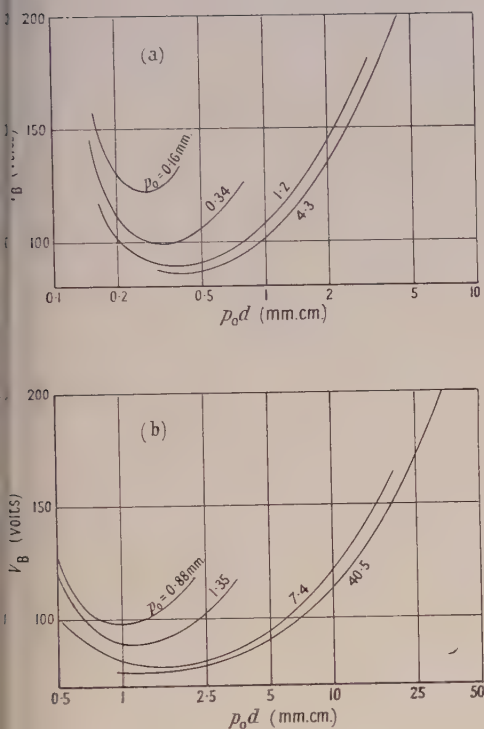


Figure 2. Breakdown potential curves with electrodes of 2.8 cm. diameter at various pressures :

(a) Pure argon; (b) 93.4% neon, 6.6% argon.

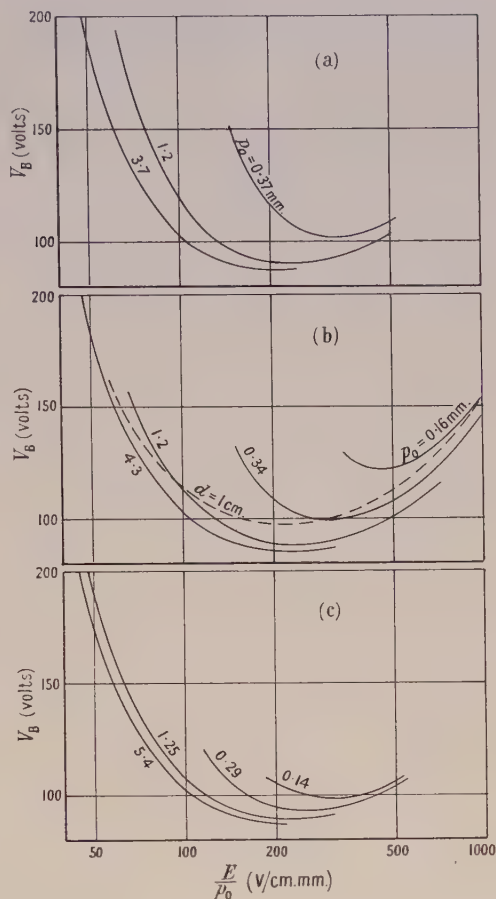


Figure 3. Breakdown potential curves as functions of  $E/p_0$  in pure argon. Electrode diameter :

(a) 1.5 cm.; (b) 2.8 cm.; (c) 6.0 cm.

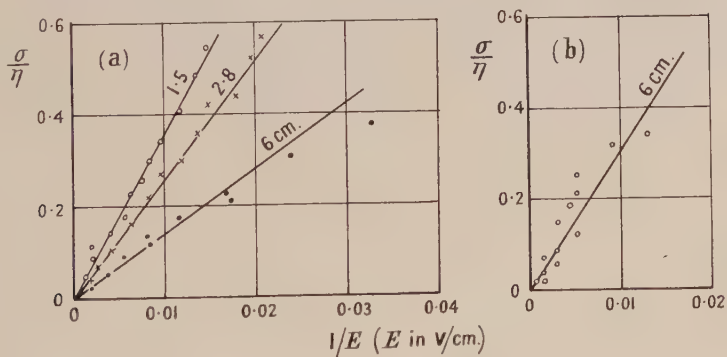


Figure 4. Experimental points representing  $\sigma/\eta = \Delta V / (\Delta V + V_R)$ .

(a) Argon : potassium-activated electrodes (electrode diameters in cm.).  
(b) Argon : nickel electrodes.

There seems to be a further objection to the theoretical expression in that the factor  $\sigma/\eta$  for nickel electrodes of 6 cm. diameter derived from Figure 4(b) does not correspond to that for potassium-activated electrodes.

The theoretical approach according to Mierdel and Steenbeck (1937) applies even less than the theory derived in this paper and cannot therefore explain the increase in breakdown voltage.

Figures quoted by McCallum and Klatzow (1934) for increase in breakdown voltage between nickel electrodes in argon are much higher than those found in this series of experiments and must be due to an additional cause not present here.

The increase of breakdown potential with small electrodes and at low pressures makes it necessary to use large electrode diameter, small spacing and high pressure to obtain a true Paschen curve. The values of breakdown potential measured on the tube of 6 cm. diameter will correspond fairly well with the values between infinite parallel planes except perhaps at high values of  $p_0d$  in argon where the pressure was about 50 mm. Hg and the separation up to 3.75 cm.

The measured curves for nickel and potassium over an extended range of  $p_0d$  are shown in Figure 5. The curve for potassium is easily reproducible and on

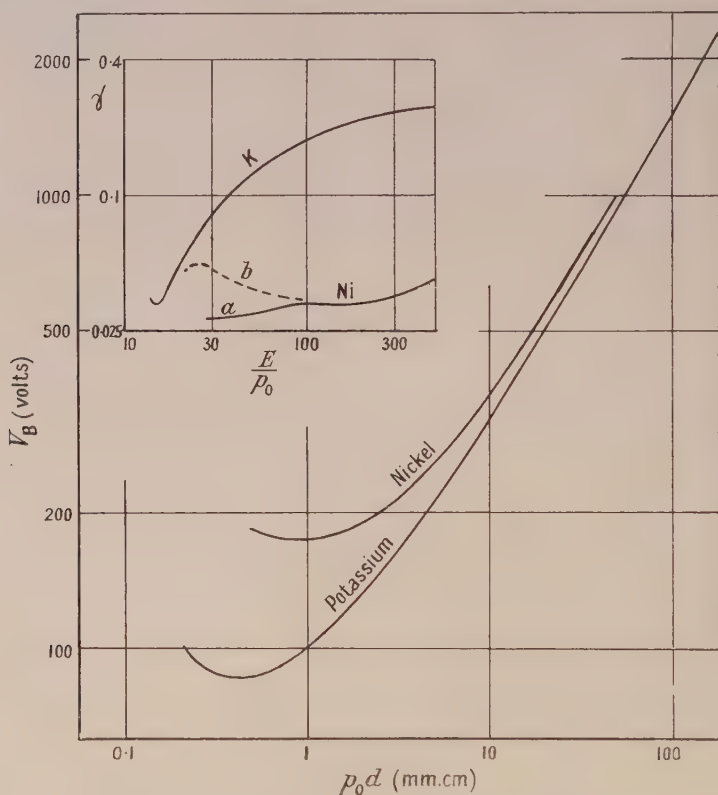


Figure 5. Experimental breakdown potential curves in argon with potassium and nickel cathodes. Inset:  $\gamma$ -curves as functions of  $E/p_0$ , for potassium and two different nickel cathodes.

using each electrode as cathode in turn, very close correspondence between the breakdown potentials occurred.

The nickel was in the form of an electro-deposit on the steel electrodes and although the treatment of both electrodes was exactly similar, the breakdown potentials with each as cathode in turn differed appreciably.

The factor  $\gamma$  was calculated from the breakdown relation in equation (8), although high accuracy is not attained by this method.

The values of  $V_0$  and  $\eta$  were taken from Penning and Druyvesteyn (1940) and Kruithof (1940). Figure 5 (inset) shows  $\gamma$ -curves for potassium and nickel as functions of  $E/p_0$ . Curve *a* for nickel corresponds with the  $p_0 d$  breakdown voltage curve shown. Curve *b* is for the other electrode and merges with *a* at higher values of  $E/p_0$ .

The curve of  $\gamma$  for potassium shows a form similar to that to be expected if the  $\gamma_b$  factors were predominant, the other factors being approximately constant. At very low values of  $E/p_0$  the curve tends to rise again as has been found for other materials by others (Penning and Druyvesteyn 1940) and is probably due to the increasing importance of  $\theta$  and  $\psi$  as  $E/p_0$  decreases.

The curves for nickel show that the metastable atom and photon action become important below a value of  $E/p_0$  of 100 volt/cm.mm. and to a different extent for the two electrodes, depending on their sensitivity to this action. Again this confirms previous results (Penning and Druyvesteyn 1940), but the full explanation is still obscure.

This illustrates the fact of the difficulty of the interpretation of  $\gamma$  and the importance of the purity of the cathode material.

#### § 5. TIME DELAY EFFECTS IN BREAKDOWN

There are two main causes of time delays in breakdown which will be treated separately and then combined. The delays involved when constant overvoltage is applied have already been dealt with by others (von Laue 1925, Zuber 1925, Schade 1936-7, Hertz 1937) and will serve as a basis for relations to be derived for the case of linearly increasing overvoltage.

The statistical time lag is due to insufficient primary electrons and formative lag comes about as a result of the time taken for positive ions to move to the cathode from their points of origin.

#### § 6. STATISTICAL TIME DELAY

Primary electrons, which are necessary to initiate breakdown, appear in a random fashion due to some external agent and therefore introduce time delays, even when the applied potential is adequate for breakdown. Let formative time delay be neglected for the time being. Von Laue (1925) has shown that the probability that breakdown will take place after a time  $t_s$  measured from the instant of applying an adequate potential, is given by

$$f(t) = \exp\left(-q_e \int_0^{t_s} W dt\right). \quad \dots\dots (16)$$

In the case of plane parallel electrodes, Hertz (1937) has shown that  $W$ , the probability that one electron will initiate discharge, is related to the factor  $M$  as follows:

$$M = \gamma[\exp\{\eta(V_a - V_0)\} - 1] = \frac{\gamma \log(1 - W)}{\log(1 - \gamma W)}.$$

At the normal value of breakdown potential  $M=1$  and  $W=0$ .

With constant overvoltage, i.e. when  $M$  is constant and greater than unity,  $W$  is constant and the probability of breakdown becomes

$$f_1(t) = \exp(-q_e W t_s) = \exp(-t_s/t_0). \quad \dots\dots (17)$$



This relation has been verified experimentally by Zuber (1925).

In order to extend the theory to the case of rising overvoltage, it is necessary to make some approximations:

If  $\gamma$  and  $W$  are small at small overvoltage  $\Delta V$ , then

$$M \simeq -\frac{1}{W} \log(1 - W) \simeq 1 + \frac{1}{2}W.$$

Using a method of Schade (1938), it follows approximately that

$$\begin{aligned} M &= \gamma [\exp \{(\alpha_B + \Delta\alpha)(d - d_0)\} - 1] \\ &\simeq \gamma [\exp \{\alpha_B(d - d_0)\} - 1] + \gamma \exp \{\alpha_B(d - d_0)\} \frac{\Delta\alpha}{\Delta E} \Delta E(d - d_0) \\ &\simeq 1 + \frac{\partial\alpha}{\partial E} \Delta V. \end{aligned} \quad \dots\dots(18)$$

Thus

$$W \simeq 2 \frac{\partial\alpha}{\partial E} \Delta V \simeq 2 \frac{\partial\alpha}{\partial E} \frac{dV}{dt} t = \frac{\partial W}{\partial t} t. \quad \dots\dots(19)$$

Therefore the probability of breakdown after a time  $t_s$  with the applied potential rising linearly from the normal breakdown value, is

$$f_2(t) = \exp \left\{ -\frac{1}{2} q_e (\partial W / \partial t) t_s^2 \right\} = \exp \left\{ -\frac{1}{2} (t_s / t_m)^2 \right\}. \quad \dots\dots(20)$$

The probability of breakdown occurring in an interval between  $t_s$  and  $t_s + dt_s$  is given by

$$f_2'(t) dt_s = -\frac{t_s}{t_m} \exp \left\{ -\frac{1}{2} (t_s / t_m)^2 \right\} d(t_s / t_m) \quad \dots\dots(21)$$

with a maximum occurring at  $t_s = t_m$ .

The functions  $f_1$  and  $f_2$  are represented in Figure 6 in terms of their characteristic time constants,  $t_0$  and  $t_m$  respectively.

Function  $f_2$  is only valid for small values of overvoltage and cannot be applied where the overvoltage becomes large. It is further restricted if the electrons do not occur singly but in  $b$  bursts of  $r$  electrons each. The factor  $q_e$  must then be replaced by  $br$  and  $W$  by  $W_r = 1 - (1 - W)^r$ . Whilst  $W$  (and therefore  $\Delta V$ ) is very small this does not differ much from  $f_2$  since  $b(\partial W_r / \partial t) = br(\partial W / \partial t) = q_e(\partial W / \partial t)$ , but  $W_r$  soon approaches unity and the function goes over into a form similar to  $f_1$ . A better approximation at larger overvoltages may be made by assuming  $W$  to have the form  $W = 1 - \exp(-t/T)$ , where  $T$  is approximately determined by finding the value of  $\Delta V_T$  which corresponds to  $W = 1 - e^{-1}$ , giving  $T = \Delta V_T / (dV/dt)$ .

The probability of breakdown for electrons occurring singly then becomes

$$f_{3a}(t) = \exp[-q_e \{t_s - T(1 - \exp(-t_s/T))\}]. \quad \dots\dots(22)$$

If the average number of electrons formed simultaneously is  $r$  with  $b$  bursts per second,

$$f_{3b}(t) = \exp[-b \{t_s - (T/r)(1 - \exp(-rt_s/T))\}]. \quad \dots\dots(23)$$

The probabilities of breakdown in any particular interval may be found by differentiation and it is found that maxima occur at the following values corresponding to equations (22) and (23) respectively:

$$f_{3a}: \quad t_s/T = \log \frac{2q_e T}{2q_e T + 1 - \sqrt{(4q_e T + 1)}}, \quad \dots\dots(24)$$

$$f_{3b}: \quad t_s/T = \frac{1}{r} \log \frac{2bT/r}{2bT/r + 1 - \sqrt{(4bT/r + 1)}}. \quad \dots\dots(25)$$

Some general curves representing  $f_{3a}$  and  $f_{3b}$  are shown in Figure 7(a). In these  $q_e T = brt = 2$  is constant and  $r$  is varied. For any other value of  $q_e T$  the probability is just raised to a proportional power.

It is evident that already with bursts of 10 electrons at a time the curve  $f_{3b}$  approaches closely the exponential curve  $\exp(-bt_0)$ .

Thus the transition is fairly rapid from one shape of probability curve to the other. The form of the statistical distribution curve will indicate the way in which the primary electrons are produced. Where these electrons are due to emission from the cathode, they are independent of each other and therefore the distribution represented by  $f_{3a}$  is to be expected.

When the primary electrons are produced by  $\alpha$ -particles, they will occur in groups, each particle giving rise to a whole train of electrons which are simultaneous for most practical purposes, so that  $f_{3b}$  should be applicable.

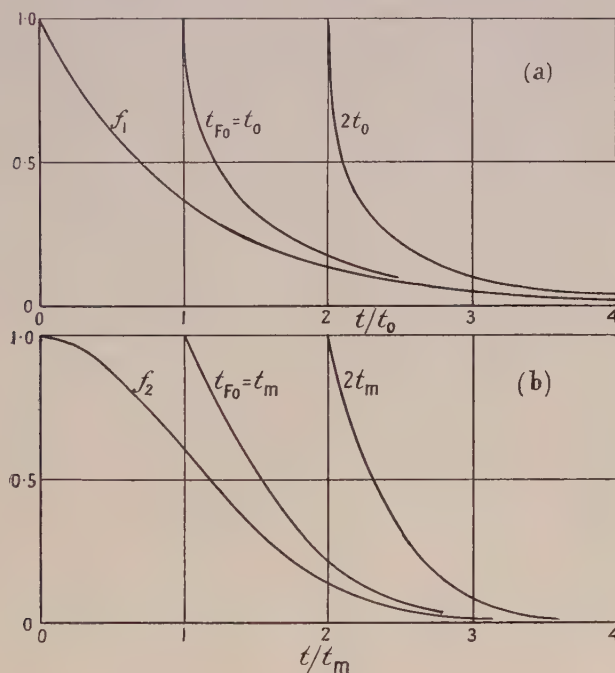


Figure 6. Statistical time delay probability curves  $f_1$  and  $f_2$  and curves of combined statistical and formative time delays.

Ionization by other types of radiation does not usually give rise to a closely spaced group of electrons and the distribution will tend to approximate to the case of single electrons.

Electrons which are produced in the body of the gas are less effective than electrons emitted from the cathode. The probability function  $W$  is based on the latter and in the case of gas ionization it may be shown that  $W$  must be divided by  $\eta(V - V_0)$  to compensate for this fact.

Some interesting experiments have been carried out in order to determine statistical delay time when a discharge tube was kept in total darkness away from radioactive sources. The only external source of ionizing radiation could have been cosmic rays and the very feeble natural radioactivity of materials.

The experimental tubes used were small sealed-off diodes with potassium activated cathodes and argon filling at 18 mm. Hg pressure. These were of the parallel plane electrode type, electrodes spaced 0.06 in. apart and  $\frac{1}{4}$  in. in diameter.

It was found that primary electrons far in excess of those to be expected from the above-mentioned causes were present in the tube when the breakdown potential was measured at intervals of three seconds. On increasing the interval between measurements to 90 seconds, the primary electrons were much less, showing that the short discharge occurring at each measurement had some influence on the subsequent time delay. Between measurements the inter-electrode field was reduced to zero.

Representative curves are shown in Figure 7(b). The distribution curve for measurements at 3 second intervals yields a calculated rate of primary electron

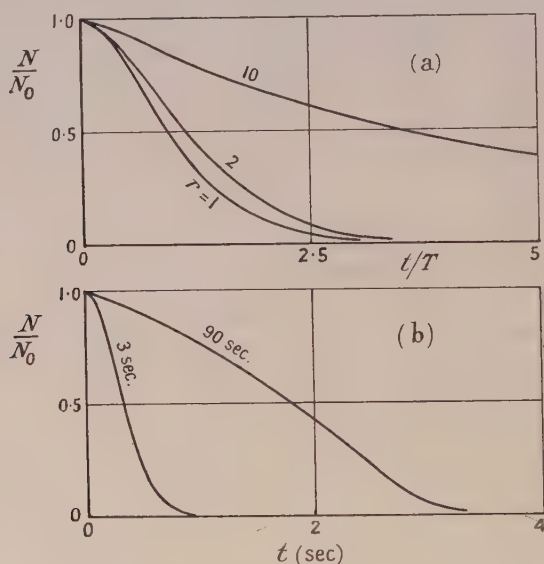


Figure 7.

- (a) Statistical time delay probability curves  $f_{3a}$  and  $f_{3b}$ .  
 (b) Experimental statistical distribution curves with different intervals between measurements. (Rate of voltage rise—40 v/sec.)

production of about 5 per second. With 90 second intervals the rate is about one electron in two seconds, whereas the number which will be produced naturally is of the order of one per minute.

This effect may be attributed to continued emission from the cathode after extinction of a discharge, as Paetow (1939) has shown. He found that this continued emission was still appreciable after 50 seconds and that it was probably due to small specks of impurity on the cathode which acquired charges during discharge and afterwards caused electron emission due to the high fields set up. It is probable that even on high purity potassium such specks may exist and give rise to this persistent emission which was still noticeable when the interval between small measurement discharges was 90 seconds.

Paetow found that the emission was very large immediately after stopping a discharge, partly due to metastable action which became negligible after about a second and thereafter due to this after-effect only.



## § 7. FORMATIVE TIME DELAY

When statistical time delay is reduced to negligible proportions by sufficient primary electrons, the discharge will not take place instantaneously on application of sufficient overvoltage, since it takes a definite time for the current to increase to the point at which conduction is appreciable.

This formative time delay has been dealt with by Schade (1936-37) for the case of constant overvoltage, yielding the following expression:

$$t_F = t_i \frac{M}{M-1} \log \left\{ \frac{1 + (M-1)j_{ke}/j_{k0}}{M} \right\}. \quad \dots\dots (26)$$

The main cause of the delay in current increase is the average transit time of positive ions from their points of creation to the cathode. The primary electron current density at the cathode is  $j_{k0}$  and the final cathode electron current density  $j_{ke}$  and their ratio which is included in the logarithmic term has a minor effect on the formative time delay.

The expression for formative delay has not previously been derived for the case of rising applied potential and will be developed below.

By the method used before in equation (18) it is possible to show that

$$M-1 \simeq \frac{\partial \alpha}{\partial E} \Delta V_F = \frac{\partial \alpha}{\partial E} \frac{dV}{dt} t_F.$$

For small overvoltages  $(M-1)$  will be small and the time delay will be approximately inversely proportional to the average value of  $(M-1)$ , according to equation (26).

If the overvoltage rises linearly, the average overvoltage will be half of the final value reached

$$(M-1)_{av} \simeq \frac{1}{2} \frac{\partial \alpha}{\partial E} \frac{dV}{dt} t_{F0},$$

and from equation (26)

$$t_{F0} = \frac{2t_i}{(\partial \alpha / \partial E)(dV/dt)t_{F0}} \log \{1 + (M-1)_{av} j_{ke}/j_{k0}\},$$

giving

$$t_{F0} = \left[ \frac{1}{dV/dt} \frac{2t_i}{\partial \alpha / \partial E} \log \{1 + (M-1)_{av} j_{ke}/j_{k0}\} \right]^{\frac{1}{2}}. \quad \dots\dots (27)$$

The final overvoltage will therefore be

$$\Delta V_m = \left[ \frac{dV}{dt} \frac{2t_i}{\partial \alpha / \partial E} \log \{1 + (M-1)_{av} j_{ke}/j_{k0}\} \right]^{\frac{1}{2}}. \quad \dots\dots (28)$$

The terms in the logarithmic function can cause very little variation so that it follows approximately that

$$t_{F0} \propto (dV/dt)^{-\frac{1}{2}}, \quad \Delta V_m \propto (dV/dt)^{\frac{1}{2}}. \quad \dots\dots (29)$$

On deriving the expression more rigorously from Schade's (1936-37) differential equation, the result is

$$t_{F0} = \left[ \frac{1}{dV/dt} \frac{2t_i}{\partial \alpha / \partial E} \log \left\{ j_{ke}/j_{k0} \left( 1 + \left( \frac{2}{\pi} \frac{\partial \alpha}{\partial E} \frac{dV}{dt} t_i \right)^{\frac{1}{2}} \right)^{-1} \right\} \right]^{\frac{1}{2}}. \quad \dots\dots (30)$$

There is not much difference when compared with equation (27) which may therefore be used.

The limiting formative time delay when  $(M-1)$  tends to zero becomes (Schade 1936-37)

$$\lim_{M \rightarrow 1} t_{F0} = t_i j_{ke} / j_{k0} \quad \dots\dots (31)$$

The average distance through which positive ions move to the cathode may be found by integrating over the whole discharge gap, yielding

$$d_{av} = d \left\{ \frac{e^{\alpha d}}{e^{\alpha d} - 1} - \frac{1}{\alpha d} \right\} \quad \dots\dots (32)$$

This is for plane parallel electrodes so that the average transit time is

$$t_i = \frac{p_0 d}{K_i V_a} d_{av} = \frac{d_{av}}{K_i E / p_0} \quad \dots\dots (33)$$

In the case of a concentric diode in which the anode radius  $R_a$  is much smaller than the cathode radius  $R_c$ , the average transit time is approximately

$$t_i = \frac{R_c - R_a}{2 K_i E_c / p_0}, \quad \dots\dots (34)$$

where  $E_c$  is the field strength at the cathode.

There is some experimental confirmation of the equation (28) in that the linear portions of measured curves have slopes which correspond well with the calculated values.

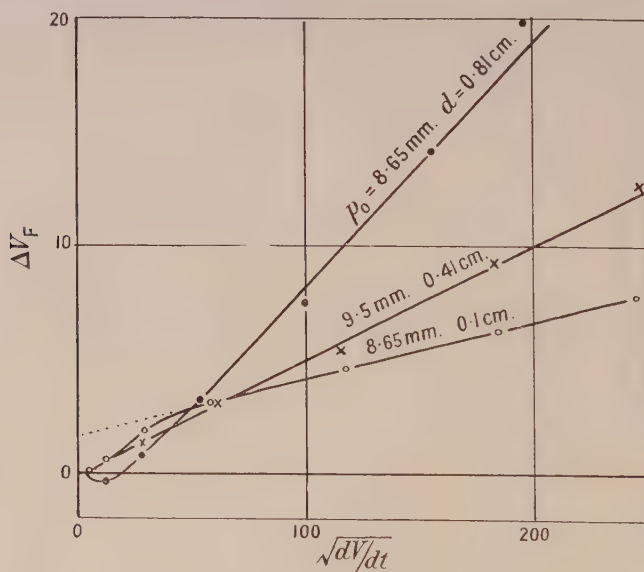


Figure 8. Experimental formative overvoltage curves at various values of  $p_0$  and  $d$ . The linear portions correspond well with the theoretical calculations.  $dV/dt$  expressed in v/sec.

Figure 8 shows typical curves from which it is evident that in general the initial portions of the curves do not conform to the theory but that the curves have a constant slope over most of the range of rate of voltage rise.

The expected slope of an experimental curve is  $\Delta V_m / \sqrt{(dV/dt)}$ , from equation (28).

Assuming  $\log \{1 + (M-1)_{av} j_{k0}/j_{k0}\}$  to be approximately constant at 18 and taking  $\partial \alpha / \partial E$  from Figure 9 (Kruithof 1940) the following table may be drawn up for argon and 6 cm. diameter potassium-activated electrodes to compare experiment with theory:

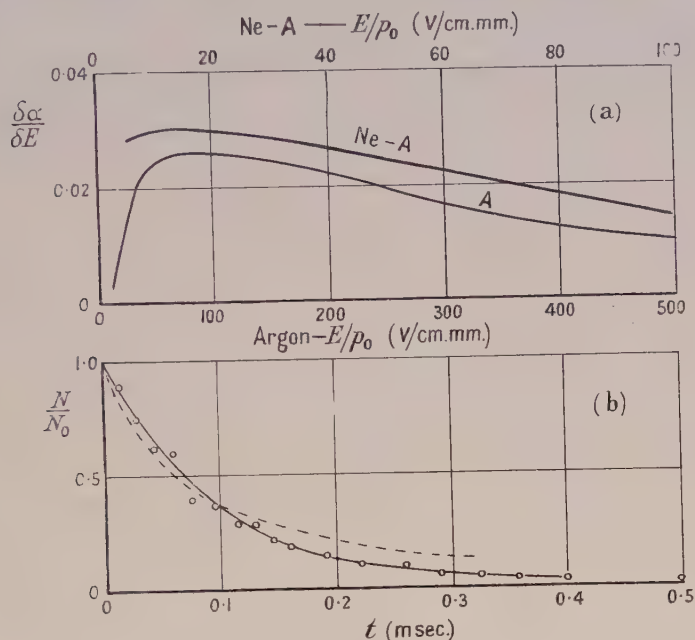


Figure 9. (a) The factor  $\partial \alpha / \partial E$  for argon and for a mixture of 93.4% neon with 6.6% argon. (b) Experimental distribution curve showing the effect of combined statistical and formative delays.

$p_0$	Experimental			Theoretical Slope
	$d$	$t_i$	Slope	
4.56	0.104	0.17	0.023	0.017
	0.195	0.53	0.031	0.028
	0.405	1.74	0.050	0.049
	0.8	4.95	0.086	0.083
9.5	0.1	0.29	0.025	0.020
	0.2	0.89	0.035	0.035
	0.41	2.74	0.065	0.064
8.65	0.1	0.27	0.025	0.020
	0.2	0.84	0.036	0.034
	0.41	2.58	0.050	0.061
	0.81	7.05	0.114	0.107

Mobility of argon positive ions at 1 mm. Hg =  $2.1 \times 10^3$  cm/sec/volt/cm.

The theory thus finds some justification in practice except at small overvoltage where more factors seem to be present than those which have been taken into account. The order of overvoltage calculated is correct and the theory may therefore be applied with reasonable accuracy.

This formative delay is not a variable quantity in a fully symmetrical discharge gap and may therefore be allowed for in cases where it becomes important.



## § 8. COMBINED STATISTICAL AND FORMATIVE DELAYS

If average statistical and formative delays are of the same order, an expression may be derived in order to take this into account for rising potential.

With statistical time delay, a certain time elapses before the discharge is initiated and therefore the overvoltage will reach a value  $\Delta V_s$  before the formative period begins.

Let the increase of overvoltage during the formative period be  $\Delta V_F$ . Then the average overvoltage during this period is  $\Delta V_s + \frac{1}{2}\Delta V_F$ .

The formative time delay is therefore given by equation (26) as

$$t_F = \frac{1}{\Delta V_s + \frac{1}{2}\Delta V_F} \cdot \frac{2t_i}{\partial \alpha / \partial E} \log \{1 + (M-1)_{av} j_{ke}/j_{k0}\},$$

$$\Delta V_F = \frac{dV}{dt} t_F = \frac{\Delta V_{F0}^2}{\Delta V_s + \frac{1}{2}\Delta V_F},$$

where  $V_{F0}$  is the formative overvoltage when  $V_s = 0$ .

The solution to the above equation is

$$\Delta V_F = -\Delta V_s + \{\Delta V_s^2 + \Delta V_{F0}^2\}^{\frac{1}{2}}. \quad \dots\dots (35)$$

The total overvoltage is

$$\Delta V = \Delta V_s + \Delta V_F = \{\Delta V_s^2 + \Delta V_{F0}^2\}^{\frac{1}{2}}, \quad \dots\dots (36)$$

$$t = \{t_s^2 + t_{F0}^2\}^{\frac{1}{2}}. \quad \dots\dots (37)$$

The statistical probability curves  $f_1$  and  $f_2$  are modified as shown in Figure 6 when the formative time delays are of the same order as the statistical delay time constants  $t_0$  and  $t_m$  (see equations (17) and (20)).

A typical statistical distribution of points for combined delay times is shown in Figure 9(b), as measured on a small concentric diode containing 15 mm. argon and about  $1 \mu\text{gm.}$   $\gamma$ -equivalent radioactive material to provide primary ionization. The measured formative time delay at a rate of voltage rise of  $3 \times 10^4$  volts/sec. was about 0.25 millisecond. The solid curve was fitted at the ordinate  $e^{-\frac{1}{2}}$  to correspond to a modified  $f_2$  probability curve with  $t_{F0} = 2t_m$ . The broken curve was fitted at the ordinate  $e^{-1}$  and corresponds to a modified  $f_1$  probability curve with  $t_{F0} = t_0$ . No better fit is possible with this latter type of distribution and it thus seems as if the  $f_2$  type of distribution given in equation (20) gives a very good fit. This is however not what would be expected if the  $\alpha$ -particles created groups of electrons containing about 50 electrons each as they should do in this case.

The number of primary electrons occurring per second on calculating with the  $f_2$  type of distribution is about  $4 \times 10^4$  per second, which is of the order of the number of  $\alpha$ -particles to be expected per second.

Theoretically the curve should follow the  $f_1$  type of distribution which in this case does not seem to be confirmed. Other tubes show similar curves which means that there may be a further factor to take into account.

## ACKNOWLEDGMENTS

Acknowledgments are due to Messrs. Ferranti Limited, who have provided the facilities for carrying out this work, and to the Admiralty who have sponsored the development and have given permission for the publication of this paper.

## REFERENCES

- HERTZ, G., 1927, *Z. Phys.*, **46**, 177 ; 1937, *Ibid.*, **106**, 102.  
 HUXFORD, W. S., and ENGSTROM, R. W., 1940, *Phys. Rev.*, **58**, 67.  
 KRUTHOF, A. A., 1940, *Physica*, **7**, 519.  
 VON LAUE, M., 1925, *Ann. Phys., Lpz.*, **76**, 261.  
 LOEB, L. B., 1939, *Fundamental Processes of Electrical Discharge in Gases* (New York : John Wiley).  
 MCCALLUM, S. P., and KLATZOW, L., 1934, *Phil. Mag.*, **17**, 291.  
 MEILI, E., 1945, *Helv. Phys. Acta*, **18**, 79.  
 MIERDEL, G., and STEENBECK, M., 1937, *Z. Phys.*, **106**, 311.  
 NEWTON, R. R., 1948, *Phys. Rev.*, **73**, 570.  
 OLIPHANT, M. L. E., 1929, *Proc. Roy. Soc. A*, **124**, 228 ; 1930, *Ibid.*, **127**, 373.  
 PAETOW, H., 1939, *Z. Phys.*, **111**, 770.  
 PENNING, F. M., 1930, *Proc. K. Ned. Akad. Wet. Amst.*, **33**, 841 ; 1933, *Physica*, **5**, 268.  
 PENNING, F. M., and DRUYVESTEYN, M. J., 1940, *Rev. Mod. Phys.*, **12**, 87.  
 POSE, H., 1928-9, *Z. Phys.*, **52**, 428.  
 ROGOWSKI, W., 1940, *Z. Phys.*, **115**, 257.  
 SCHADE, R., 1936-7, *Z. Phys.*, **104**, 487 ; 1938, *Ibid.*, **108**, 353.  
 THOMSON, J. J., 1928, *Conduction of Electricity through Gases* (Cambridge : University Press), **1**, 466.  
 ZUBER, K., 1925, *Ann. Phys., Lpz.*, **76**, 231.

## The Behaviour of Multiple Circuit Magnetrons in the Neighbourhood of the Critical Anode Voltage

BY W. E. WILLSHAW AND R. G. ROBERTSHAW

Research Laboratories of The General Electric Company, Limited, Wembley, Middx.

*MS. received 30th June 1949*

**ABSTRACT.** It is pointed out that the mechanism of operation of the multiple circuit magnetron oscillator in the region of minimum magnetic field and voltage, where the efficiency is commonly assumed to approach zero, should approach that of an oscillator of the travelling wave tube type, providing that a cathode of suitable size is used. Useful efficiencies should thus be obtainable under these conditions.

Details of experiments are given in which an electronic efficiency of 12% was obtained at a wavelength of 3 cm. at values of magnetic field and voltage several times lower than those used for high efficiency operation. The mode of operation was determined by the value of the magnetic field, a given mode being maintained over a range of magnetic field of the order of 8%. The anode voltage was about 70% of the critical value.

The experimental results generally support the hypothesis and suggest that the minimum voltage regime should be of extreme importance for work at the highest radio frequencies.

### § 1. INTRODUCTION

THE main characteristics of performance of the high efficiency multiple circuit magnetron oscillator are well known. Operation in one mode starts at minimum values of magnetic field strength and anode voltage, and continues with increasing efficiency as these parameters are increased. In the higher efficiency region it is assumed that electrons interacting favourably with the oscillating field leave the main electron cloud, which extends only part of the way from cathode to anode, and being gradually focused into tight bunches finally arrive at the anode with a velocity which is the same as that of a rotating wave component of the anode field. On this assumption a very good approximation to the observed efficiency is derived directly, i.e.  $\eta = 1 - \frac{1}{2} m \Omega^2 a^2 / e V$ .

where  $\Omega$  is the rotating wave angular velocity,  $a$  the anode radius, and  $V_a$  the anode voltage (Willshaw and Rushforth 1946). Change of mode, giving a change in  $\Omega$  may occur at any value of magnetic field strength as  $V_a$  is changed in order to change current. For the lower efficiency region, where the anode voltage and magnetic field strength are much lower, the main electron cloud extends much nearer to the anode, so that electrons leaving it do not have time to be formed into bunches before reaching the anode, and to acquire the velocity of the rotating wave component. Thus the observed efficiency is much lower than that given by the above expression.

## § 2. BEHAVIOUR NEAR THE CRITICAL VOLTAGE

At the limiting lower values of magnetic field and anode voltage the electron cloud extends quite close to the anode surface, and there is experimental evidence to show that in the absence of oscillations electrons may describe circular paths which are coaxial with the anode cylinder (Wassermann 1948). Now the electron velocity at radius  $r$  is  $eH/2m(1 - b^2/r^2)$ ,  $H$  being the magnetic field strength, and  $b$  the cathode radius. If the radius of the cathode is not too large relative to that of the anode, this velocity will vary very little in the neighbourhood of the anode. The variation in electron density in the neighbourhood of the anode is similarly small, being proportional to  $1 + (b/r)^4$ . Conditions are thus similar to those in a travelling wave tube (Kompfner 1947), in that there is a stream of electrons of given velocity and density passing across the mouths of several cavities and therefore capable of interacting with the fields due to oscillations in these cavities. By direct analogy there is then the possibility of oscillations being generated when the electron velocity close to the anode is equal to the velocity of the wave generated in the anode circuit. This condition will obtain when  $(eH/2m)(1 - b^2/r_m^2) = \Omega = (2eV_a/m)^{1/2}$  where  $r_m$  is the maximum radius reached by the space charge. A change in mode of oscillation corresponding to a change in  $\Omega$  should result when  $H$  or  $V_a^{1/2}$  are correspondingly changed, this being in distinct contrast to the behaviour in the high efficiency region. We shall call this the 'minimum voltage' regime of operation.

## § 3. EXPERIMENTAL PERFORMANCE IN THE MINIMUM VOLTAGE REGIME

Some experiments have recently been carried out in the minimum voltage regime with a magnetron having 28 cavities of the 'rising sun' form (Hollenberg, Kroll and Millman 1948) with a circuit ratio of 2.25/1, anode diameter of 16 mm., cathode diameter of 3 mm., and wavelength of  $\pi$  mode of 3.31 cm. Figure 1. This valve, fitted with a much larger cathode (11.5 mm. dia.) had previously been designed and used for high power operation with an anode voltage of the order of 15 kv., magnetic field of 2,500 oersteds and efficiency of 20%. Figure 2 shows the relationship between anode voltage and mean current for the minimum voltage regime for a range of magnetic field values, and contours of constant power output are included. The valve was operated with a 50 c/s. voltage applied to the anode through a 5,000 ohm series resistance so that current passed for approximately one fifth of the time. The corresponding wavelength of operation is shown together with the mode number  $n$  of the wave component with which the electron is interacting. The mode number is physically the number of



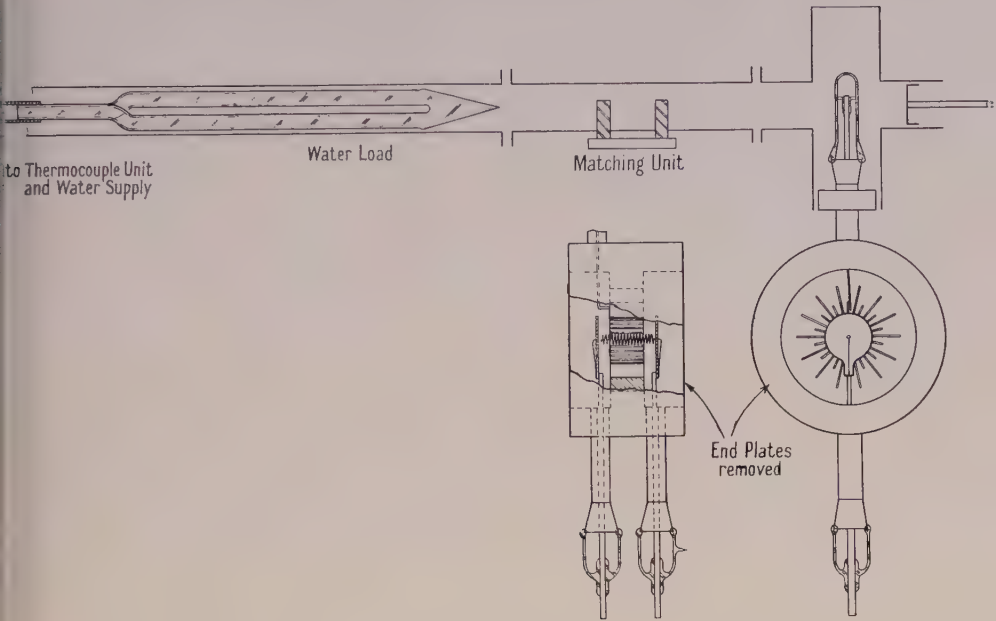


Figure 1. Rising sun magnetron for 3.3 cm. wavelength, and water load.

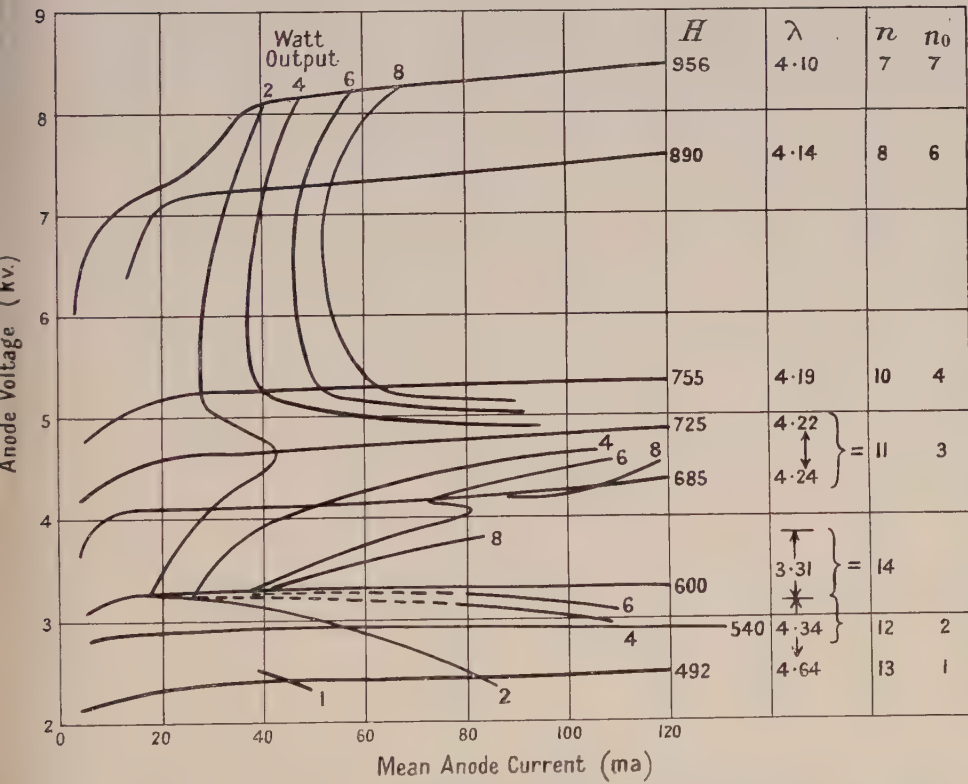


Figure 2. Variations of anode current and mode of operation with anode voltage and magnetic field strength. ( $H$ =magnetic field strength in oersteds,  $\lambda$ =wavelength in cm.,  $n_0$ =fundamental mode number,  $n$ =wave component mode number.)

times a wave is repeated round the circumference of the anode (Willshaw *et al.* 1946). The mode number  $n_0$  shown in the Figure is the fundamental mode of which  $n$  is a component. It can be seen that the mode of oscillation depended entirely in the magnetic field, and oscillations are maintained in a given mode over a range of magnetic field of the order of 8%, a maximum efficiency of 60%

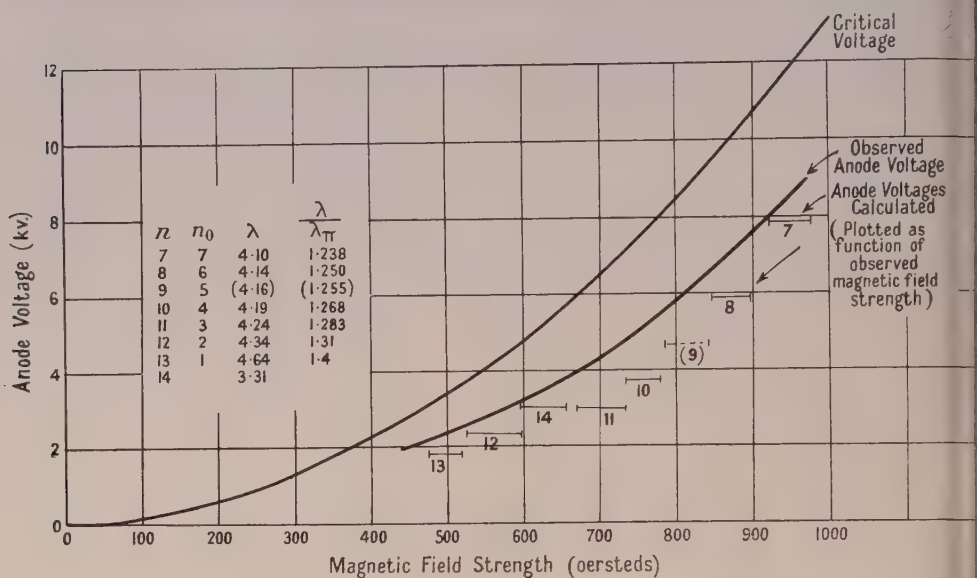


Figure 3. Relation between the observed and calculated anode voltage and magnetic field strength.

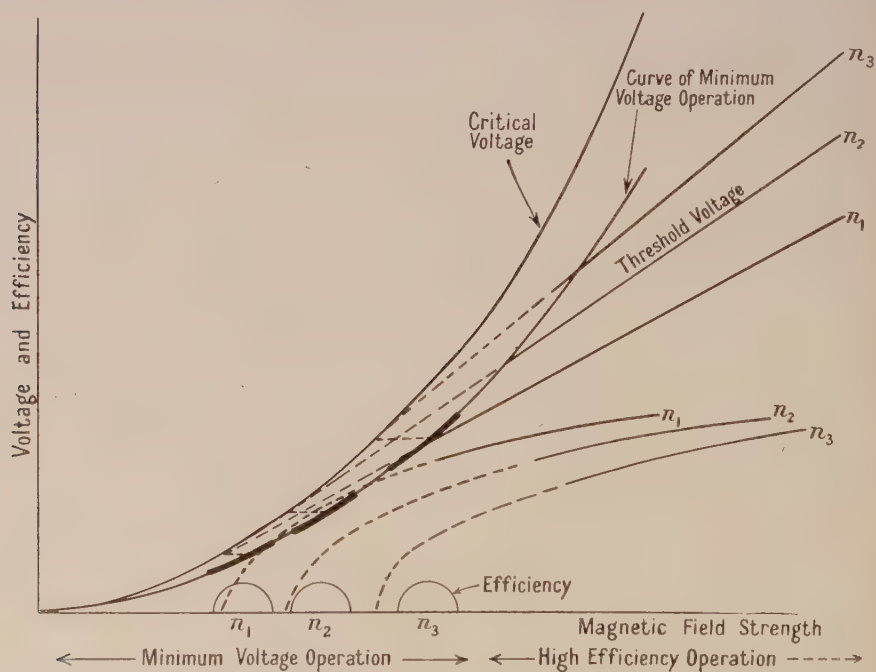


Figure 4. Relation between voltage, efficiency and magnetic field strength for minimum voltage and high efficiency operation.

being obtained in the mode  $n=14$ . The electronic efficiency in this mode, estimated from the ratio between power dissipated in the load and in the valve circuit, is 12%. In contrast to this, when operating as a higher efficiency pulsed valve, at an anode voltage of about 15 kv., oscillations are obtained in the mode  $n=14$  (the  $\pi$  mode) over a wide range of magnetic field strength, as is usual for valves operated in this regime. Figure 3 shows the observed operating voltages plotted as a function of magnetic field, together with the values calculated for the different modes of operation on the hypothesis of the minimum voltage regime, assuming that the outside of the electron cloud reaches the surface of the anode so that  $r_m = a$ . These calculated voltages are plotted as a function of the magnetic fields at which oscillations are observed and are rather lower than the observed voltages. The critical voltages are also indicated and it is seen that operation takes place at voltages which are roughly 70% of these. Finally Figure 4 shows diagrammatically the relationship between the various parameters for the high efficiency and minimum voltage regimes of operation. The dotted extensions of the curves of high efficiency represent the values calculated from the simple expression mentioned earlier, the practical values lying much below these and falling to zero at a magnetic field greater than that at which 'minimum voltage' operation occurs.

#### § 4. FIELD OF APPLICATION

It is evident from the results which have so far been achieved that useful efficiency may be obtained with a multiple circuit magnetron operating like a travelling wave tube in the minimum voltage regime. Values of anode voltage and magnetic field are several times smaller than for the high efficiency regime. The size of the valve for a given voltage is thus a maximum, and this fact and the low magnetic field involved make this mode of operation of extreme importance for work at the shortest wavelengths.

#### REFERENCES

- HOLLENBERG, A. V., KROLL, N., and MILLMAN, S., 1948, *J. Appl. Phys.*, **19**, 624.  
KOMPFFNER, R., 1947, *Proc. Inst. Radio Engrs.*, N.Y., **35**, 124.  
WASSERMANN, I. I., 1948, *J. Tech. Phys.*, USSR, **18**, 785.  
WILLSHAW, W. E., and RUSHFORTH, L., 1946, *J. Instn. Elect. Engrs.*, **93**, IIIA, 180.  
WILLSHAW, W. E., *et al.*, 1946, *J. Instn. Elect. Engrs.*, **93**, IIIA, 985.



## Measurements of the Reflection Coefficient of Water at a Wavelength of 8.7 mm.

By D. G. KIELY

Royal Naval Scientific Service

*Communicated by L. H. Bainbridge-Bell ; MS. received 25th April 1949,  
and in amended form 3rd August 1949*

**ABSTRACT.** An account is given of measurements (carried out in March 1947) of the reflection coefficient of water at a wavelength of 8.7 mm. over a range of angles of incidence.

The method employed is to measure the relative field strengths of the direct waves and waves reflected from a trough of water using free-space propagation and high-gain aerials.

The following electrical constants of water have been computed from the measured results (water temperature  $11.1^{\circ}\text{C.}$ ): refractive index  $4.40 \pm 0.24$ , dielectric constant  $10.86 \pm 2.21$ , absorption coefficient  $2.91 \pm 0.06$ , conductivity/frequency  $12.82 \pm 0.42$ , Brewster angle  $79^{\circ}$ .

### § 1. INTRODUCTION

THIS note describes some experimental work carried out at a wavelength of 8.7 mm. to determine the reflection coefficient, conductivity, dielectric constant and absorption coefficient of water. The reflection coefficient was measured for different angles of incidence, and from these results the other constants were calculated. At this wavelength the problem of measuring the reflection coefficient was considered more optical than radio in nature and the method employed was to measure the relative field strengths of direct and reflected free-space waves using high-gain (narrow beam width) aerials and a trough of water.

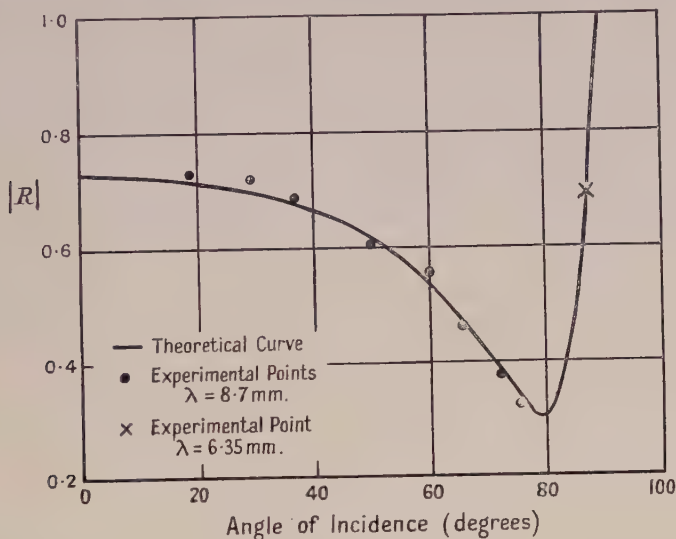
### § 2. DESCRIPTION OF APPARATUS

The experimental apparatus consisted of a transmitter and receiver, mounted on metal racks, which allowed the heights of the aerials to be varied, above a trough of water placed between them. The horizontal distance between the receiver and the transmitter was maintained constant and the total variation in height of either aerial above the water surface was approximately 4 feet. The trough dimensions were 8 ft. 9 in. by 3 ft. The aerials and radio-frequency circuits were mounted on tilting platforms attached to the racks; this allowed them to be pointed down at the water surface or directly across it. The beam width was sufficiently small for the direct and reflected rays to be received independently. Polarization was vertical.

### § 3. EXPERIMENTAL PROCEDURE

The horizontal distance between the receiving and the transmitting aerials was kept fixed. The heights of the two aerials were adjusted so that for each angle of incidence the aerials were directed at the centre of the trough. The experimental procedure was extremely simple and straightforward. The power was switched on, 30 minutes was allowed for the klystrons to become warm and stable in frequency, the transmitter and receiver were tuned, and the receiver gain was turned to a suitable level. For each angle of incidence a direct transmission across the trough

as received, and the receiver output,  $V_1$ , and the transmitter power monitor reading noted. The aeriels were then set to the required angle of incidence, the reflected wave received, receiver output  $V_2$  noted and the transmitter power monitor reading checked. This was repeated several times for each angle of incidence and the average value of  $V_1$  and  $V_2$  obtained. Only very small variations in  $V_1$  and  $V_2$  were noted in these repetitions. A correction was made in the value of  $V_2$  for the difference in path length for direct and reflected waves using the inverse-distance law to give  $V_3$ ; the ratio  $V_3/V_1$  was then equal to  $|R' + iR''|$ , the modulus of the reflection coefficient,  $R'$  and  $iR''$  being the real and imaginary components. The water temperature during the measurements was  $11.1^\circ\text{C}$ . The experimental results are shown in the Figure as a function of angle of incidence. The point



at  $87.5^\circ$  was obtained at a wavelength of 6.35 mm. by reflections from the sea during another experiment. This point has not been used in the following theoretical work.

An experiment was carried out to check the validity of the inverse-distance law of propagation for the distances involved in the above work. This experiment showed that the inverse-distance law was valid for the six measurements from  $37.5^\circ$  to  $76^\circ$ , but was not strictly valid for the two measurements at  $19^\circ$  and  $30^\circ$  incidence. These two observations have not been used in the following calculations.

#### § 4. THEORETICAL ANALYSIS OF RESULTS

The symbols used are as follows:  $\mu^2$  = complex dielectric constant of water,  $n$  = real part of refractive index of water,  $\epsilon$  = real part of dielectric constant of water,  $\kappa$  = absorption coefficient of water,  $f$  = frequency of radiation,  $R = R' + iR''$  = complex coefficient of reflection of water,  $\theta$  = angle of incidence,  $\phi$  = complex angle of refraction,  $\sigma$  = conductivity of water.

It is suspected that  $\epsilon \gg 1$  and  $\sigma/f \gg 1$ . Now

$$\epsilon - i \frac{2\sigma}{f} = \mu^2 = (n - i\kappa)^2. \quad \dots\dots(1)$$

If  $\sin \phi = \mu^{-1} \sin \theta$ , the reflection coefficient is

$$|R| = \left| \frac{\mu \cos \theta - \cos \phi}{\mu \cos \theta + \cos \phi} \right|. \quad \dots\dots (2a)$$

Now, as there is *a priori* reason to suspect that  $|\mu^2| = |\epsilon - i(2\sigma/f)| \gg 1$ , and since  $\sin \theta < 1$ ,

$$\cos \phi = \sqrt{1 - \frac{\sin^2 \theta}{\mu^2}} = 1 - \frac{1}{2} \frac{\sin^2 \theta}{\mu^2} + \dots \quad \dots\dots (2b)$$

and the error in adopting this approximation will be at the most of the order of 2%. Hence

$$|R^2| = \frac{|\mu^2| \cos^2 \theta + 1 - 2n \cos \theta}{|\mu^2| \cos^2 \theta + 1 + 2n \cos \theta}.$$

Let

$$y = \frac{1 + |R^2|}{1 - |R^2|} = \frac{|\mu^2| \cos^2 \theta + 1}{2n \cos \theta}, \quad \dots\dots (3)$$

i.e.

$$y = ax + b/x, \quad \dots\dots (3a)$$

where  $x = \cos \theta$ ;  $a = |\mu^2|/2n$ ;  $b = 1/2n$ . In order to determine the best values of  $a$  and  $b$ , the method of least squares was adopted with suitable weighting factors. This gives the values  $a = 3.163 \pm 0.065$ ;  $b = 0.114 \pm 0.006$ .

Having found  $a$  and  $b$ , the physical constants for water were obtained as follows:

$$\begin{aligned} n &= 1/2b &= 4.40 \pm 0.24, \\ \epsilon &= 1/2b^2 - a/b &= 10.86 \pm 2.21, \\ \kappa &= \sqrt{(a/b - 1/4b^2)} &= 2.91 \pm 0.06, \\ \sigma/f &= (1/2b^2) \sqrt{(4b - \frac{1}{4})} &= 12.82 \pm 0.42. \end{aligned}$$

Using the values of  $a$  and  $b$ , a curve of  $|R|$  against  $\theta$  was computed from (3a). This is shown in the Figure by the experimental points. The Brewster angle, obtained by differentiation of (3a), to give the minimum value of  $|R|$  is found to be  $79^\circ$ , as indicated in the curve. The experimental point at  $87.5^\circ$  incidence is in good agreement with the theoretical curve, which indicates that there is possibly little difference between the constants governing reflection from water at 8.7 and 6.35 mm.

Saxton (1947) gives theoretical curves of the variation of absorption coefficient and refractive index of water with wavelength and temperature. Comparing the above experimental results with these curves it will be seen that the agreement is quite good when the temperature difference is taken into consideration.

#### ACKNOWLEDGMENTS

This work was carried out for the Royal Naval Scientific Service, and permission to publish this paper is gratefully acknowledged.

The author wishes to acknowledge the assistance of his colleagues with the theoretical and experimental work carried out for the production of this paper.

#### REFERENCE

SAXTON, J. A., 1947, *Meteorological Factors in Radio-Wave Propagation* (London: Physical Society), p. 278.



# Coupling of the Ordinary and Extraordinary Rays in the Ionosphere

By T. L. ECKERSLEY \*

*Communicated by G. I. Finch; MS. received 8th March 1949,  
in amended form 23rd June 1949*

**ABSTRACT.** In this paper an approximate solution to the wave equation is given for propagation in an ionosphere in which the gradient of the density  $N$  is in the vertical,  $z$ , direction only, and in which account is taken of the earth's magnetic field. It corresponds exactly to the ray theory and expresses a quantity  $Z$ , which is the  $z$  derivative of the phase function  $S$ , by a quartic equation.  $Z$  can be represented as a function of  $\zeta$  (which is proportional to  $N$ ) on a four-sheeted Riemann surface, and the branch points are studied for the case of vertical incidence for which  $Z$  becomes the refractive index. By considering the branch points in the complex  $\zeta$  plane, the amount of the coupling between the ordinary and the isolated extraordinary branches of the  $(Z, \zeta)$  curves can be expressed as a function of the obliquity of the magnetic field. The triple splitting of rays reflected from the ionosphere, observable where the field is nearly vertical, can thus be explained, and the theory is substantiated by the observation that the polarizations of the echoes on the  $(P', f)$  records are ordinary, ordinary and extraordinary in order of increasing critical frequencies, as given by the branches of the  $(Z, \zeta)$  curves.

THE problem of how a wave travels in the ionosphere is complicated by the effect of the earth's magnetic field, but a very good approximate theory can be obtained. It is the more accurate the more uniform the layer is, and it corresponds exactly to the ray theory.

By the use of Maxwell's equation we get the original wave equation in the vector form

$$\frac{1}{c^2} \frac{d^2 E}{dt^2} + \nabla^2 E - \nabla \operatorname{div} E = \left( \frac{2\pi}{\lambda} \right)^2 \frac{\nu_0'^2}{\nu_H^2 - \nu'^2} \left[ \frac{\nu_H^2}{\nu'^2} \frac{H(HE)}{H^2} - \frac{i\nu_H}{\nu'} \frac{[HE]}{H} \right],$$

where  $\nu_0'^2 = \nu_0^2(1 + i\alpha)$ , in which  $\nu_0$  is the usual critical frequency of the medium,  $\alpha = \nu_c/2\pi\nu$  the absorption term,  $\nu_c$  the collisional frequency,  $\nu$  the wave frequency  $\nu' = \nu(1 + i\alpha)$ , and  $\nu_H = eH/2\pi m$ , and is the resonant frequency of the electron in the magnetic field  $H$ .

We now assume that the solution of the wave equation can be represented in the form of Jeffrey's approximate solution,

$$E = \frac{1}{(dS/dz)^{\frac{1}{2}}} E_{1,2,3} \exp(2\pi i S - 2\pi i \nu t),$$

where  $E_1, E_2, E_3$  are the three components of  $E$ , and  $S = \text{const.}$  is the phase surface, and make the approximation that the  $\nabla^2 S$  term can be neglected in comparison with the  $(dS/dx)^2$  terms, which implies that the gradient of the refractive index  $\mu$  is everywhere small.

On reduction, we obtain three equations that can be represented in matrix form by

$$\begin{vmatrix} 1 - m^2 - Z^2 + \alpha_{11} & \alpha_{21} & \alpha_{31} \\ \alpha_{12} & 1 - Z^2 + \alpha_{22} & mZ + \alpha_{32} \\ \alpha_{13} & mZ + \alpha_{23} & 1 - m^2 + \alpha_{33} \end{vmatrix} \times E = 0. \quad \dots (1)$$

\* Private address—Weatheroak, Danbury, Essex.

Here we have assumed that the gradient of density in the ionosphere is purely in the vertical  $z$  direction, so that we make  $\lambda(dS/dx)=l$  and  $\lambda(dS/dy)=m$ , where  $l$  and  $m$  give the initial direction cosines of the wave, and  $\lambda(dS/dz)=Z$ .  $\alpha_{11} \dots$  are given by

$$\begin{aligned}\alpha_{11} &= \xi \rho_1^2 + \zeta & \alpha_{12} &= \xi \rho_1 \rho_2 + i \eta \rho_3 & \alpha_{21} &= \xi \rho_1 \rho_2 - i \eta \rho_3 \\ \alpha_{22} &= \xi \rho_2^2 + \zeta & \alpha_{13} &= \xi \rho_1 \rho_3 + i \eta \rho_2 & \alpha_{31} &= \xi \rho_1 \rho_3 - i \eta \rho_2 \\ \alpha_{33} &= \xi \rho_3^2 + \zeta & \alpha_{23} &= \xi \rho_2 \rho_3 + i \eta \rho_1 & \alpha_{32} &= \xi \rho_2 \rho_3 - i \eta \rho_1\end{aligned}$$

in which

$$\rho_{1,2,3} = H_{1,2,3}/H,$$

where  $H_1, H_2, H_3$  are the components of  $H$ , and

$$\xi = -\frac{\nu_0'^2}{\nu'^2 - \nu_H^2} \frac{\nu_H^2}{\nu'^2}; \quad \eta = \frac{\nu_0'^2}{\nu'^2 - \nu_H^2} \frac{\nu_H}{\nu'}; \quad \zeta = \frac{\nu_0'^2}{\nu'^2 - \nu_H^2}.$$

From the matrix we obtain an equation for  $Z$  which is biquadratic. We can thus represent  $Z$  on a four-sheeted Riemann surface, and this is sufficiently accurate except near the branch, or reflection points.

We can express the equation in terms of  $\zeta$  and  $\tau$ , where  $\zeta$  is now defined by  $\zeta = \nu_0'^2/\nu^2$ . This is the previous  $\zeta$  with  $\nu_H$  neglected, and  $\tau = \nu_H/\nu$ , which may be resolved into the components  $\tau_x, \tau_y, \tau_z$ .

If we know  $\zeta$  and the components of  $\tau$ , we can express  $Z$  as a function of its position on the Riemann surface (Forsyth 1900).

We presume  $\zeta$  and the components of  $\tau$  to be known, because we cannot attack a problem without knowing the density  $N$  in the ionosphere, so that the topography of the surface is known and does not depend upon what we represent on it. All the branch points and reflection points are known and depend on  $\zeta$ .

The behaviour of propagation can be represented as the behaviour of  $Z$ , and the four-sheeted Riemann surface gives everything that we require. Thus the transmission of electric waves in an ionized medium with a magnetic field present can be expressed most suitably in terms of this four-sheeted biquadratic Riemann surface. This, though not perfectly accurate, is very nearly so, except in the neighbourhood of the branch points.

For the particular case of vertical incidence, the branch points can be determined from the formula

$$Z^2 = \lambda^2 \left( \frac{dS}{dz} \right)^2 = \frac{(1 - \zeta)(\gamma - \zeta) - \frac{1}{2} \zeta \tau_x^2 \pm \zeta \left[ \frac{1}{4} \tau_x^4 + \tau_z^2 (1 - \zeta)^2 \right]^{\frac{1}{2}}}{\gamma (1 - \zeta) - \zeta \tau_x^2} \dots \dots (2)$$

where  $\gamma = 1 - \tau^2$  and  $\tau_y = 0$ .

Jeffrey's solution, which gives the waves on the earth, depends upon  $S$ , and  $S$  is given by the above formula, derived from matrix (1).

Jeffrey's solution is

$$E = \frac{A}{\lambda(dS/dz)^{\frac{1}{2}}} \exp \left( \frac{2\pi i}{\lambda} S_z - 2\pi i \nu t \right), \dots \dots (3)$$

which depends almost entirely on the phase  $S$ .

For vertical transmission,  $dS/dz$  can be expressed in the above form. It is biquadratic, and represents the variation of the phase of the wave. This formula gives the refractive index and all the branch points of  $S$ , which are either zeros or infinities of the above expression.

We find that the group velocity is zero at all these points, which means that a pulse will come up to the branch points, stop, and then go down again. These branch points are therefore the reflection points. We give an example in Figure 1, which shows the refractive index  $\lambda(dS/dz)$  as a function of the quantity  $\xi$ , which is the ratio of the frequencies  $\nu_0^2/\nu^2$ , where  $\nu_0^2 = Ne^2/\pi mc^2$ .

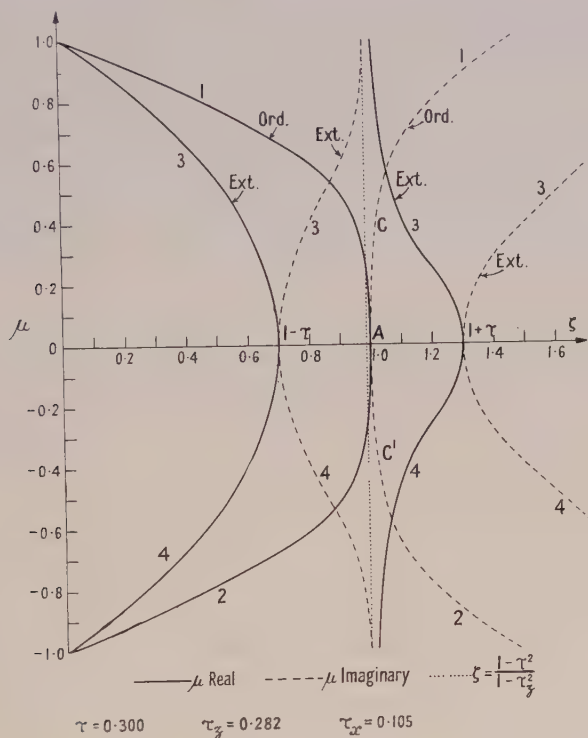


Figure 1. Refractive index as a function of  $\xi(\propto N)$ , showing reflection at the branch points.

We give here the four branch points in terms of  $\nu_0$ :

1.  $\nu_1 = \nu_0/(1 - \tau)^{\frac{1}{2}}$  Extraordinary
2.  $\nu_2^* = \{(1 - \tau_z^2)/(1 - \tau^2)\}^{\frac{1}{2}} \nu_0$
3.  $\nu_3 = \nu_0$
4.  $\nu_4 = \nu_0/(1 + \tau)^{\frac{1}{2}}$

approximately, since the  $\tau$ 's are functions of  $\nu_1, \nu_2$  etc.

More explicitly, they can be expressed in the form

1.  $\nu_1^2 - \nu_1 \nu_H = \nu_0^2$ ,
2.  $\nu_2^2 \{(\nu_2^2 - \nu_H^2)/[\nu_2^2 - (\nu_H^2)^2]\} = \nu_0^2$ ,
3.  $\nu_3^2 = \nu_0^2$ ,
4.  $\nu_4^2 + \nu_4 \nu_H = \nu_0^2$ .

\* Brought to notice by Rai (1937).



The branch or reflection points are shown in Figure 2. This gives the nature of the four-sheeted Riemann surface. The branch points correspond to the normal ordinary and extraordinary rays.

One thing is clear. The ordinary and extraordinary rays are on different sheets of the Riemann surface. When the transmission is vertical and the magnetic field is completely vertical, the sheets are in two unconnected pairs, and there is no means of passing from an ordinary sheet to an extraordinary one or vice versa. There is no coupling between the rays. This is discussed in fuller detail later, but this outline gives an idea of the nature of the coupling between the two.

We can now go on to consider the Riemann surface method of representation. The results contained in the following pages give us an understanding of the coupling process. No criterion of the relative probability of appearance or the

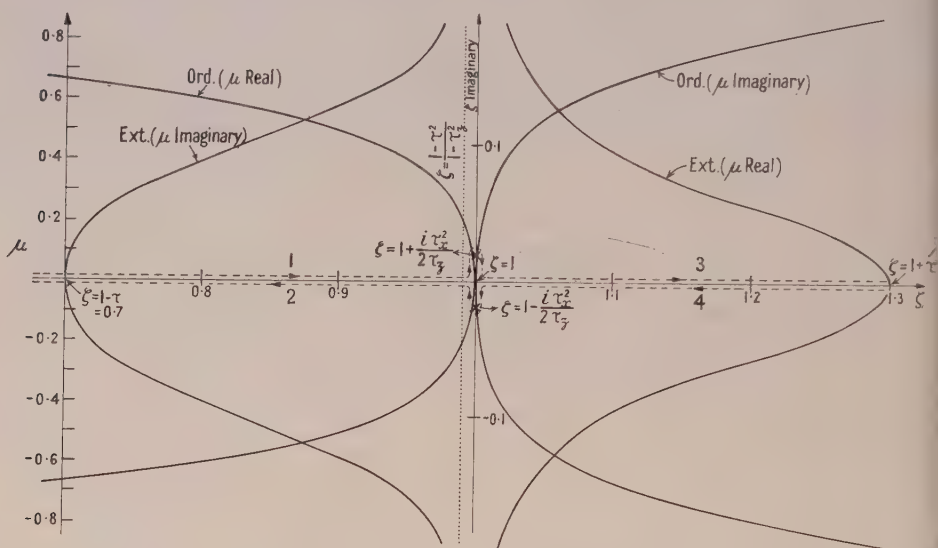


Figure 2. Refractive index as a function of  $\zeta (\propto N)$ , showing branch points in the complex  $\zeta$  plane.

degree of intensity of the rays or pulses of these critical frequencies has ever been given, and the following method of analysis gives definite conclusions with regard to this point. The original analysis, giving critical frequencies alone, is like the older phase integral quantum theory, in which the various spectral lines were given (corresponding to the critical frequencies) without any indication of their intensities.

We have represented the waves on a four-sheeted Riemann surface on which the branch (or reflection) points will be seen. It has been pointed out that the phase and group time increase continually up to and through the branch points and follow on the downward branch to  $\zeta = 0$ , giving the complete phase and group delay of a wave or impulse travelling along the upward branch ( $dS/dz$  positive) to the reflection point ( $dS/dz = 0$ ) (generally but not necessarily) and down the lower branch ( $dS/dz$  negative) to the starting point.

The conditions of reflection can therefore be best studied by examining the branch points and branch lines of the four-sheeted Riemann surface on which ( $dS/dz$ ) is most suitably represented.

This surface, for the case discussed above, is shown in Figure 2, where the surface represents the complex  $\zeta$  plane. The study of expression (2) shows that branch points occur at

$$\begin{aligned} \zeta = 1 - \tau \text{ (one),} & \quad \zeta = 1 \text{ (one),} & \quad \zeta = 1 + (i\tau_x^2/2\tau_z) \text{ (two),} \\ \zeta = 1 - (i\tau_x^2/2\tau_z) \text{ (two),} & \quad \zeta = 1 + \tau \text{ (one),} & \quad \zeta = \infty \text{ (unless } \zeta = z^2), \\ \text{and} & \quad \zeta = \gamma/(1 - \tau_z^2) \text{ (one),} \end{aligned}$$

when the refractive index becomes infinite.

If  $\zeta$  negative is cut off by a perfectly conducting plane, there are two further branch points at  $\zeta = 0$  representing the complete reflection of the ordinary and extraordinary rays at the surface. The branch lines ending at the branch points should be noted.

Any path which crosses a branch line goes from one sheet, say 1, to another sheet, say 2. The branch line ends at any branch point where the two are interchanged.

The analysis of the four-valued expression for  $\mu$  in this manner reveals significant features. When the incidence is vertical and the earth's magnetic field is also vertical, then there are two independent solutions on two independent pairs of sheets, i.e. the 1-2 pair and the 3-4 pair, and there is no interchange between the pairs.

When, however, the magnetic field is at all oblique, both the longitudinal and the transverse components of  $H$  are present. All four sheets are then linked together. There are branch points where 1 and 3 and where 2 and 4 are interchanged, and it is always possible to choose a path which goes from any one sheet to any other. The ordinary and extraordinary rays are then coupled together, as well as the ordinary and isolated rays, although usually to a very slight extent.

This analysis may be used for estimating or computing the intensities of the echoes corresponding to the four critical frequencies already given, and for calculating the coupling between the ordinary and extraordinary rays.

In the first place it should be noted that it will be very improbable that the ray with critical frequency  $\nu_2$  (pointed out by Rai 1937) will ever be obtained with observable intensity, for the path of the extraordinary echo which is reflected at  $\zeta = \gamma/(1 - \tau_z^2)$  (see Figure 2), corresponding to the critical frequency  $\nu^2$ , has to traverse the region from  $\zeta = 1 - \tau$  to  $\zeta = \gamma/(1 - \tau_z^2)$ , where the refractive index is large and entirely imaginary, before being reflected.

There is, however, a much more likely case, in which, instead of the normal ordinary and extraordinary doublet, which separates as a split echo near the critical frequency, there is a triplet ordinary, ordinary, extraordinary: o., o., ex. (see Figures 2, 3 and 4).

The three critical frequencies here shown are given by

$$\begin{array}{ccc} \zeta = (1 + \tau), & \zeta = 1 & \text{and} & \zeta = (1 - \tau). \\ \text{o.} & \text{o.} & & \text{ex.} \end{array}$$

Since  $\zeta = \nu_0^2/\nu^2$ , where  $\nu$  is the critical frequency, the three critical frequencies are

$$\begin{array}{ccc} \nu_0/(1 + \tau)^{\frac{1}{2}}, & \nu_0 & \text{and} & \nu_0/(1 - \tau)^{\frac{1}{2}} \\ \text{o.} & \text{o.} & & \text{ex.} \end{array}$$

where  $\nu_0^2 = Ne^2/\pi mc^2$ .

The last two are the normal critical frequencies and the first an extra one.

This split into three branches was first observed by Harang (1936), who showed the three branches (a), (b) and (c) each separated by a frequency interval  $\nu_H/2$  appropriate to the critical frequencies given above.

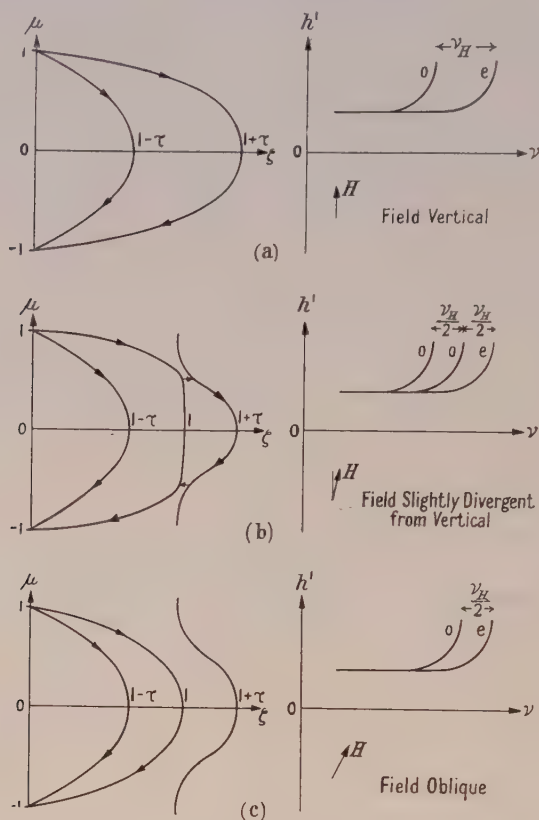


Figure 3. Similar to Figure 1, showing the corresponding  $(h', \nu)$  curves with the production of a triplet.

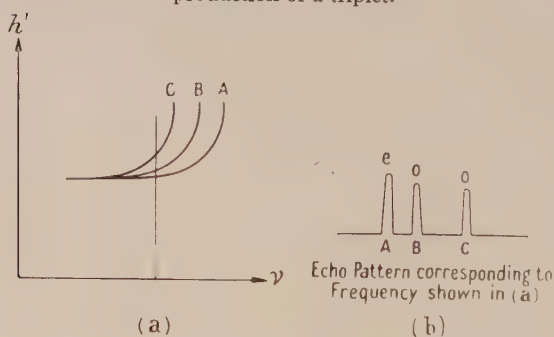


Figure 4.  $(h', \nu)$  curve, showing the triplet with the corresponding echo pattern and polarizations.

The mechanism of this is illustrated in Figures 1, 2 and 3. Turning first to Figure 1, it will be seen that if we could bridge the gap from the ordinary ray (1) to the isolated ray (3) at C, and then move along the 3-4 path through the apex at D to C', bridging the gap again at C' on to the downward ordinary branch 2, we should form a path the critical frequency of which would be  $\nu_0/(1+\tau)^{1/2}$ ,



corresponding to the added ordinary ray observed by Harang. This ray was also observed by the author on the cathode-ray oscillograph in 1933, the order of delay being ex., o., o. (Eckersley 1933, also Meek 1948, Newstead 1948).

The polarization of this extra ray, determined as it is by the conditions when leaving the ionosphere on the downward ordinary path, will obviously correspond to that of the ordinary ray.

That the physics of such a transmission is possible will be seen by proceeding to the limit where  $\tau_x \rightarrow 0$  and  $H$ , the magnetic field, is purely vertical. When  $\tau_x$  is very small, but  $H$  not quite vertical, the analysis shows that the isolated branch 3-4 very nearly touches the ordinary ray branch at  $CC'$ , and in the limit when  $\tau_x \rightarrow 0$ , the two actually join, and the paths  $CAC'$  and  $C\infty$  disappear. We are then left with the two simple rays with critical values of  $\zeta$ , viz.  $1 - \tau$  and  $1 + \tau$ . These are the extreme rays of the triplet, and have a frequency difference  $\nu_H$  instead of the usually observed difference  $\nu_H/2$ .

It is hardly conceivable, physically, that this process should occur discontinuously at  $\tau_x = 0$ , and we should expect, on physical grounds, to find all three branches in the neighbourhood of  $\tau_x = 0$  for the reason that the isolated branch 3-4 is closely coupled to the ordinary branch 1-2 when  $\tau_x$  is small.

We can express these ideas in a more exact form by considering the Riemann surface again. We have to find the total attenuation on integrating this along a path which, starting in sheet 1, passes continuously to sheet 3 round the 1-3 branch point, again passes continuously from sheet 3 to sheet 4 round the 3-4 branch point at  $\zeta = 1 + \tau$ , and then from sheet 4 to sheet 2 round the 4-2 branch point and back to earth. In sheet 2, as in sheet 1,  $N$ , the number of electrons, is zero at  $\zeta = 0$ .

This represents, in a more exact mathematical form, the physical path previously discussed. Thus it passes, in sheet 1, as far as  $\zeta = 1$ ; then it goes from 1 to  $1 + i(\tau_x^2/2\tau_z)$ , where,  $\zeta$  being complex, there is an attenuation. After passing round the branch point 1-3, it reaches sheet 3, and  $\zeta$  decreases on this sheet from  $1 + i(\tau_x^2/2\tau_z)$  to the neighbourhood of  $\zeta = 1$ , again making a contribution to the attenuation. We then integrate along the path from  $\zeta = 1$  to  $\zeta = 1 + \tau$  in sheet 3, where the path is along the real axis and the integral is real, so that there is no contribution to the attenuation. At this point,  $1 + \tau$ , it goes from sheet 3 to sheet 4.

Finally, we require to pass from sheet 4 to sheet 2 to continue the path down to earth, and to do so we have again to introduce attenuation by rounding the branch point at  $\zeta = 1 - i(\tau_x^2/2\tau_z)$  where  $\zeta$  and the integrand are again both complex. We then reach branch 2, the ordinary ray, at  $\zeta = 1$  and proceed, without attenuation, along this path to earth again at  $\zeta = 0$ .

The imaginary part of  $\mu$  is definitely specified at each point of the path, so that the attenuation can be uniquely determined.

It will be observed that the path and integrand are only complex in the regions between  $\zeta = 1$  and  $\zeta = 1 + i(\tau_x^2/2\tau_z)$  and between  $\zeta = 1$  and  $\zeta = 1 - i(\tau_x^2/2\tau_z)$ , and that this path tends to zero as  $\tau_x \rightarrow 0$ . Therefore the total attenuation of this spurious ordinary echo decreases as  $\tau_x \rightarrow 0$ . This was also obvious in the previous more definitely physical treatments.

Another point must be considered: The integral should be taken with respect to  $z$ , i.e. the distance, but as expressed on the Riemann surface,  $\mu$ , or  $\lambda(dS/dz)$ , is a function of  $\zeta$  only.

The attenuation or imaginary part,

$$\int \lambda \frac{dS}{dz} dz = \int f(\zeta) d\zeta,$$

can be expressed in the form  $\int f(\zeta) d\zeta (dz/d\zeta)$ .

Now the first part of this integral is a quantity only depending on  $\tau_x, \tau_z, \tau$ , not on the distribution of density in the layer. The whole integral is small when the gradient of density in the layer is large, and vice versa.

Therefore the attenuation equals  $\int f(\zeta) \frac{d\zeta}{d\zeta/dz}$ , and is likely to be small when  $d\zeta/dz$ , the ionic gradient, is large, and vice versa.

It follows that the conditions in which the triplet form with critical frequencies  $\nu_0/(1-\tau)^{\frac{1}{2}}, \nu_0, \nu_0/(1+\tau)^{\frac{1}{2}}$  is likely to appear are: (i) in northern latitudes where  $\tau_x$  is small, and (ii) in regions where the gradient of  $N$  with respect to  $z$  is large. It is significant that this triplet form has only been observed in high latitudes.

Cases which may well represent this type of transmission were noted in 1933 (Eckersley 1933). On such occasions well defined triplets were observed on frequencies in the neighbourhood of the critical frequency. The polarization observed in the cathode-ray indicator was invariably as shown in Figure 4.

A and B are the normal extraordinary and ordinary pair, the extra echo C being of ordinary polarization.

These three correspond to the branches with critical frequencies:

A	B	C
$\nu_0/(1-\tau)^{\frac{1}{2}},$	$\nu_0$	and $\nu_0/(1+\tau)^{\frac{1}{2}}$ (the extra echo).
ex.	o.	o.

We may use the curves in Figure 1 in the way just described to calculate the coupling coefficient between the ordinary and extraordinary rays. Thus, considering an up-going ray in the ordinary 1-2 sheet, we may bridge the gap, as before, to the isolated ray in the 3-4 sheet. We then pass to the branch point at

$$\zeta = \gamma/(1-\tau_z)^{\frac{1}{2}}, \quad dS/dz = \infty$$

and back along the imaginary branch in the 3-4 sheet to D, and finish along the real part of the extraordinary branch which goes down to earth again. It is clear that the total attenuation is large and, therefore, that the coupling will be small. The contribution to the attenuation is especially large between S and D. The same remarks as regards the gradient of  $\zeta$  with respect to  $z$  apply equally well here. Thus if  $d\zeta/dz$  is large enough, the total attenuation along the path may be made as small as we please.

The truth of this statement may readily be seen by proceeding to the limit where  $d\zeta/dz$  becomes so large at one point that we may consider this to be the surface of separation. This case may easily be worked out according to the full wave theory. Without going into detail, it may be said that in medium 1 (see Figure 5) there may be two characteristic waves,  $o_{.1}$  and  $ex_{.1}$ . Let the polarization ratio  $X/Y$  be given by  $P_{o.1}, P_{ex.1}$ .

Therefore, in medium 2, we shall have  $P_{o.2}, P_{ex.2}$ .

Suppose a wave of the type o. is sent through the first medium. Since  $P_{o.2}$  and  $P_{ex.2}$  are not the same as  $P_{o.1}$  and  $P_{ex.1}$ , and since there is an appreciable

component of the electric force, the reflected wave will not be only of the o. type, but will consist of o. and ex. in suitable proportions to satisfy the boundary conditions.

If the path in medium 1 is sufficiently long, and if the incoming signal consists of a short wave impulse, the reflected wave will consist of an o. and an ex. impulse which, after travelling sufficiently far, will be separated into two pulses.

Thus, by sending into the medium an  $o_1$  impulse, we get a pair,  $R_{o,1}$  and  $R_{ex,1}$ , reflected or refracted back into medium 1 again.

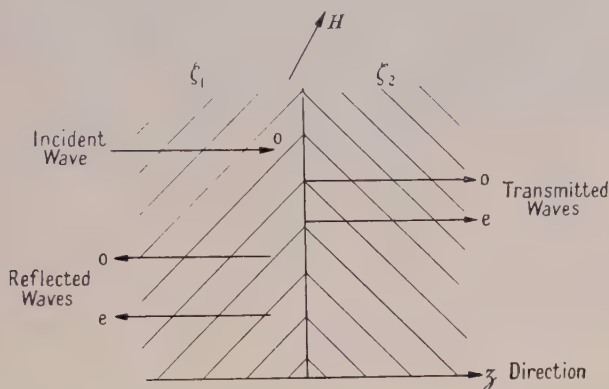


Figure 5. Illustrating the full wave solution at a surface of separation between  $\zeta_1$  and  $\zeta_2$ .

Thus there is obviously a coupling between the  $o_1$  and  $ex_1$  rays where the gradient is so steep that in the limit we may consider it to form a definite surface of separation.

This is an extreme illustration of the effect of coupling already referred to.

This coupling has, in general, been calculated by the relatively inaccurate four-sheeted Riemann surface method because it is very difficult to get a suitable solution of a fourth order differential equation. As reckoned by this method, the amount of coupling may be a little inaccurate, but where the media on each side of the surface of separation are uniform, it is possible to use a completely definite wave solution which agrees with the above and shows, as in the last analysis, that there is a definite coupling between the o. and ex. waves. Some German papers also show this, and I think we may rest assured that this coupling exists.

## RECAPITULATIONS

1. Triple splitting of rays reflected from the ionosphere has been observed in the polar regions where the earth's magnetic field is nearly vertical (see Figure 4). Well defined triplets are almost invariably of the type o., o., ex. in terms of critical frequency. In terms of delay time they are ex., o., o. They have been observed by Harang in Norway, J. M. Meek in Canada and by the author as far south as England. They have also been observed by Newstead in Hobart, Tasmania, but as far as is known they have never been observed in any equatorial region.

2. These triplets can be explained in terms of the four-sheeted Riemann surface, which expresses the propagation in the ionosphere. They are due, as shown in Figure 3 (b), to the coupling between the isolated and ordinary rays



This coupling does not occur in equatorial regions. The Riemann surface theory, which is approximate, has been confirmed in certain cases by the wave theory, which is absolutely correct.

3. It is in virtue of a coupling between the o. and isolated rays that a triplet is formed. When  $\tau_x$  is zero, and we are consequently at the pole, there is no definite isolated ray, and the two extremes of the triplets are formed with a frequency separation of  $\nu_H$  approximately, and not the usual  $\nu_H/2$  approximately.

4. The fact that the observed features of the triplets can be explained by the Riemann surface theory, and can be derived from it, is a very good proof that this theory is correct. These features are: (i) the triplet is of the ex. o., o. type; (ii) it is confined to high positive and negative latitudes.

Triplets were noted by the writer in England as early as 1933; experimental results were given, but the explanation was not published at the time.

#### REFERENCES

- ECKERSLEY, T. L., 1933, *Proc. Roy. Soc. A*, **141**, 710; 1948, *Nature, Lond.*, **161**, 597.  
 FORSYTH, A., 1900, *Theory of Functions* (Cambridge: University Press).  
 HARANG, L., 1936, *Terr. Mag. Atmos. Elect.*, **41**, 160.  
 MEEK, J. M., 1948, *Nature, Lond.*, **161**, 597.  
 NEWSTEAD, G., 1948, *Nature, Lond.*, **161**, 312.  
 RAI, R. N., 1937, *Proc. Nat. Inst. Sci.*, **3**, 307-317.

## LETTERS TO THE EDITOR

### The Debye Effect in Electrolytes

P. Debye (1932) has predicted the existence of an alternating electric potential  $\Phi$  at a point in an electrolyte through which a sound wave is passing. His equation is

$$\Phi = \frac{m_H}{\epsilon} g a_0 \frac{\sum (p_j \zeta_j M_j / \rho_j)}{\sum (p_j \zeta_j^2 / \rho_j)} \left\{ \frac{4\pi l / D\omega}{[1 + (4\pi l / D\omega)^2]^{\frac{1}{2}}} \right\}$$

where  $\omega$  is the angular frequency,  $g$  the velocity of sound in solution,  $a_0$  the particle velocity amplitude,  $l$  the conductivity of the solution,  $D$  the dielectric constant of the solvent,  $m_H$  the mass of a hydrogen ion,  $\epsilon$  the electronic charge,  $p_j$  the relative number per unit volume of ions of valency  $\zeta_j$ , gram ionic mass  $M_j$  and frictional coefficient  $\rho_j$ . The deduction of this result has been followed by mathematical work by which corrections for various smaller effects have been proposed.

For frequencies less than tens of megacycles per second the last factor in the equation is of the order of unity and frequency becomes unimportant. For a binary salt with univalent ions Debye's result then reduces to

$$\Phi = 1.4 \times 10^{-7} a_0 \frac{M_1/\rho_1 - M_2/\rho_2}{1/\rho_1 + 1/\rho_2} \text{ volts.}$$

With dilute solution in a given solvent, electrolysis experiments give values for ionic mobilities differing little from ion to ion or with concentration. Hence for the purpose of determining the order of magnitude of the effect, we may put  $\rho_1 \simeq \rho_2$  so obtaining a result roughly proportional to  $(M_1 - M_2)$ . The order of  $\Phi$  should therefore be about 1 microvolt when  $a_0$  is 1 cm/sec.: a sound intensity of about 1/100 watt/cm<sup>2</sup>. This led Debye to express confidence in the early detection of the effect. In fact, no experimental evidence for it in electrolytes was found until the recent work of Yeager, Bugosh, Hovorka and McCarthy (1949), although an effect of about one hundredth of the estimated order of magnitude was recorded by Rutgers (1946) for colloidal solutions.

For purposes of calculation we should use for  $M_1$  and  $M_2$  the effective masses of the ions, including the mass of any solvation sheath. The use of the available conflicting results for solvation numbers for calculation of the relative values of  $\Phi$  for the five salts used by the above workers shows no correlation with their experimental results. In fact these results vary so little between one salt and another in water as to suggest that the solvent is largely responsible for the effective masses of the ions. That is, there is either a large solvation sheath masking the effect of the ions proper, or the equation does not take into account all the factors involved. Available results from which conclusions may be drawn are insufficient and work with selected salts and a variety of solvents is obviously very necessary. Such results should serve to obtain quantitative data, not only about the Debye effect, but also about the mechanism of solvation.

A principal experimental difficulty is the possibility of direct electromagnetic coupling between the radiofrequency source and the detecting apparatus. Such coupling would limit the sensitivity of the amplifier which could usefully be employed. Yeager, Bugosh, Hovorka and McCarthy used elaborate screening precautions to detect the effect and their method thereby made measurement of the sound intensity impracticable. However their results appear to confirm that the effect is smaller than expected from the Debye equation and for reasonable sound intensities is therefore not much above noise level.

A solution would seem to be the use of a method by which a pulse of sound is sent through the experimental liquid, the duration of the pulse being such that, with the length of sound path used, the source is inoperative during detection of the effect.

An apparatus of this kind, by which any electromagnetic pick-up is separated in time from the desired signal, is nearing completion in this laboratory. The frequency of 465 kc/s. has been chosen so that the sound wavelength in the experimental liquid may be sufficiently long for the use of probes spaced half a wavelength apart for detection of the potential variations; at the same time standard intermediate frequency transformers may be used for the amplifier. At this frequency the absorption of sound in the electrolyte will be small and a long sound path may consequently be used. This makes it possible to use a long pulse, of the order of one millisecond in duration. The amplifier required for such a pulse need have a bandwidth of only 1,000 c/s. and the noise level will therefore be low. The method is essentially a progressive wave method, reflections from the end of the tank being avoided by the use of an absorbing device. Since a large tank may be used the sound field at the detecting probes is calculable and no difficulty is expected in determining the intensity there. The pulses are to be displayed on a cathode-ray tube and compared with signals from a standard generator. It is hoped to investigate thoroughly the dependence of the effect on the various parameters involved.

A. N. HUNTER.

Physics Department,  
University College,  
Leicester.  
7th October 1949.

DEBYE, P., 1933, *J. Chem. Phys.*, **1**, 13.

RUTGERS, A., 1946, *Nature, Lond.*, **157**, 74.

YEAGER, E., BUGOSH, J., HOVORKA, F., and MCCARTHY, J., 1949, *J. Chem. Phys.*, **17**, 411.

## Electron Optics of the Three-Stage Electron Microscope

Electron microscopes employing three stages of electronic magnification are now becoming more generally used, but as yet no adequate account of their electron optics has been published. Le Poole (1947) gave some ray diagrams, which, while they are accurate, are not sufficiently comprehensive to give a clear picture of the situation.

In connection with the building of an electron microscope in collaboration with Mr. J. F. Brown, and under the direction of Professor G. I. Finch, the conditions of conjugate foci between the electron lenses were examined by Gaussian optical methods, which, while they do not give a strictly accurate quantitative analysis of the situation, do indicate the approximate positions and method of formation of the images. The analysis is reproduced in the Table, and Figures 1, 2, 3 and 4 are the ray diagrams which were deduced from the data summarized in this Table.

### Condition of Conjugate Foci between Objective Lens and Intermediate Lens of a Three-Stage Electron Microscope.

$u$  (objective lens) = 0.8 cm.;  $v$  (intermediate lens) = 17 cm.; objective-intermediate lens separation = 15 cm.; magnification of projector lens =  $M_P = 120\times$ .

Objective lens			Intermediate lens			$M_0 \times M_1 \times M_P$	Corresponding ray diagram
$v$ (cm.)	$f$ (cm.)	Magn. ( $M_0$ )	$f$ (cm.)	Magn. ( $M_1$ )	$u$ (cm.)		
32.5	0.785	38	—	1	—	4560	2-stage  Figure 3. Low magnification (a)
44.6	0.786	55.8	40	0.575	— 29.6	3860	
54.3	0.788	67.9	30	0.433	— 39.3	3550	
68.1	0.791	85	25	0.32	— 53.1	3380	
157	0.797	196.5	20	0.12	— 142	2830	
321	0.798	400	18	0.0555	— 306	2660	
2905	0.7998	3635	17.1	0.0059	— 2980	2565	
$\infty$	0.8		17	$1/\infty$	$\infty$	2555*	Figure 4. Low magnification (b)
— 247	0.803	309	16	0.0684	256	2530	
— 64.3	0.81	84	14	0.220	79.3	2090	
— 25.8	0.825	32.2	12	0.43	40.8	1645	
— 4.1	0.981	5.13	9	0.916	19.1	565	
			8.08	1.168	15	0	Figure 2. Diffraction
5.72	0.701	7.15	6	1.885	9.28	1000	Figure 1. High magnification
7.91	0.728	9.9	5	2.47	7.09	2920	
9.77	0.741	12.21	4	3.35	5.23	7700	

\* Interpolated.

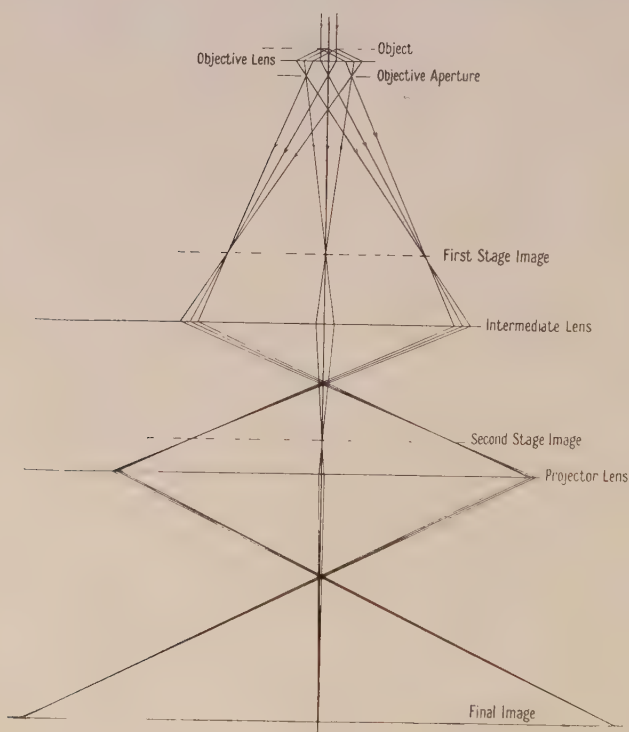


Figure 1. High magnification.

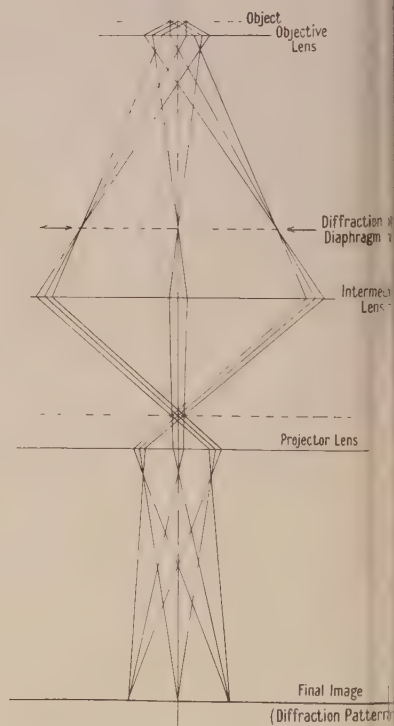


Figure 2. Diffraction.



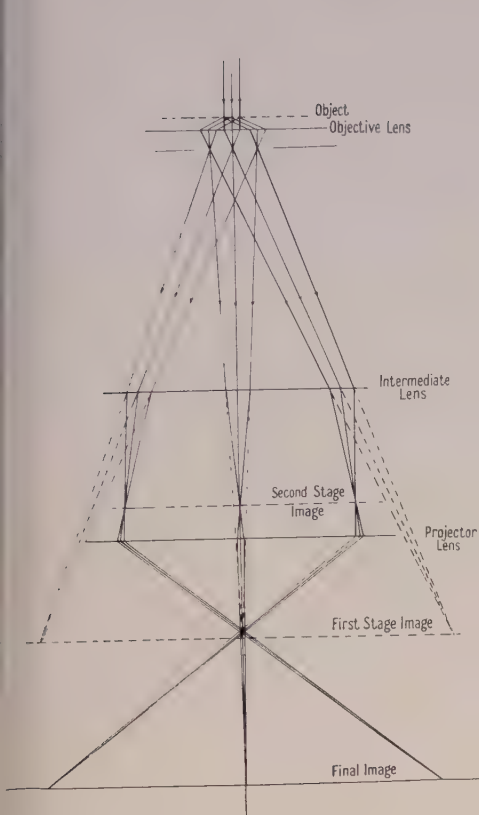


Figure 3. Low magnification (a).

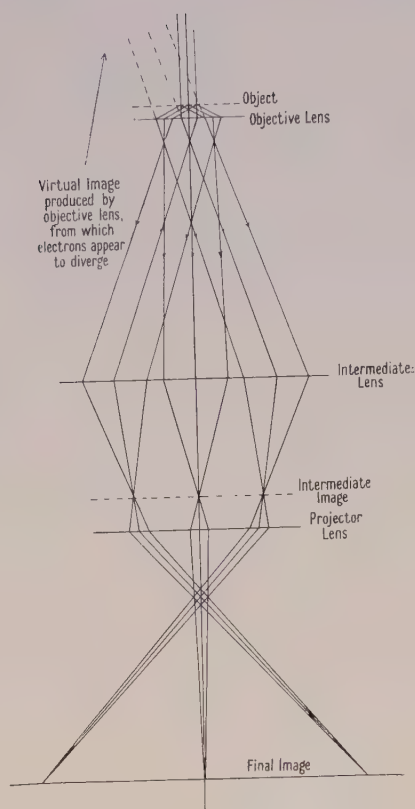


Figure 4. Low magnification (b).

Figure 1 indicates the electron paths when the microscope is producing a high magnification final image. If from this condition the power of the intermediate lens is decreased sufficiently, it is possible to obtain a zero magnification image, and if no objective aperture is present to remove the higher order diffracted rays, a diffraction pattern of the specimen is seen on the final screen (Figure 2). If the power of the intermediate lens is further decreased and the objective lens refocused, then a low magnification image is produced on the final screen, and the optics of this image are best explained in the following way.

If the intermediate lens is switched off, and the objective lens refocused, a two-stage image is formed. If now the intermediate lens is switched on at very low power, then the magnification of the image is slightly decreased; this condition is shown in Figure 3. Upon further increasing the power of the intermediate lens, a stage is reached where the objective lens no longer produces a real image; this is the case illustrated by Figure 4. Further increases in intermediate lens power produces again the diffraction pattern.

These theoretical deductions were borne out by practical measurements of focal lengths of the lenses of the electron microscope for the various conditions of image formation. It was also found that, when a low magnification was required, the image formed by using the intermediate lens in the condition corresponding to Figures 3 or 4 showed less distortion than that produced when the conditions of Figure 1 obtained.

I am indebted to Mr. J. F. Brown, with whom the work was carried out, and to Professor G. I. Finch for his helpful supervision.

Applied Physical Chemistry Laboratory,  
Imperial College, London S.W. 7.\*  
20th September 1949.

C. E. CHALICF.

LE POOLE, J. B., 1947, *Philips Tech. Rev.*, **9**, 33.

\* Now at National Institute for Medical Research, Hampstead, London N.W. 3.

## REVIEWS OF BOOKS

*Metal Rectifiers*, by H. K. HENISCH. Pp. xi + 156. First Edition. (Oxford: University Press, 1949.) 15s.

This book belongs to the series of monographs on Physics and Chemistry of Materials. I always find it difficult to define exactly the cross section of physicists or engineers to whom such a monograph is addressed. In general the practical expert will find little new in the chapters on manufacture, while he might find the chapters dealing with theory hard going because they are, of necessity, rather condensed. On the other hand the theoretical physicist often finds that the description of the practical methods is somewhat incomplete. It appears to me that in this volume the author has managed to find a happy combination of describing the essentials of practical manufacturing methods without getting lost in details, and of presenting the theory in such a way that it is not too difficult to follow for the practical engineer, though I myself would have liked to have seen the theoretical Chapter V somewhat amplified and some of the figures in it described in more detail. On the other hand, a full bibliography enables the interested reader to study the subject in greater detail.

After a short history of rectifier development the manufacture of the most important types of rectifiers is described. These comprise cuprous oxide, selenium, sulphide and germanium rectifiers.

In the third chapter characteristic rectifier properties are described. Starting with the rather complex voltage-current characteristics of the various types of rectifier, D.C. resistance and incremental or A.C. resistance are described as well as the phenomena of hysteresis, creep, ageing and the effects of temperature. The self capacitance represents an A.C. shunt and a number of equivalent networks are given together with an account of the variations of the self capacitance with the conditions of measurement such as direct voltage, time, etc. In view of the importance of "noise" in modern circuitry, the question of noise would appear to deserve more than one short paragraph at the end of the chapter.

Chapter IV deals with measurements of rectifier properties and the pitfalls that may be encountered in these.

The longest chapter in the book is, quite rightly, the one dealing with modern theories of rectification. After a discussion of the structure of semiconductors and the mechanism of electrical conduction in solids, modern concepts of insulators, intrinsic semiconductors and impurity semiconductors are given.

Next, the theories of the chemical and physical barrier layers are explained and the theoretical and experimental results compared. Chapter VI deals shortly with earlier theories of rectification.

Two short chapters on rectifier operation and future developments conclude this highly recommendable book. As far as the bibliography is concerned, replacement of the simple asterisks by numbers or by an indication of the corresponding page in the text would facilitate finding one's way back into the text when scanning through the list of references. Seven of the references mentioned in the text have not received an asterisk, and the one mentioned on page 129 has the wrong number.

H. G. LUBSZYNSKI.

## CONTENTS FOR SECTION A

	PAGE
ditorial . . . . .	1
Dr. K. MENDELSSOHN and Mr. J. L. OLSEN. Heat Transport in Superconductors . . . . .	2
Dr. E. R. ANDREW and Mr. J. M. LOCK. The Magnetization of Superconducting Plates in Transverse Magnetic Fields . . . . .	13
Prof. M. H. L. PRYCE. A Modified Perturbation Procedure for a Problem in Paramagnetism . . . . .	25
Dr. R. P. PENROSE and Dr. K. W. H. STEVENS. The Paramagnetic Resonance from Nickel Fluosilicate . . . . .	29
Prof. M. H. L. PRYCE and Dr. K. W. H. STEVENS. The Theory of Magnetic Resonance-Line Widths in Crystals . . . . .	36
Dr. T. R. KAISER. On the Capture of Particles into Synchrotron Orbits . . . . .	52
Dr. T. R. KAISER and Mr. J. L. TUCK. Experiments on Electron Capture and Phase Stability in a 14 mev. Synchrotron . . . . .	67
Letters to the Editor :	
Dr. W. EHRENBERG. The Electric Conductivity of Simple Semiconductors . . . . .	75
Reviews of Books . . . . .	77
Contents for Section B . . . . .	78
Abstracts for Section B . . . . .	79

## ABSTRACTS FOR SECTION A

*Heat Transport in Superconductors*, by K. MENDELSSOHN and J. L. OLSEN.

**ABSTRACT.** The heat conduction processes in superconductors have been discussed on the basis of the analogy with liquid helium II. It is suggested that under certain conditions the superconductive metal can exhibit a type of heat transport corresponding to the heat flow associated with the fountain effect. The heat conductivity of a number of pure metals and alloys has been measured in the normal and in the superconductive state and the results have been analysed with reference to the hypothesis mentioned above. In addition to the change of heat conduction with temperature, the magnetic hysteresis of the heat conduction has been investigated. The use of these phenomena as make-and-break thermal contacts at very low temperatures has been suggested.

*The Magnetization of Superconducting Plates in Transverse Magnetic Fields*, by E. R. ANDREW and J. M. LOCK.

**ABSTRACT.** The magnetization curves of thin superconducting tin plates were measured in transverse magnetic fields in order to investigate the nature of the intermediate state in such specimens. The curves showed peak magnetizations much higher than  $H_c/4\pi$ , indicating the presence of fields much greater than the critical field at the edge of the plates. This effect is qualitatively similar to that predicted by Landau's theory of the intermediate state, but quantitative agreement is not obtained. Resistance measurements on thin strips of tin in transverse fields showed that resistance only reappears for fields considerably greater than those required to start the destruction of superconductivity.



*A Modified Perturbation Procedure for a Problem in Paramagnetism*, by M. H. L. PRYCE.

**ABSTRACT.** A modified perturbation technique is described for problems in which second-order effects are comparable in magnitude with first-order effects, where orthodox methods break down. It is applied to the energy levels of paramagnetic ions in a crystal, giving an effective Hamiltonian in which the Stark splitting, the anomalous  $g$ -value and the temperature-independent paramagnetism are clearly exhibited.

*The Paramagnetic Resonance from Nickel Fluosilicate*, by R. P. PENROSE and K. W. H. STEVENS.

**ABSTRACT.** The paramagnetic resonance from the nickel ion in nickel fluosilicate has been investigated at a number of frequencies and temperatures. It has previously been suggested that the ion is in an electric field of trigonal symmetry. The results obtained are in good agreement with this hypothesis. It is also found that the magnitude of the splitting of the levels varies with temperature.

*The Theory of Magnetic Resonance-Line Widths in Crystals*, by M. H. L. PRYCE and K. W. H. STEVENS.

**ABSTRACT.** A theory is developed for calculating the mean displacements and mean square widths of resonant absorption lines in crystals for which the spin-lattice relaxation time is long compared with the spin-spin relaxation time. The theory is applied to a number of different cases; in particular, the effects of nuclear hyperfine structures and exchange forces in ionic resonances are discussed at length. It is shown that the theory holds, provided that the temperature is high compared with the Curie temperature.

*On the Capture of Particles into Synchrotron Orbits*, by T. R. KAISER.

**ABSTRACT.** A theory is developed for the capture of particles into synchrotron orbits when the radio-frequency accelerating voltage rises from zero to its maximum value in a finite time. It is shown that if this time of rise is sufficiently long, all particles originally occupying a band of width  $1/\sqrt{2}$  times the maximum width of the final stable region for synchrotron phase oscillations will be captured, irrespective of the initial phase at which they enter the accelerating gap. This conclusion would seem to be in agreement with the observed characteristics of existing electron synchrotrons.

*Experiments on Electron Capture and Phase Stability in a 14 mev. Synchrotron*, by T. R. KAISER and J. L. TUCK.

**ABSTRACT.** Experiments were made by interrupting the radio-frequency accelerating voltage for intervals during the acceleration in a synchrotron, and observing the effects on the output. The process of capture is found to be more efficient than would be expected for an instantaneously developed radio-frequency accelerating voltage. The synchrotron acceleration may be interrupted for a short period without losing more particles than would be accounted for by contraction of the beam radius during the interruption, so that for sufficiently short periods of interruption the loss is negligible. This demonstrates that the phase at which electrons enter the resonator during capture is of no consequence under the conditions prevailing. The results are in quantitative agreement with a theory put forward by Kaiser which takes into account the finite rate of rise of resonator voltage, and with the general theory of synchrotron stability.



## PHYSICAL SOCIETY PUBLICATIONS

Fellows and Student Members of the Society may obtain ONE copy of each publication at the price shown in brackets. In most cases the cost of postage and packing is extra.

- Resonant Absorbers and Reverberation.* Report of the 1947 Summer Symposium of the Acoustics Group of the Physical Society. Pp. 57. In paper covers. 7s. 6d. (5s.) Postage 6d.
- The Emission Spectra of the Night Sky and Aurorae*, 1948. Papers read at an International Conference held under the auspices of the Gassiot Committee in London in July 1947. Pp. 140. In paper covers. 20s. (12s. 6d.) Postage 6d.
- The Strength of Solids*, 1948. Report of Conference held at Bristol in July 1947. Pp. 162. In paper covers. 25s. (15s. 6d.) Postage 8d.
- Report of International Conference on Fundamental Particles (Vol. I) and Low Temperatures (Vol. II)*, 1947. Conference held at Cambridge in July 1946. Pp. 200 (Vol. I), pp. 184 (Vol. II). In paper covers. 15s. each vol. (7s. 6d.) Postage 8d.
- Meteorological Factors in Radio-Wave Propagation*, 1947. Report of Conference held jointly with the Royal Meteorological Society in April 1946. Pp. 325. In paper covers. 24s. (12s.+postage 1s.)
- Handbook of the 33rd Exhibition of Scientific Instruments and Apparatus*, 1949. Pp. 272. In paper covers. 5s. (2s. 6d.) Postage 1s.
- Catalogue of the 32nd Exhibition of Scientific Instruments and Apparatus*, 1948. Pp. 288. In paper covers. 5s. (2s. 6d.) Postage 1s. (Half price from 5th April 1949).
- Catalogue of the 31st Exhibition of Scientific Instruments and Apparatus*, 1947. Pp. 298. In paper covers. 2s. 6d. (1s. 6d.) Postage 1s.
- Report on Colour Terminology*, by a Committee of the Colour Group. Pp. 56. In paper covers. 7s. (3s. 6d.)
- Report on Defective Colour Vision in Industry*, by a Committee of the Colour Group. 1946. Pp. 52. In paper covers. 3s. 6d. (1s. 9d.+postage 4d.)
- Science and Human Welfare.* Conference held by the Association of Scientific Workers, Physical Society and other bodies. 1946. Pp. 71. In paper covers. 1s. 6d. (9d.) Postage 4d.
- Report on the Teaching of Geometrical Optics*, 1934. Pp. 86. In paper covers. 6s. 3d. Postage 6d.
- Report on Band Spectra of Diatomic Molecules*, 1932. By W. JEVONS, D.Sc., Ph.D. Pp. 308. In paper covers, 25s.; bound in cloth, 30s. (15s.) Postage 1s.
- Discussion on Vision*, 1932. Pp. 327. In paper covers. 6s. 6d. (3s. 3d.) Postage 1s.
- Discussion on Audition*, 1931. Pp. 151. In paper covers. 4s. (2s.) Postage 1s.
- Discussion on Photo-electric Cells and their Application*, 1930. Pp. 236. In paper covers. 6s. 6d. (3s. 3d.) Postage 8d.
- The Decimal Bibliographic Classification (Optics, Light and Cognate Subjects)*, 1926. By A. F. C. POLLARD, D.Sc. Pp. 109. Bound in cloth. 4s. (2s.) Postage 8d.
- Motor Headlights*, 1922. Pp. 39. In paper covers. 1s. 6d. (9d.) Postage 4d.
- Report on Series in Line Spectra*, 1922. By A. FOWLER, C.B.E., Sc.D., F.R.S. Pp. 182. In paper covers. 30s. (15s.) Postage 8d.
- A Discussion on the Making of Reflecting Surfaces*, 1920. Pp. 44. In paper covers. 2s. 6d. (1s. 3d.) Postage 4d.
- Reports on Progress in Physics.* Vol. XI (1946-48). Pp. 461. Bound in cloth. 42s. (25s.) Postage 1s.
- Reports on Progress in Physics.* Vols. IV (1937, reprinted 1946) and X (1944-45). Bound in cloth. 30s. each. (15s.) Postage 1s.
- The Proceedings of the Physical Society.* From Vol. I (1874-75), excepting a few parts which are out of print. Prices on application.
- The Transactions of the Optical Society.* Vols. 1 (1899-1900) -33 (1931-32), excepting a few parts which are out of print. Prices on application.

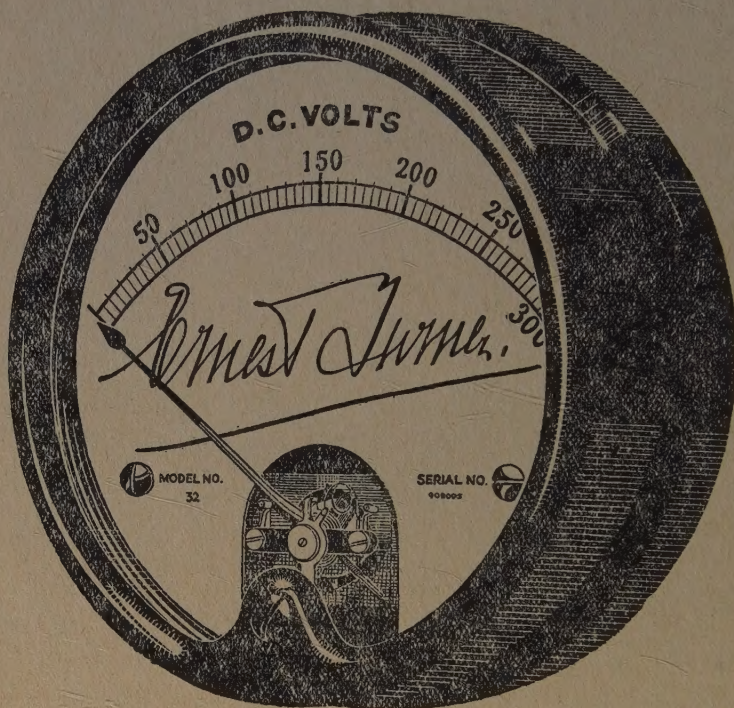
Orders, accompanied by remittances, should be sent to

THE PHYSICAL SOCIETY

1 Lowther Gardens, Prince Consort Road, London S.W.7



# ELECTRICAL MEASURING INSTRUMENTS OF THE HIGHER GRADES



**ERNEST TURNER  
ELECTRICAL INSTRUMENTS  
LIMITED  
CHILTERN WORKS  
HIGH WYCOMBE  
BUCKS**

**Telephone :**  
**High Wycombe 1301/2**

**Telegrams**  
**Gorgeous, High Wycombe**